Aus der medizinischen Klinik für Kardiologie, Angiologie und Pneumologie
des Universitätsklinikums Heidelberg
Direktor: Prof. Dr. Norbert Frey

Hypertrophic Growth Control by Activating Transcription Factor 6 in the Neonatal and Adult Heart

Inauguraldissertation
zur Erlangung des medizinischen Doktorgrades

an der Medizinischen Fakultät der
Ruprecht-Karls-Universität Heidelberg

vorgelegt von
Christoph Hofmann
aus Heppenheim

2021

Dekan: Herr Prof. Dr. med. Hans-Georg Kräusslich

Doktormutter: Frau Shirin Doroudgar, Ph.D.

To my family

Table of Contents

Index of Abbreviations

18S	18S ribosomal RNA
AAV	Adeno-associated virus
ACCF	American College of Cardiology Foundation
AHA	American Heart Association
ATF	Activating transcription factor
ATF4	Activating transcription factor 4
ATF6	Activating transcription factor 6 alpha
ATF6(N)	N-terminal fragment of activating transcription factor 6 alpha
ATF6β	Activating transcription factor 6 beta
ATP	Adenosine triphosphate
BAK	B-cell lymphoma-2 homologous antagonist/killer
BAX	B-cell lymphoma-2-associated X protein
BBF2H7	BBF2 human homolog on chromosome 7
BI-1	Bax inhibitor 1
BCL-2	B-cell lymphoma-2
BID	BH3-interacting domain death agonist
BIM	B-cell lymphoma-2-like protein 11
BiP	Binding immunoglobulin protein
Ca^{2+}	Calcium
Caspase-1	Cysteinyl-aspartate specific protease 1
Caspase-2	Cysteinyl-aspartate specific protease 2
Caspase-8	Cysteinyl-aspartate specific protease 8
C. elegans	Caenorhabditis elegans

CHOP	CCAAT-enhancer-binding protein homologous protein
CREB	Cyclic AMP-responsive element-binding protein
CREBH	Cyclic AMP-responsive element-binding protein H
CREB3	Cyclic AMP-responsive element-binding protein 3
CREBL1	Cyclic AMP-responsive element-binding protein-like 1
CREB3L1	Cyclic AMP-responsive element-binding protein 3-like protein 1
CREB3L2	Cyclic AMP-responsive element-binding protein 3-like protein 2
CREB3L3	Cyclic AMP-responsive element-binding protein 3-like protein 3
CREB3L4	Cyclic AMP-responsive element-binding protein 3-like protein 4
CREB4	Cyclic AMP-responsive element-binding protein 4
Cyt C	Cytochrome c
D. melanogaster	Drosophila melanogaster
DNA	Deoxyribonucleic acid
DR5	Death receptor 5
ECG	Electrocardiography
eIF2	Eukaryotic initiation factor 2
eIF2α	Alpha subunit of eukaryotic initiation factor 2
ER	Endoplasmic reticulum
ERAD	Endoplasmic reticulum-associated protein degradation
ERp18	Endoplasmic reticulum resident protein 18
ERSE	Endoplasmic reticulum stress response element
ERSE-II	Endoplasmic reticulum stress response element II
et al.	Et alii
GADD34	Growth arrest and DNA damage–inducible 34
GAPDH	Glycerinaldehyd-3-phosphat-Dehydrogenase
GRINA	Glutamate Receptor Ionotropic NMDA-Associated Protein 1

GRP78	Glucose-regulated protein 78 kD
GRP94	Glucose-regulated protein 94 kD
GDP	Guanosine diphosphate
GTP	Guanosine triphosphate
HF	Heart failure
HFmrEF	Heart failure with mid-range ejection fraction
HFpEF	Heart failure with preserved ejection fraction
HFrEF	Heart failure with reduced ejection fraction
HFsnEF	Heart failure with supra-normal ejection fraction
Hspa5	Heat Shock Protein Family A (Hsp70) Member 5
Hsp90b1	Heat Shock Protein 90 Beta Family Member 1
HSR	Heat shock response
IL1β	Interleukin 1 beta
IP3R	Inositol-1,4,5-trisphosphate receptor
IRE1	Inositol requiring protein 1
IRE1α	Inositol requiring protein 1 alpha
IRE1β	Inositol requiring protein 1 beta
ISO	Isoproterenol
JNK	c-Jun N-terminal kinase
MANF	Mesencephalic astrocyte-derived neurotrophic factor
Met-tRNA	Methionyl-transfer ribonucleic acid
miRNA	Micro-ribonucleic acid
mm	Millimeter
MOMP	Mitochondrial outer membrane permeabilization
MRI	Magnetic resonance imaging
mRNA	Messenger ribonucleic acid

NCK	Non-catalytic region of tyrosine kinase adaptor protein 1
NF-κB	Nuclear factor kappa-light-chain-enhancer of activated B cells
NLRP3	NOD-, LRR- and pyrin domain-containing protein 3
NOXA	Latin for damage (also known as PMAIP1)
NYHA	New York Heart Association
OASIS	Old astrocyte specifically induced substance
P	Phosphoryl group / phosphorylated
p53	Cellular tumor antigen p53
PCR	Polymerase chain reaction
PDIA5	Protein disulfide-isomerase A5
PDIA6	Protein disulfide-isomerase A6
PE	Phenylephrin
PERK	Protein kinase RNA-like ER kinase
pH	Power of hydrogen
PMAIP1	Phorbol-12-myristate-13-acetate-induced protein 1
PP1	Protein phosphatase 1
Proteostasis	Protein homeostasis
PTP	Mitochondrial permeability transition pore
PUMA	p53 upregulated modulator of apoptosis
RIDD	Regulated IRE1-dependent decay
RNA	Ribonucleic acid
RNase	Ribonuclease
ROS	Reactive oxygen species
RtcB	RNA 2',3'-Cyclic Phosphate And 5'-OH Ligase
S. cerevisiae	Saccharomyces cerevisiae
SR	Sarcoplasmic reticulum

SRP	Signal recognition particle
Syvn1	Synoviolin 1
Thbs4	Thrombospondin 4
TM	Tunicamycin
TRAF	Tumor necrosis factor receptor associated factor
TRAF	Tumor necrosis factor receptor associated factor 2
T-tubules	Transverse tubules
TXNDC12	Thioredoxin domain-containing protein 12
TXNIP	Thioredoxin Interacting Protein
tRNA	Transfer ribonucleic acid
uORF	Upstream open reading frame
UPR	Unfolded protein response
UPRE	Unfolded protein response element
UPRmt	Mitochondrial Unfolded Protein Response
Veh	Vehicle
WBP1	WW domain-binding protein 1
XBP1	X box-binding protein 1
XBP1s	Spliced XBP1

List of Figures

List of Tables

1 Introduction

This dissertation is based on the research article ‘Age-related decline of the unfolded protein response in the heart promotes protein misfolding and cardiac pathology’ (Hofmann et al. 2021) and the review article ‘Protein Misfolding in Cardiac Disease’ (Hofmann et al. 2019). The first publication examines the mammalian unfolded protein response during postnatal cardiac aging and the consequence of an age-associated decline of its ATF6 branch for hypertrophic growth, cardiac function, and protein misfolding in response to neurohumoral stimulation or pressure overload. The second publication summarizes the regulation of protein homeostasis and the implications of protein misfolding in cardiac disease with a specific emphasis on the transition towards clinical practice. Sections of this dissertation, especially the description of the methods and the figures, are based on and replicated from the preprint article ‘Age-related decline of the unfolded protein response in the heart promotes protein misfolding and cardiac pathology’ (Hofmann et al. 2021). This introduction aims to give an overview of the research areas relevant for this study and tries to illustrate and summarize previous work this study is based on. Chapter 1.1 outlines general aspects of heart failure and cardiac remodeling, which is essential for the understanding of the pathophysiology that is examined in this study. Cardiac hypertrophy, which is one specific aspect of cardiac remodeling, is then introduced in more detail in Chapter 1.2. This is followed by a detailed description of proteostasis and its role in cardiac health and disease in Chapter 1.3. Chapter 1.4 summarizes the unfolded protein response of the endoplasmic reticulum and how it determines cell fate in response to proteotoxic stress; how this becomes affected during cardiac aging is then described in Chapter 1.5. The rationale of this study is outlined in Chapter 1.6 and is followed by a discussion of limitations in Chapter 1.7 that have to be considered for translational intentions.

1.1 Heart Failure

Heart failure, which is the final common endpoint of many different forms of heart disease, is a rapidly growing public health issue that affects approximately 40 million individuals worldwide (Ziaeian and Fonarow 2016). According to current guidelines, heart failure is defined as a clinical syndrome that is associated with typical symptoms and signs such as fatigue, dyspnea, or peripheral and pulmonary edema that are caused by structural or functional cardiac abnormalities (Ponikowski et al. 2016; Yancy et al. 2017). Diagnosis is therefore currently primarily based on symptoms, physical findings and echocardiography. Heart failure is a progressive syndrome in which cardiac function further declines overtime, worsening the signs of heart failure and eventually resulting in death (Ponikowski et al. 2016; Yancy et al. 2017). Even though the treatment for heart failure has improved over the recent years, it remains a severe condition with a poor prognosis. Novel therapies are therefore urgently needed. Especially those that target the underlying causes of heart failure may improve clinical outcomes yet further. Understanding the detailed mechanisms of the pathophysiology of heart failure is therefore essential to identify novel therapeutic targets for the treatment of heart failure.

1.1.1 Epidemiology of Heart Failure

The global incidence of heart failure is estimated to range from 100 to 900 cases per 100,000 person years, which largely depends on the diagnostic criteria used and the population studied (Ziaeian and Fonarow 2016). The estimated prevalence of heart failure in developed countries ranges from 1% to 2% of the adult population and has increased drastically in terms of absolute numbers (Cowie et al. 1997; Ziaeian and Fonarow 2016). This increase in heart failure burden can be largely explained as a

secondary effect of global population aging and general population growth (Roth et al. 2015). In contrast to the increase in absolute numbers, the standardized age-adjusted rates of heart failure are decreasing in developed countries, especially in women. This reduction is thought to be driven by a better primary prevention of cardiovascular disease and an improved treatment of ischemic heart disease (Brouwers et al. 2013; Levy et al. 2002; Zhao et al. 2015; Ziaeian and Fonarow 2016).

Despite some progress in the care of patients with heart failure, it remains a serious disease that is extremely difficult to treat. While the symptoms and signs of heart failure may resolve, especially under sufficient medical treatment, cardiac function can remain compromised, leaving the patient at risk for further decompensation (Ponikowski et al. 2016). Even though the mortality of heart failure decreased significantly over the last years, the 1-year mortality for patients first hospitalized with heart failure still remains at approximately 20% and the 5-year mortality at about 50%, highlighting the critical need of novel therapies for the treatment of heart failure (Figure 1) (Gerber et al. 2015; Ohlmeier et al. 2015; Zarrinkoub et al. 2013; Ziaeian and Fonarow 2016).

Figure 1 | Prevalence and Mortality of Heart Failure.

(A) Proportion of the population living with heart failure in individual countries across the globe. Estimates based on a single center or hospital are indicated by an H. (B) Death rates for patients hospitalized with heart failure across the globe. Each symbol represents data from a published study. Vertical shaded areas show the range in reported death rates within each time frame. Horizontal shaded areas show regions. The data categorized as ‘Europe’ is from the EuroHeart Failure Survey (24 countries), the EuroHeart Failure Survey II (30 countries) and the ESC-HF pilot survey (12 countries). The data are not age adjusted. Figures and figure legends of (A) and (B) were taken and adapted with permission from ‘Heart failure: preventing disease and death worldwide’ (Ponikowski et al. 2014).

Figure 1 | Prevalence and Mortality of Heart Failure.

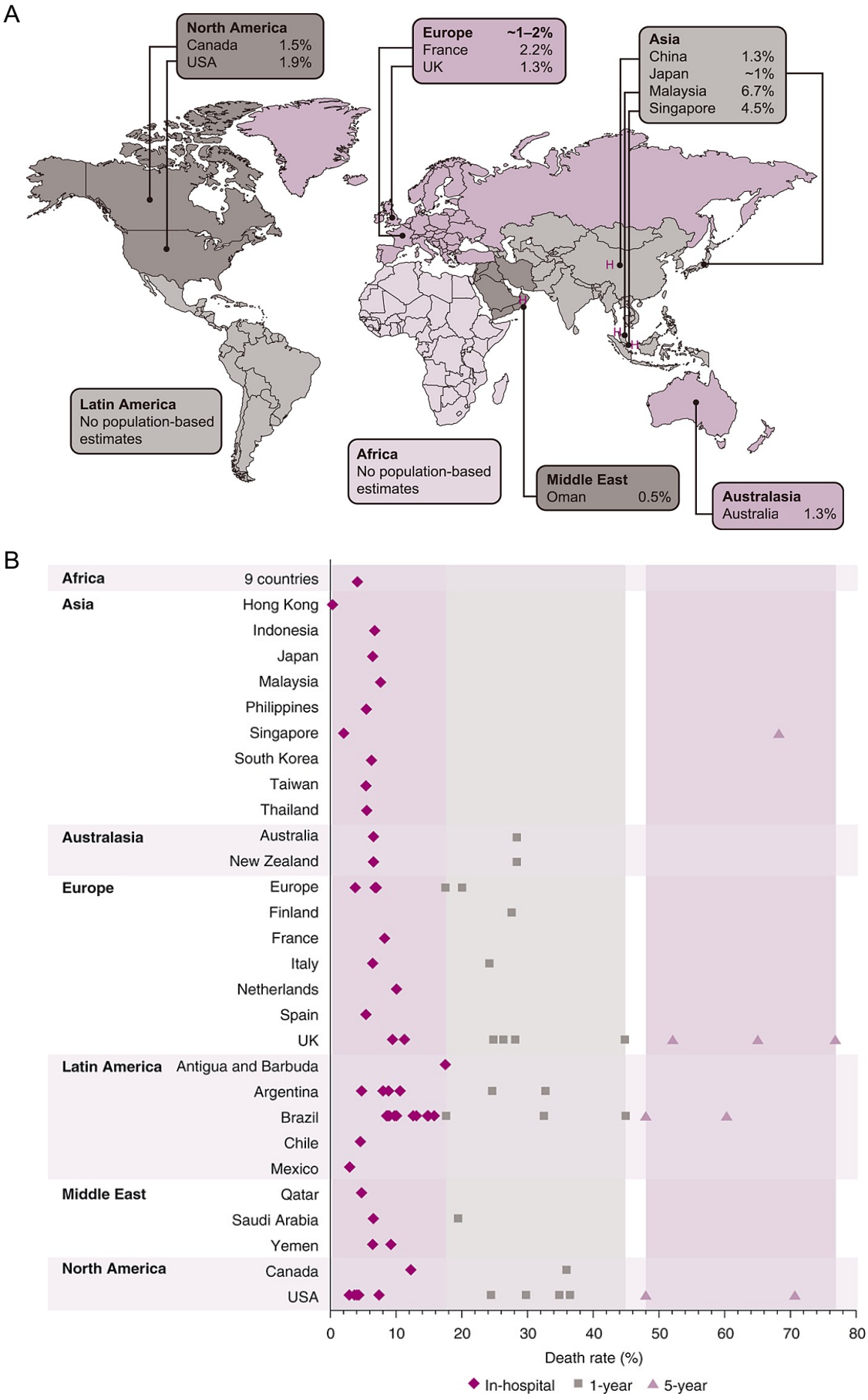

1.1.2 Classification of Heart Failure

To objectively assess the severity of heart failure, several classification systems have been developed (Albakri 2018). The two most widely used classification systems are the 'American College of Cardiology Foundation (ACCF) / American Heart Association (AHA) stages of heart failure' (Hunt et al. 2009) and the 'New York Heart Association (NYHA) functional classification of heart failure' (The Criteria Committee of the New York Heart Association. Boston 1994). The ACCF/AHA classifies heart failure into four stages according to the presence of structural heart disease and the severity of heart failure symptoms, whereas the NYHA functional classification of heart failure divides heart failure based on the occurrence of symptoms and the remaining exercise capacity (Table 1) (Albakri 2018; Hunt et al. 2009; The Criteria Committee of the New York Heart Association. Boston 1994). In addition to the classification of heart failure by symptomatic severity, current guidelines further divide heart failure based on the left ventricular ejection fraction. Previously, heart failure was classified into the two main phenotypes: heart failure with reduced ejection fraction (HFrEF), with a left ventricular ejection fraction of <40%, and heart failure with preserved ejection fraction (HFpEF), with a left ventricular ejection fraction of ≥ 50%. Recently, the shared heart failure guidelines from the American College of Cardiology, the American Heart Association, and the Heart Failure Society of America, which was published in 2017, adopt the 2013 introduced term of heart failure with borderline ejection fraction for patients with heart failure and a left ventricular ejection fraction of 40% to 49% (Hsu et al. 2017; Yancy et al. 2017). Similarly, the most recent guidelines of the European Society of Cardiology define heart failure with an ejection fraction of 40% to 49% as mid-range ejection fraction (HFmrEF) (Hsu et al. 2017; Ponikowski et al. 2016). Therefore, heart failure is currently classified into the three main categories HFrEF, HFmEF, and HFpEF, even though recent studies indicate that this system may require

Table 1 | ACCF/AHA Stages of Heart Failure and the NYHA Functional Classifications.

ACCF/AHA Stages of HF		NYHA Functional Classification	
A	At high risk for HF but without structural heart disease or symptoms of HF	None	
B	Structural heart disease but without signs or symptoms of HF	I	No limitation of physical activity. Ordinary physical activity does not cause symptoms of HF.
C	Structural heart disease with prior or current symptoms of HF	I	No limitation of physical activity. Ordinary physical activity does not cause symptoms of HF.
		II	Slight limitation of physical activity. Comfortable at rest, but ordinary physical activity results in symptoms of HF.
		III	Marked limitation of physical activity. Comfortable at rest, but less than ordinary activity causes symptoms of HF.
		IV	Unable to carry on any physical activity without symptoms of HF, or symptoms of HF at rest.
D	Refractory HF requiring specialized interventions	IV	Unable to carry on any physical activity without symptoms of HF, or symptoms of HF at rest.

ACCF indicates American College of Cardiology Foundation; AHA, American Heart Association; HF, heart failure; and NYHA, New York Heart Association.

Table 1 adapted with permission from '2013 ACCF/AHA Guideline for the Management of Heart Failure - A Report of the American College of Cardiology Foundation/American Heart Association Task Force on Practice Guideline' (Yancy et al. 2013).

modifications such as the inclusion of a heart failure type for supra-normal ejection fraction (HFsnEF) (Cleland et al. 2020; Wehner et al. 2019). Heart failure can also occur due to failure of the right ventricle, which is then called right-sided heart failure (Konstam Marvin et al. 2018). The three main heart failure categories comprise distinct subpopulations of heart failure and are thought to be associated with different risk factors and pathomechanisms. While it is clear that they have to be treated differently, the optimal treatment strategies are currently unclear and limited, especially for HFpEF and HFmEF (Hsu et al. 2017; Ponikowski et al. 2016; Yancy et al. 2017).

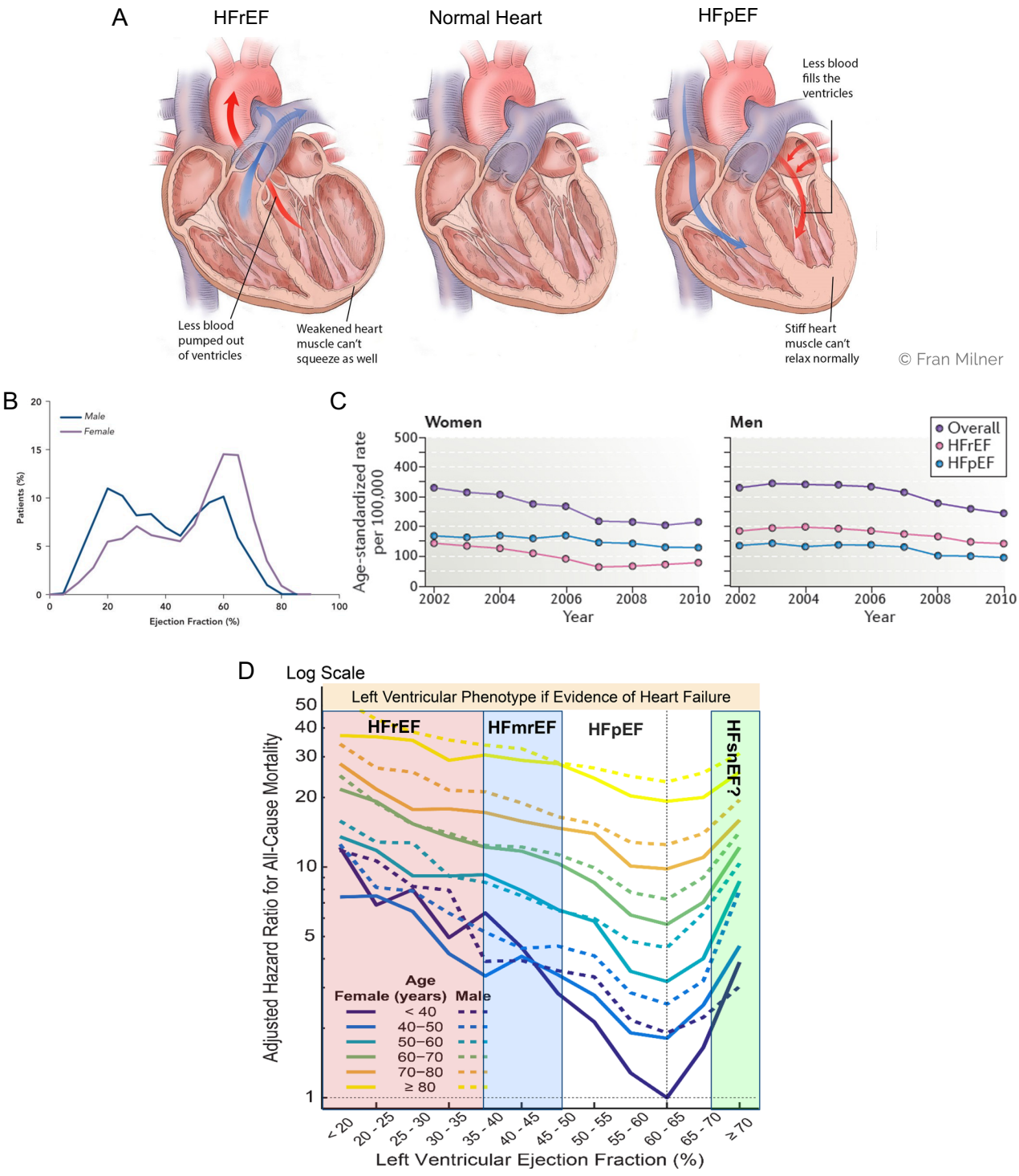

Figure 2 | Comparison of Ejection Fraction based Types of Heart Failure.

(A) The two best described ejection fraction-based types of heart failure are currently HFrEF and HFpEF. HFrEF is characterized by a weakened heart muscle that largely impairs systolic contractility, whereas HFpEF is associated with aggravated myocardial relaxation that impairs diastolic function. Figure 2A reproduced with permission from Fran Milner, Medical Illustration and Design. Copyright Fran Milner. (B) Distribution of left ventricular ejection fraction in heart failure patients. Figure taken with permission from 'Global Public Health Burden of Heart

Failure' (Savarese and Lund 2017). (C) Incidence of HFrEF and HFpEF for women and men. Figure taken with permission from 'Epidemiology and aetiology of heart failure' (Ziaeian and Fonarow 2016). (D) All-cause mortality according to left ventricular ejection fraction stratified by age and sex. Figure and figure legend was adapted from 'The year in cardiology: heart failure: The year in cardiology 2019' (Cleland et al. 2020).

1.1.3 Etiology of Heart Failure

Due to differences in disease definitions, the incidence and prevalence of the heart failure subgroups varies in different epidemiological studies, however both HFrEF and HFpEF are thought to comprise approximately half of all heart failure cases (Figure 2) (Ziaeian and Fonarow 2016). While HFrEF is sometimes also referred to as systolic heart failure, it should be noted that most patients with HFrEF also experience diastolic dysfunction (Ponikowski et al. 2016). Similarly, some patients with HFpEF, which is sometimes referred to as diastolic heart failure, present with changes in systolic function (Ponikowski et al. 2016). Importantly, the etiology of heart failure is diverse and complex and many patients present with several different risk factors and pathologies that may have contributed to the occurrence of heart failure (Ponikowski et al. 2016). Among the most relevant etiologies of heart failure are ischemic heart disease, hypertension or other abnormal loading conditions, arrythmias, and genetic diseases (Ponikowski et al. 2016). It has been suggested that the etiology of heart failure has shifted over time in the developed countries, a phenomenon that is also evolving in less-developed countries (Balmforth et al. 2019). While heart failure was not classified by ejection fraction in the initial reports from the 1949 initiated Framingham Heart Study, hypertension was described to be the most prevalent etiology for heart failure at that time (McKee et al. 1971). More recent studies however reported that for HFrEF, coronary heart disease has become the predominant cause for disease development (Balmforth et al. 2019). In contrast to HFrEF, the greatest risk

factor for HFpEF remains hypertension (Yancy et al. 2017; Ziaeian and Fonarow 2016). In addition, female sex, age, diabetes and more rare etiologies such as hypertrophic cardiomyopathies or cardiac amyloidosis were reported to be associated with HFpEF (Ziaeian and Fonarow 2016). However, it remains mostly unknown which etiologies ultimately lead to HFrEF or HFpEF, since most risk factors can be found in both HFrEF and HFpEF patients. For example, in a more recent cohort, 73.6% of HFrEF patients and 89.3% of HFpEF patients had hypertension (Gerber et al. 2015), which makes it difficult to define specific causes for HFrEF and HFpEF.

1.1.4 Ventricular Remodeling in Heart Failure

The clinical progress of both HFrEF and HFpEF is accompanied by a continuous development of cardiac remodeling; a plasticity response that results in molecular, cellular, and interstitial changes within the heart (Cohn et al. 2000). This process is a culmination of a complex series of cellular events that ultimately impair cardiac function and contribute to cardiac dysfunction and heart failure. Clinically, cardiac remodeling manifests as a consequence to increased cardiac workload and neurohormonal stimulation such as in response to myocardial injury, ventricular wall stress, or manifested congenital heart disease. Among many other events, cardiac remodeling involves cardiomyocyte death, cardiac hypertrophy, fibrosis, metabolic adaption, vascular remodeling, inflammation, and electrophysiological changes (Burchfield et al. 2013). This intrinsic cardiac response to a variety of pathological insults is thought to initially adapt the heart to myocardial stress. However, if those remodeling events continue, they become maladaptive and significantly contribute to cardiovascular morbidity and mortality (Burchfield et al. 2013). Only recently it has become evident that the heart holds the capacity to reverse its maladaptive remodeled phenotype,

which is described as reverse cardiac remodeling (Kim et al. 2018). Understanding and targeting the complex mechanisms of remodeling is therefore an ongoing major goal of current cardiac research with the aim to specifically target maladaptive features of cardiac remodeling. This may reverse the pathological phenotype and may have the potential to improve the outcome of heart failure patients yet further (Cohn et al. 2000).

1.2 Cardiac Hypertrophy

One key element of cardiac remodeling that can occur in all forms of heart failure is cardiac hypertrophy (Figure 3) (Nakamura and Sadoshima 2018). According to Laplace's law, ventricular wall stress is proportional to ventricular pressure and radius, but indirectly proportional to ventricular wall thickness. Therefore, the hypertrophic cardiac growth response was seen as a compensatory mechanism to reduce wall stress in response to pressure or volume overload (Grossman et al. 1975; Hood et al. 1968; Meerson 1961). However, more recent studies are beginning to question the concept that cardiac hypertrophy in response to pathological stress is adaptive and protective, highlighting the concept of the inhibition of pathological cardiac hypertrophy to improve outcomes in heart disease (Hill and Olson 2008; Schiattarella and Hill 2015; Schiattarella et al. 2017).

1.2.1 Diagnosis of Cardiac Hypertrophy

Cardiac hypertrophy is commonly diagnosed by echocardiography when interventricular septum or left ventricular wall thickness is ≥12mm (Katholi and Couri 2011; Kawel et al. 2012; Levy et al. 1987), right ventricular wall thickness is ≥6mm in adults (Ho and Nihoyannopoulos 2006), or when the ventricular mass index and the relative wall thickness, which can be normalized by body surface area, height, or fat-

free mass, exceeds certain cutoff values (Lang et al. 2015). Cardiac hypertrophy can also be diagnosed by other methods such as magnetic resonance imaging (MRI) or electrocardiography (ECG), with MRI being the most accurate and ECG, with a reported sensitivity below 25%, the least accurate method for the diagnosis of anatomic cardiac hypertrophy (Aro and Chugh 2016; Bottini et al. 1995; Grothues et al. 2002). Of note, recent accumulating evidence suggests that anatomic ventricular hypertrophy and ECG diagnosed ventricular hypertrophy may be clinically distinct entities with different pathophysiological and prognostic manifestations, which should be kept in mind when using the term cardiac hypertrophy (Aro and Chugh 2016).

1.2.2 Types of Cardiac Hypertrophy

Based on ventricular wall thickness and relative ventricular internal diameter, anatomic cardiac hypertrophy is classified into the three groups: concentric remodeling, eccentric hypertrophy, and concentric hypertrophy (Artham et al. 2009; Lang et al. 2015). Concentric remodeling is defined as increased relative wall thickness with normal ventricular mass index (Artham et al. 2009; Lang et al. 2015). In contrast, both eccentric hypertrophy and concentric hypertrophy are defined by increased ventricular mass index, with normal relative wall thickness in the case of eccentric hypertrophy and increased relative wall thickness for concentric hypertrophy (Artham et al. 2009; Lang et al. 2015). Even though all three forms can be found in HFrEF and HFpEF, left ventricular hypertrophy is often eccentric in HFrEF and mostly concentric in HFpEF (Heinzel et al. 2015). Related to this observation is the finding that patients with eccentric hypertrophy are more likely to develop HFrEF, whereas those with concentric hypertrophy are at higher risk for developing HFpEF (Velagaleti et al. 2014).

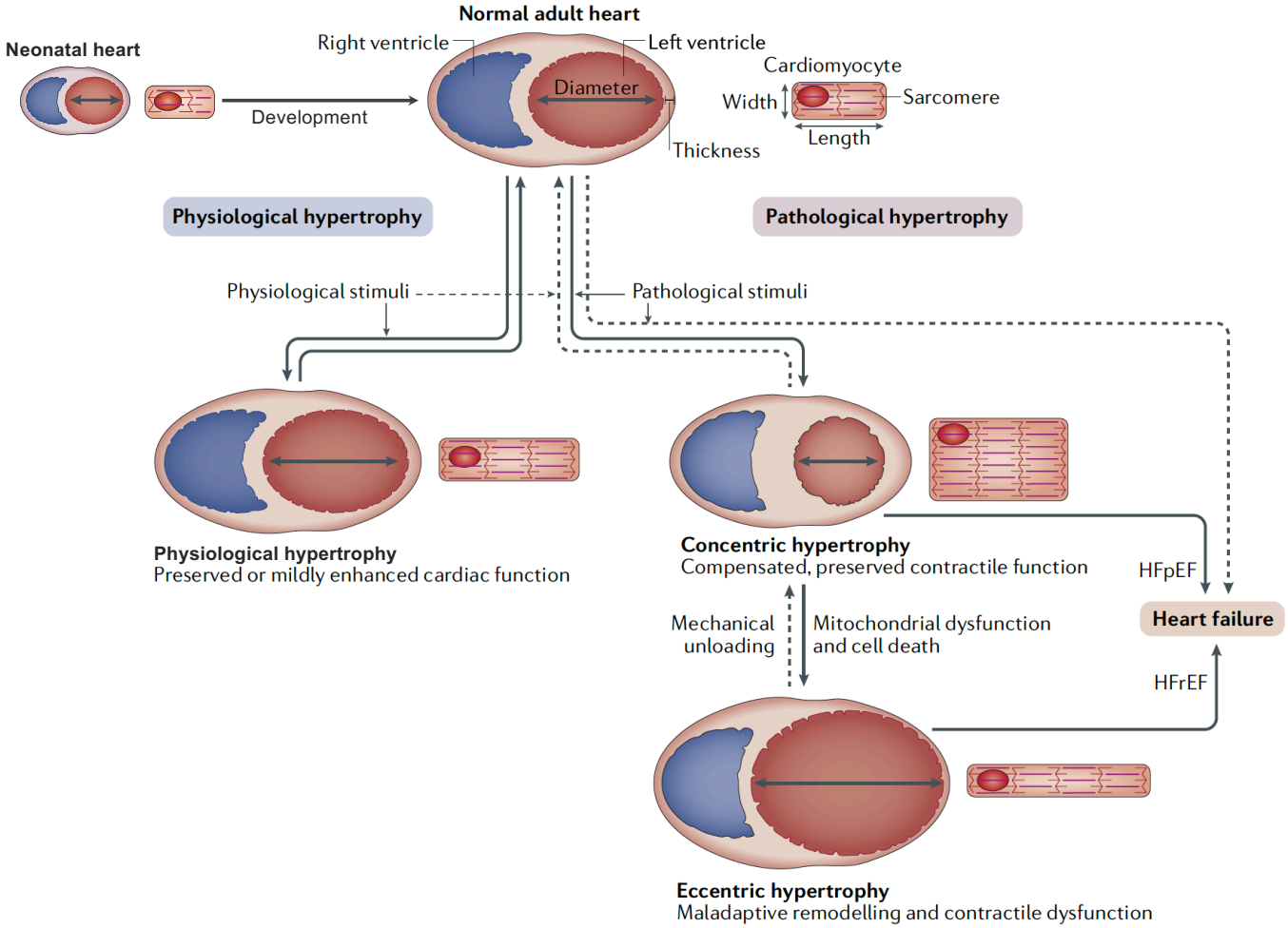

Figure 3 | Overview of Cardiac Hypertrophy.

Cardiac hypertrophy occurs during normal postnatal development when the heart increases in size. The adult heart can further undergo hypertrophic growth in response to physiological or pathological stimuli. Physiological cardiac hypertrophy is characterized by preserved or mildly enhanced cardiac function and normal architecture and organization of the heart. In contrast, pathological hypertrophy is characterized by impaired cardiac function and disturbed ventricular dimensions, leading to concentric or eccentric hypertrophy. Although not fully understood, concentric hypertrophy is more often associated with HFpEF, whereas patients with eccentric hypertrophy are at increased risk for developing HFrEF. Adapted with permission from 'Molecular basis of physiological heart growth: fundamental concepts and new players' (Maillet et al. 2013) and 'Mechanisms of physiological and pathological cardiac hypertrophy' (Nakamura and Sadoshima 2018). Dashed arrows represent hypothetical or controversial pathways, solid arrows represent proven pathways.

1.2.3 Physiological and Pathological Hypertrophy

Adult cardiac hypertrophy, especially left ventricular hypertrophy, can occur in response to pathological stress such as chronic pressure or volume overload but also in response to physiological stress such as endurance training or pregnancy (Hill and Olson 2008; Nakamura and Sadoshima 2018). Other entities associated with the development of cardiac hypertrophy despite chronic pressure or volume overload include, among many others, age, race, obesity, diabetes, hypercholesterolemia, high job strain, or prior myocardial infarction (Artham et al. 2009). Interestingly, more recent evidence suggests that it is primarily the type of stress and not its duration that defines the clinical presentation and phenotype of cardiac hypertrophy, even though the duration of the stress correlates with the degree of hypertrophic growth (Perrino et al. 2006). While cardiac growth can be facilitated by cardiomyocyte proliferation in the neonatal heart, soon after birth this capacity for proliferation of cardiomyocytes is largely lost (Mohammadi et al. 2019). In the postnatal heart both physiological and pathological cardiac hypertrophy is mediated by cellular enlargement of individual cardiomyocytes. However, the hypertrophic characteristics are distinct between both forms (Figure 3). In physiological cardiac hypertrophy, cardiomyocytes increase both in length and width (Nakamura and Sadoshima 2018) and the increase in cardiac mass is mostly mild, with left ventricular wall thickness normally not exceeding 15mm (Li et al. 1996) and a total cardiac mass increase of approximately 10-20% (Nakamura and Sadoshima 2018). Physiological cardiac hypertrophy is fully reversible; it is characterized by normal heart function and does not progress to heart failure (Nakamura and Sadoshima 2018). In addition, cardiac contractile function remains preserved; no overt cardiac fibrosis or cardiomyocyte cell death can be observed, and expression of the cardiac fetal gene program, which becomes induced in a variety of pathologic myocardial conditions, remains unchanged (Nakamura and Sadoshima

2018). It should be noted, that even though left ventricular function remains preserved and increased ventricular wall thickness is fully reversible in physiological hypertrophy, some reports indicate that the resolution of cavity enlargement is incomplete in most cases and substantial chamber dilatation persists even after 5 years in over 20% in deconditioned athletes (Dorn 2007; Pelliccia et al. 2002). In contrast to physiological cardiac hypertrophy, pathological hypertrophy is associated with impaired cardiac function, fibrosis, inflammation, metabolic, electrical, and vascular remodeling that ultimately results in cardiomyocyte cell death and heart failure (Schiattarella and Hill 2015).

1.2.4 Clinical Implications of Cardiac Hypertrophy

Defining the prevalence of cardiac hypertrophy is challenging and inconsistent due to different definitions and diagnostic methods. Epidemiological reports indicate that anatomical left ventricular hypertrophy is prevalent in approximately 2-20% in a general western population, which further increases with age and may reach a prevalence of approximately 20-70% in hypertensive patients (Cuspidi et al. 2012; Drazner et al. 2005; Levy et al. 1987; Schirmer et al. 1999). Independent from the diagnostic method selected, both anatomic and ECG diagnosed cardiac hypertrophy are well established major risk factors and predictors of cardiovascular events and mortality (Artham et al. 2009; Kannel et al. 1970; Koren et al. 1991; Levy et al. 1990; Velagaleti et al. 2014) with anatomic and ECG diagnosed cardiac hypertrophy carrying somewhat different and independent prognostic information (Aro and Chugh 2016). Importantly, left ventricular hypertrophy is consistently reported to be a more powerful risk factor than other conventional cardiovascular risk factors for morbidity and mortality (Artham et al. 2009; Schiattarella and Hill 2015). The presence of anatomical left ventricular

hypertrophy increases the risk of death independent of age, sex, and the occurrence of other risk factors, with eccentric cardiac hypertrophy having a worse risk profile than concentric hypertrophy (Artham et al. 2009; Bang et al. 2017; Koren et al. 1991). Similarly, ECG diagnosed left ventricular cardiac hypertrophy is associated with an increase in mortality (Havranek et al. 2008; Kannel et al. 1970; Levy et al. 1990). Since cardiac hypertrophy is associated with poor cardiovascular outcome and increased risk of death, cardiac hypertrophy has been proposed as a therapeutic target for different cardiovascular disease (Schiattarella and Hill 2015). Indeed, preclinical studies indicate that the inhibition of left ventricular hypertrophy is associated with increased cardiac function and improved outcomes (Artham et al. 2009; Schiattarella and Hill 2015; Schiattarella et al. 2017). It is important to highlight that those observations remain correlative, and it is necessary to clearly demonstrate that inhibition of cardiac hypertrophy can directly increase cardiovascular outcome and survival in patients (Schiattarella and Hill 2015). Until now it also remains unclear if the heart can fully reverse its pathological hypertrophic phenotype. While some studies showed that ventricular unloading of the failing heart can decrease cardiac mass, it remains unknown if a heart that previously underwent significant remodeling can sufficiently reverse its phenotype, since the decrease of cardiac hypertrophy is not predictive for improved cardiac function when ventricular unloading is stopped (Dandel et al. 2014). To exploit the full potential of targeting cardiac hypertrophy, therapeutic interventions might therefore be preferably initiated in the early phase of hypertrophy when the heart is not failing.

1.3 Cardiac Proteostasis

In order to grow in size, the heart requires increased protein synthesis, which is driven primarily by increased rates of translation during cardiac hypertrophy (Heineke and Molkentin 2006; Nakamura and Sadoshima 2018). During protein synthesis, mRNA is decoded by ribosomes to create a polypeptide chain, that later folds with assistance by chaperones into its functional three-dimensional structure. The ribosome mediates the decoding of the mRNA by facilitating the stepwise binding of tRNAs to complementary mRNA codons. These amino acids are then chained together to create the polypeptide that later folds into the functional protein. Eukaryotic cells contain two primary populations of ribosomes; one cytosolic fraction that is generally thought to mediate translation of mRNAs encoding cytosolic proteins, and endoplasmic reticulum-bound ribosomes that translate mRNAs encoding secretory and membrane proteins or those that reside in the ER, Golgi apparatus or lysosomes (Palade 1975). Besides these two populations, mitochondria contain their own distinct subset of ribosomes, which do not play a major role in global protein synthesis of eukaryotes (Greber and Ban 2016).

In preclinical models, signaling pathways that regulate protein synthesis are activated within minutes after a stress stimulus. Increased protein synthesis along with an enlarged heart mass may be detected within a brief timeframe beginning with several hours and up to one or two days (Doroudgar et al. 2019; Ravi et al. 2018; Wang et al. 2017). Increases in protein folding demand by a growth-dependent induction of protein synthesis puts a strain on the cardiac protein quality control network. Sufficient handling of protein synthesis, however, is critical for cellular protein homeostasis (proteostasis) (Blackwood et al. 2020). Increases in protein synthesis without an equivalent induction of the cellular protein folding and quality control environment, such

as it might occur during pathological cardiac hypertrophy, can promote protein misfolding (Blackwood et al. 2020). Since misfolded proteins can be toxic, protein synthesis, folding, and degradation must be highly coordinated to maintain cardiomyocyte viability during growth. If protein handling is insufficient, protein misfolding and accumulation may occur. This might impair cellular function, lead to cell death and may ultimately result in the progression of heart disease (Blackwood et al. 2020; McLendon and Robbins 2015).

1.3.1 The Proteostasis Network

Creating a functional protein is a difficult cellular task and mistakes can occur especially during the complex folding of the polypeptide chain that is necessary to establish the correct three-dimensional structure of the protein (Balch et al. 2008; Gruebele et al. 2016; Sala et al. 2017). Even though the final conformation of a protein is determined by its amino acid sequence, chaperones and other folding catalysts such as protein disulfide isomerases are needed to assist the folding to the proteins final state. Chaperones generally support folding in an ATP-dependent manner or by binding folding-intermediates, thereby preventing newly synthesized polypeptide chains and assembled protein subunits from aggregation into nonfunctional or toxic structures during the folding process (Sala et al. 2017). Proteotoxic stress that can be caused by environmental fluctuations can rapidly effect the integrity of the proteome and induce protein misfolding (Sala et al. 2017).

The integrity of the proteome is mediated by the proteostasis network (Sala et al. 2017). The cellular proteostasis network consist of interconnected systems that regulate proteins synthesis, folding, transport, and degradation (Figure 4) (Hofmann et al. 2019; Sala et al. 2017).

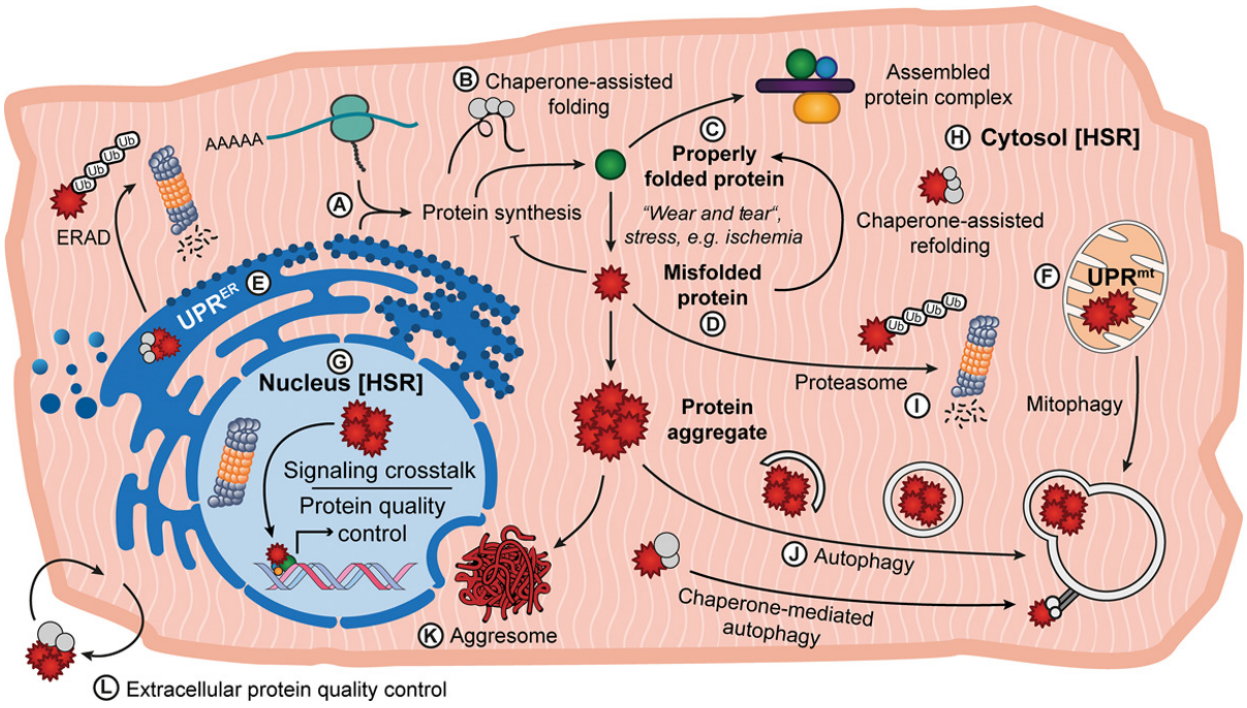

Figure 4 | Proteostasis Checkpoints in Cardiomyocytes.

Proteostasis is maintained by a series of protective mechanisms in various subcellular compartments that can be overwhelmed in the diseased heart. In physiological conditions, protein synthesis at the endoplasmic reticulum (ER), or on free ribosomes (A), is aided by chaperones (B), is tightly regulated, and results in the production of properly folded, functional proteins (C). Conditions of stress, or wear and tear, result in protein misfolding (D). Cells have evolved the ER unfolded protein response (UPR), which includes ER-associated protein degradation (ERAD; E), as well as mitochondrial UPR (UPRmt; F), and nuclear (G) and several cytoplasmic stress response pathways, including the cytoplasmic heat shock response (HSR; H), the ubiquitin-proteasome system (I), and autophagy (J), aimed at preventing and resolving protein damage, misfolding, and aggregation. Aggregation of misfolded proteins in aggresomes (K) happens when protein misfolding is not resolved. In addition to intracellular protein misfolding, extracellular protein aggregates contribute to impaired cardiac function and are cleared by chaperones and proteases (L). Figure and figure legend was taken with permission from 'Protein Misfolding in Cardiac Disease' (Hofmann et al. 2019).

All cellular sub-compartments, such as the cytoplasm, nucleus, endoplasmic reticulum, or mitochondria, possess common, as well as specific proteostasis elements that are dedicated to the respective microenvironments (Sala et al. 2017). While the proteostasis network is mostly sufficient to buffer transient or mild disturbances of

proteome integrity, it can become insufficient during prolonged proteotoxic stress. To counteract the accumulation of misfolded proteins, the levels of individual components of the proteostasis network can be rapidly adjusted upon changes in protein folding load (Sala et al. 2017). For this, multiple pathways continuously monitor the cellular proteostasis environment and upregulate protein quality control elements such as chaperones or protein degradation networks during proteotoxic stress. These pathways include the heat shock response, the oxidative stress response, and the unfolded protein response, which control gene expression through the activation of distinct transcription factors (Sala et al. 2017). In addition, this is accompanied by an overall decrease of protein synthesis to reduce protein load to the already overwhelmed compartments. This reduces further misfolding and assists in the preferred translation of stress-specific mRNAs that aid in the restoration of proteostasis (Sala et al. 2017).

1.3.2 Endoplasmic Reticulum-associated Protein Synthesis

In muscle cells, including cardiomyocytes, an interconnected membrane network known as the endoplasmic reticulum (ER) or the sarcoplasmic reticulum (SR) regulates protein handling, calcium homeostasis, lipid synthesis, and cellular metabolism (Doroudgar and Glembotski 2013). As in other cell types, protein synthesis was described to occur on ER-bound ribosomes in muscle cells, which might be of special relevance based on the large proportion of this membrane network that can be found in those cell types. Surprisingly, not much is known about the relative locations, protein synthetic functions, and protein expression profiles of the ER or SR of cardiomyocytes. Even though some studies hypothesized that both systems coexist in cardiomyocytes and execute unique functions (McFarland et al. 2010; Slade and Severs 1985; Sleiman

et al. 2015), systematic investigations that examine the differences of the ER and SR are missing (Doroudgar and Glembotski 2013). While some data suggests that a perinuclear localized tubular network may execute classical ER associated functions such as secretion and protein processing in cardiomyocytes, whereas a more peripheral network that surrounds the myofilaments and interacts with invaginations of the sarcolemma, known as transverse (T)-tubules, may primarily regulate calcium handling for contraction (Figure 5) (Doroudgar and Glembotski 2013), the membrane systems in cardiomyocytes will be collectively called ER from here on, primarily based on the insufficient data to clearly distinguish between an ER and SR network in cardiomyocytes and the extensively studied unfolded protein response of other cell types in which a SR is lacking. The ER is a tubular membrane network that regulates synthesis, folding, and posttranslational processing of approximately one third of all cellular proteins (Hetz and Papa 2018). Proteins that are targeted and processed inside the ER include secreted proteins, membrane proteins, and proteins that reside in the ER itself, the Golgi apparatus, and lysosomes (Hetz and Papa 2018; Nyathi et al. 2013). In the classical model of ER-associated protein synthesis, translation is generally initiated in the cytosol (Nyathi et al. 2013). Here, ER targeted peptides are recognized by the signal recognition particle (SRP), a ribonucleoprotein complex that binds to an hydrophobic signal sequence, in the early phase of translation (Nyathi et al. 2013).

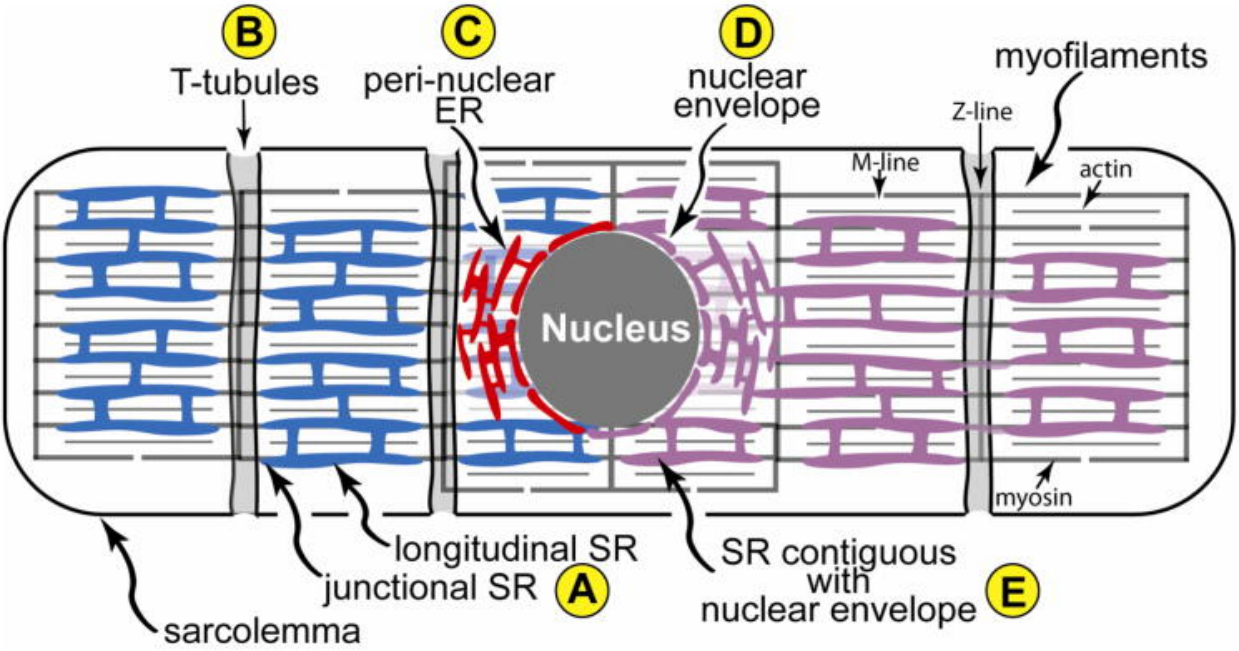

Figure 5 | The Cardiomyocyte Sarco- / Endoplasmic Reticulum Network.

Shown is a diagram of a cardiomyocyte depicting the relationships between the region of the SR near the T-tubule, junctional SR, the longitudinal SR (A), transverse, or T-tubules (B), the peri-nuclear ER (C) and nuclear envelope (D), and a depiction of SR that is contiguous with the nuclear envelope (E) The T-tubules are invaginations of the sarcolemma that reside over the Z-line of the sarcomeres. Also shown are the actin and myosin that comprise major portions of myofilaments, as well as the M- and Z-line regions of the sarcomeres. The nuclear envelope and peri-nuclear ER are contiguous and constitute a location for secreted and membrane protein synthesis, as well as calcium storage and release. The hypothetical localization of secreted and membrane protein synthesis to only the nuclear envelope and peri-nuclear ER, depicted in red, and not to the SR, depicted in blue, is shown on the left of the diagram. The hypothetical localization of secreted and membrane protein synthesis to the nuclear envelope, peri-nuclear ER and the SR, depicted as a contiguous membranous system, shaded purple, is shown on the right of the diagram. Figure and figure legend was taken with permission from 'New Concepts of Endoplasmic Reticulum Function in the Heart: Programmed to Conserve' (Doroudgar and Glembotski 2013).

Upon SRP binding, translation is paused and the SRP shuttles the unfinished peptide to the ER membrane, while still attached to the ribosome. Here, the ribosome binds to the ER translocon, where translation is continued, with the nascent protein forming into the ER lumen or membrane (Nyathi et al. 2013). The signal peptide is then removed

by a protease in the ER lumen, typically before translation of the polypeptide is completed (Hetz and Papa 2018; Nyathi et al. 2013). Recently, it is however becoming evident that this model of ER located translation is incomplete and several mechanisms exist that facilitate similar functions and form a more complex system that regulates translation associated with the ER. To this end, two systems, the SRP-dependent and SRP-independent targeting, were shown to target mRNAs cotranslational to the ER (Aviram et al. 2016). During SRP-independent targeting, the selection of the cotranslational transport system is dependent on the position of the transmembrane domain of the substrate. In addition, several mechanisms of posttranslational translocation of proteins to the ER were recently reported and it is possible that there are other, currently unknown systems, that can facilitate co- or posttranslational substrate delivery to the ER (Johnson et al. 2013). Although not examined in the heart or cardiomyocytes, recent studies in other cell types also suggest that ER- bound ribosomes might be capable of translating mRNAs that encode cytosolic proteins (Kraut-Cohen et al. 2013; Reid and Nicchitta 2012; Zhou et al. 2014). However, this view of general translation on ER-bound ribosomes remains controversial and further investigation is needed to clarify the regulation of ER localized translation (Jan et al. 2014; Jan et al. 2015; Reid and Nicchitta 2015). ER-associated protein synthesis remains complex and several systems maintain the sufficient synthesis and translocation of the selected peptides to the ER, which is followed by an extensive network of posttranslational protein processing inside the ER to ensure correct folding and function of the newly synthesized protein.

1.3.3 Protein Processing in the Endoplasmic Reticulum

The ER holds a specific environment that is needed for proper protein folding and posttranslational modification. For example, a high oxidizing redox potential inside the ER lumen is needed for the formation of disulfide bonds and a high calcium concentration supports the function of calcium-dependent ER resident chaperones. Under these conditions, chaperones, oxidoreductases, and glycosylating enzymes work together to produce correctly folded and functional proteins inside the ER. Since this special and highly controlled environment is crucial for correct ER protein processing, the ER is sensitive to stresses that disturb this environmental homeostasis and thereby eventually interfere with protein folding inside the ER, which is known as 'ER stress' (Walter and Ron 2011). Several environmental challenges, such as hypoxia, glucose starvation, disturbance of calcium storages or toxic insults, can disrupt ER homeostasis by causing an imbalance between the protein folding demand and the capacity of ER-dependent folding (Maurel et al. 2014). However, even under physiological conditions, folding mistakes are frequent, leading to misfolded proteins that need to be refolded or degraded to maintain cellular homeostasis. About one third of newly synthesized proteins are rapidly degraded, likely because of errors in translation and incorrect folding (Schubert et al. 2000). Especially proteins of the secretory pathway were reported to have a low success rate of proper folding, eventually due to their complicated folding, posttranslational modification, and assembling into multi-protein complexes in the ER (Hetz and Papa 2018). Incompletely folded proteins are quickly degraded by the ER-associated protein degradation system (ERAD), a cellular pathway which conducts ubiquitination, retro-translocation into the cytosol, and subsequent proteasome mediated degradation of misfolded ER proteins (Ruggiano et al. 2014). Further, autophagy aids in the clearance of misfolded protein

aggregates and damaged ER membranes, especially under phases of proteotoxic stress (Tannous et al. 2008).

1.3.4 Endoplasmic Reticulum Stress during Cardiac Hypertrophy

The accumulation of misfolded proteins is known to contribute to a variety of diseases, and it has been suggested that protein misfolding may occur during pathological cardiac hypertrophy and may serve as a contributor to the progression towards heart failure (Figure 6) (Blackwood et al. 2020; Willis and Patterson 2013). In other cardiac diseases such as cardiac amyloidosis or desmin-related cardiomyopathy, the excessive accumulation of misfolded proteins is known to directly impair cardiac function and is sufficient to induce heart failure (Pattison et al. 2008; Rubin and Maurer 2020; Sanbe et al. 2004; Wang et al. 2001). However, even though protein misfolding has been observed during cardiac aging and heart failure (Ayyadevara et al. 2016; Mohammed et al. 2014; Rainer et al. 2018; Sanbe et al. 2004; Tannous et al. 2008), it remains unknown if protein misfolding occurs in the early phase of heart disease before the heart is failing and if misfolded proteins in general significantly contribute to disease development and progression (Singh and Robbins 2018). While in some cardiac diseases that show a hypertrophic phenotype, such as desmin-related cardiomyopathy or hypertrophic cardiomyopathy, protein misfolding was observed when the hearts were failing (Sanbe et al. 2004), it is not known if the increased amount of protein synthesis during cardiac hypertrophy directly promotes protein misfolding or if cardiac hypertrophy and protein misfolding are independently present in those diseases. It however has been consistently observed that increasing protein quality pathways, such as the unfolded protein response, protects from heart failure in different preclinical cardiac disease models. At least in some studies, this was shown to be associated

with decreased protein misfolding, which indirectly implies that protein misfolding may indeed contribute to cardiac dysfunction (Bhuiyan et al. 2013; Blackwood et al. 2019a; Lynch et al. 2012; Lyon et al. 2013; Schiattarella et al. 2019; Schlossarek et al. 2014; Wang and Robbins 2006; Yao et al. 2017).

Figure 6 | Protein Misfolding in the Heart.

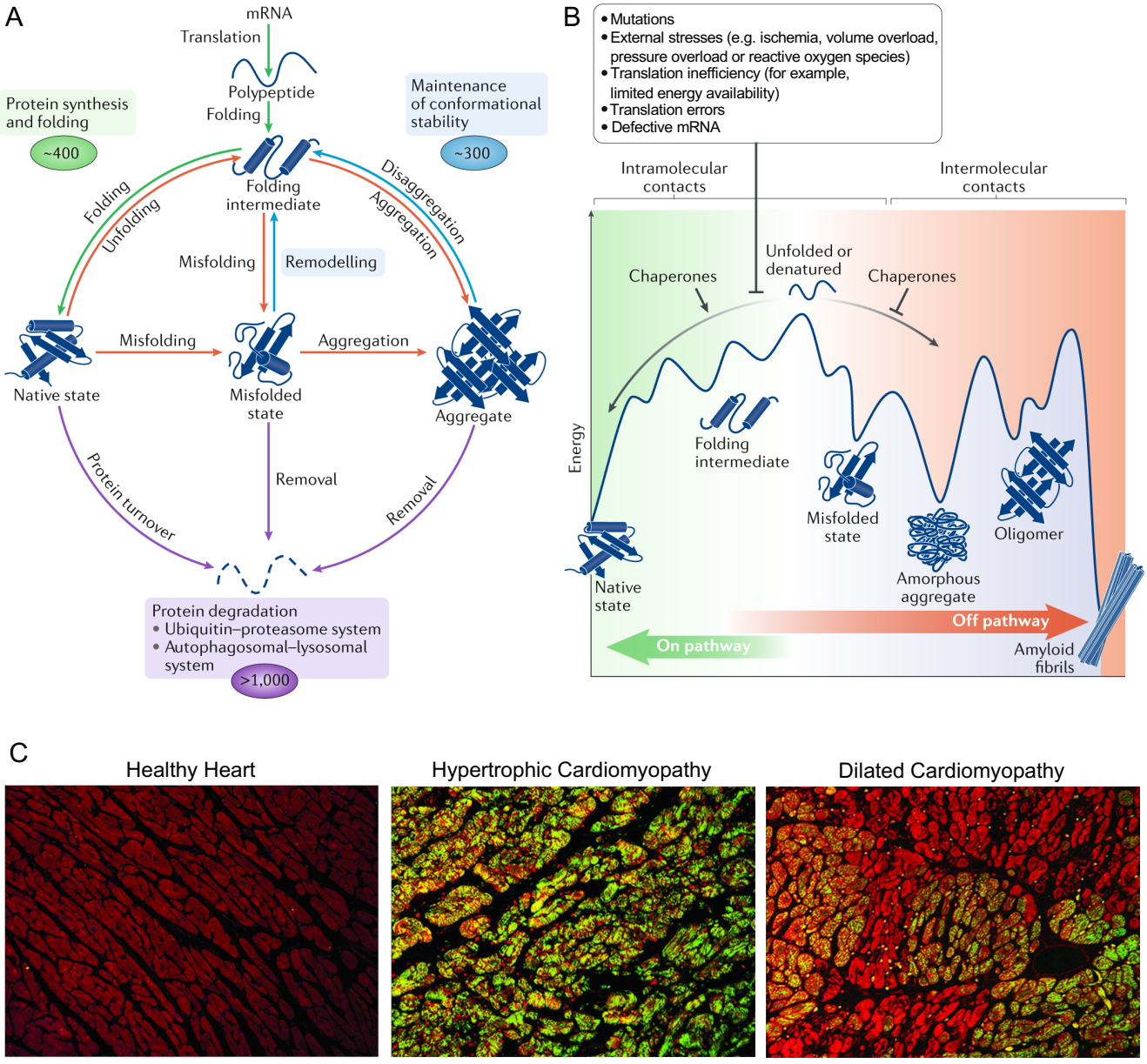

Figure 6 | Protein Misfolding in the Heart.

(A) Diagram of different pathways of protein misfolding, aggregation and degradation. The human proteostasis network comprises approximately 2000 proteins, which control all aspects of protein quality control and thereby minimize non-productive or harmful off-pathway reactions (generation of unfolded proteins or aggregates; red). The elements of the proteostasis network can be operationally assigned to three major arms: protein synthesis and folding (green), conformational maintenance (blue) and degradation (purple). Numbers indicate approximal amounts of proteins that participate in the respective pathways. (B) Proteins acquire different conformations during folding, where they increasingly form native intramolecular contacts while progressing towards the thermodynamically stable, native state, which possesses a minimum of free energy. Folding intermediates and misfolded states may accumulate as kinetically trapped species that need to traverse free-energy barriers to form functional proteins. Intermolecular contacts between non-native states may result in the formation of various aggregate species, including oligomers, amorphous aggregates and amyloid fibrils, the latter of which may even be thermodynamically more stable than the native state. Molecular chaperones enhance on-pathway reactions that support progression of folding intermediates towards the native state and block off-pathway reactions that lead to misfolded and aggregated species. Various factors, such as mutations, stress, translation aberrations or defects in mRNA, inhibit the on-pathway reactions, favoring protein misfolding and aggregation. Figures and figure legends of (A) and (B) were taken and adapted with permission from 'The proteostasis network and its decline in ageing' (Hipp et al. 2019). (C) Amyloid oligomer reactivity in human ventricular samples derived from a healthy heart and from patients with hypertrophic cardiomyopathy and dilated cardiomyopathy, respectively. Reactivity against an anti-oligomer antibody is shown in green, Actin is stained in red. Adapted with permission from 'Desmin-related cardiomyopathy in transgenic mice: A cardiac amyloidosis' (Sanbe et al. 2004). Copyright (2004) National Academy of Sciences.

During growth the ER is one of several synthetic cell compartments that undergoes an increased workload by producing a large subunit of proteins and lipids needed for cellular enlargement (Blackwood et al. 2020). Proteotoxic stress or an excessive protein load to the ER, such as it occurs during cardiac hypertrophy, might cause ER stress (Doroudgar and Glembotski 2013; Okada et al. 2004). In order to reduce ER stress and maintain a functional environment for the increased amount of protein

synthesis, the cell is thought to activate the unfolded protein response pathway (Ozcan et al. 2008), which aids in the maintenance of proteostasis trough the induction of several protein quality control elements (Hetz and Papa 2018; Walter and Ron 2011). Importantly, the unfolded protein response has been shown to become activated during cardiac hypertrophy, where at least some of its elements are adaptive (Blackwood et al. 2019b; Doroudgar et al. 2015; Lynch et al. 2012; Okada et al. 2004; Schiattarella et al. 2019). In several of those studies, an insufficient activation of the unfolded protein response was associated with an altered hypertrophic growth response. Still, most of the mechanisms by which the unfolded protein response affects cardiac growth remains unexplored.

1.4 The Endoplasmic Reticulum Unfolded Protein Response

The unfolded protein response of the ER, which is sometimes also referred to as the ER stress response, is a highly conserved molecular pathway that serves to reduce the amount of misfolded proteins inside the ER through the regulation of translation, increase of protein folding regulators, and protein degradation (Hetz and Papa 2018; Walter and Ron 2011). Even though the unfolded protein response is classically described to be related to protein misfolding, emerging data suggests that this signaling cascade is also involved in the regulation of a variety of other physiological and pathological conditions, which is often transduced by crosstalk to other signaling pathways (Hetz and Papa 2018). It is becoming clear that these intensive interactions are bidirectional and also play a major role during protein misfolding-mediated activation of the unfolded protein response. However, most aspects regarding this signaling crosstalk remain incompletely characterized, which is why this summary will

focus on the canonical functions of the unfolded protein response for protein quality control.

During ER stress the protein folding status inside the ER is transduced by a complex network of signaling pathways that ultimately determine cell fate. This mediates the expression of genes that support cell survival or induce cell death, dependent on the duration and intensity of ER stress. While transient activation of the unfolded protein response is adaptive, long-term ER stress, as it may occur during chronic disease, lets the unfolded protein response transduce pro-inflammatory and pro-death signals (Hetz and Papa 2018). Activation of the unfolded protein response by ER stress triggers two temporally distinct cellular responses in order the reduce the amount of protein misfolding (Hetz and Papa 2018). An initial response inhibits the amount of protein synthesis, to attenuate further protein load on the ER and additionally enhances the degradation of misfolded proteins, whereas a second wave triggers a large gene expression response through the activation of specific transcription factors. While those temporal dynamics have been investigated extensively in other cell types, most of those temporal aspects remain relatively unexplored in cardiomyocytes, especially *in vivo*.

The canonical unfolded protein response is executed by three transmembrane proteins on the ER; inositol requiring protein 1 (IRE1), protein kinase RNA-like ER kinase (PERK), and activating transcription factor 6 (ATF6) (Figure 7) (Hetz and Papa 2018). Of note, other noncanonical transducers of the unfolded protein response have been described, even though most of their roles in physiology and disease remains unresolved (Arensdorf et al. 2013; Stauffer et al. 2020a). During ER stress these sensors of protein misfolding initiate several mechanisms that increase the folding

capacity of the ER, reduce the influx of newly synthesized proteins into the ER, and further diminish the amount of misfolded proteins by clearing those that have already accumulated. Relatively recently, an additional mechanism to reduce further protein load to the ER has been described, which involves the release of mRNAs from the ER to the cytosol, thereby removing them from their site of ER translocation (Reid et al. 2014).

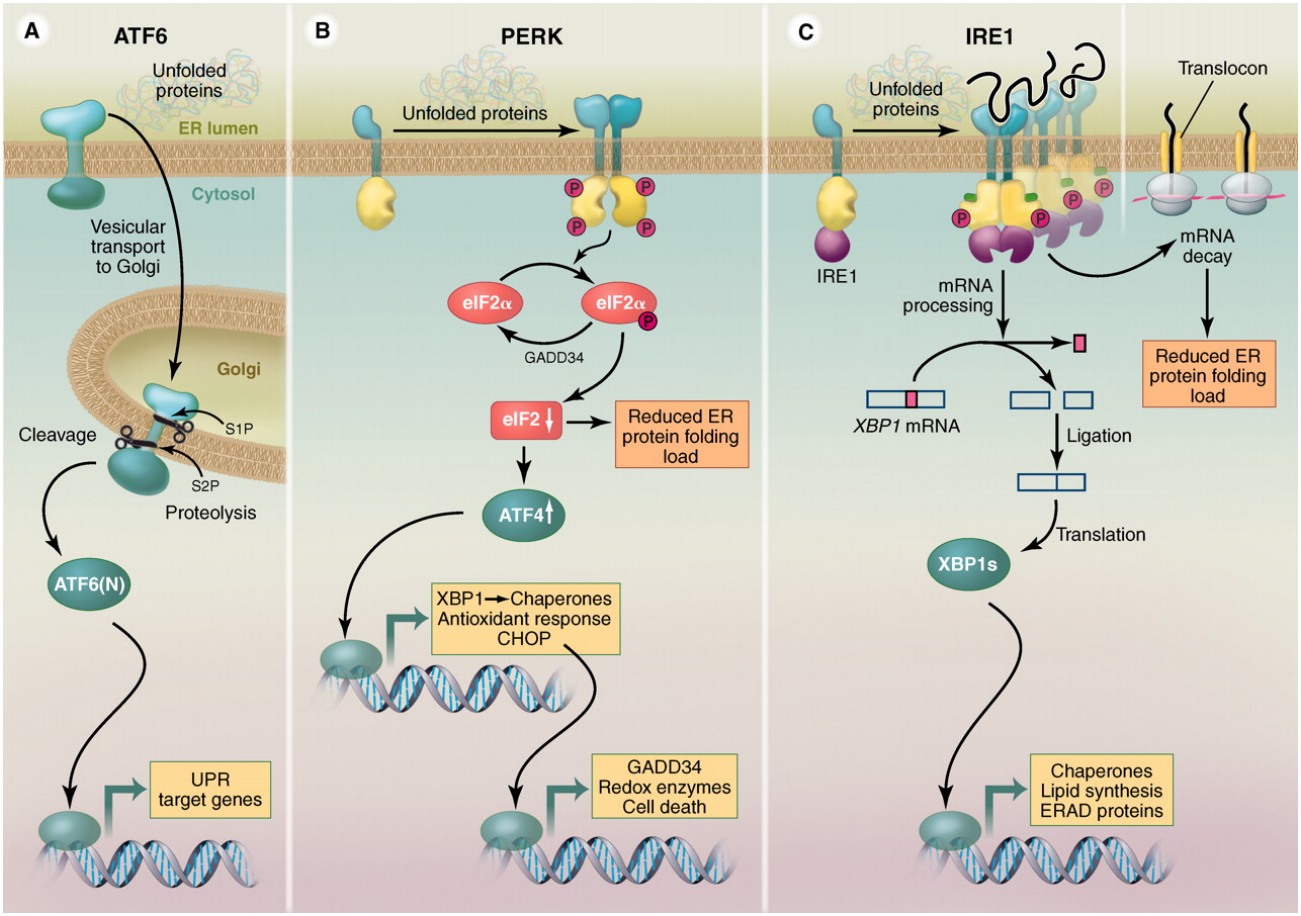

Figure 7 | The Canonical Unfolded Protein Response.

A signaling network of three transmembrane sensors of ER protein misfolding induces a gene response that may restore proteostasis during ER stress or induce cell death in response to prolonged proteotoxic stress. This conserved protein quality control pathway is known as the canonical unfolded protein response, which consists of the three branches ATF6 (A), PERK (B) and IRE1 (C). From 'The Unfolded Protein Response: From Stress Pathway to Homeostatic Regulation' (Walter and Ron 2011). Reprinted with permission from AAAS.

1.4.1 Unfolded Protein Response - The IRE1 pathway

During ER stress, the type 1 transmembrane protein IRE1, which initiates the most conserved branch of the unfolded protein response, oligomerizes and trans-autophosphorylates leading to the activation of its cytosolic RNase domain (Shamu and Walter 1996). This oligomerization can be triggered by direct binding of misfolded proteins to the luminal domain of IRE1 or the release of oligomerization-inhibiting chaperones from IRE1, that may dissociate when the protein folding demand increases inside the ER (Ron and Walter 2007). Chaperone binding to IRE1 has been well characterized for glucose-regulated protein 78 kD (GRP78), which is also known as BiP, and one of the major chaperones of the ER (Bertolotti et al. 2000). In a process known as regulated IRE1-dependent decay (RIDD), selective mRNAs which harbor specific sequences and secondary structure are then degraded by the RNase activity of IRE1, thereby regulating glucose metabolism, inflammation, and apoptosis (Hetz and Papa 2018; Hollien and Weissman 2006; Maurel et al. 2014; Moore and Hollien 2015). Here, RIDD may favor the degradation of ER-localized mRNAs to decrease protein load on the ER (Maurel et al. 2014).

In addition, IRE1 catalyzes the splicing of the mRNA encoding the transcription factor X box-binding protein 1 (XBP1) through an unconventional and specific mechanism using its endoribonuclease activity (Hetz and Papa 2018). Unspliced XBP1 mRNA produces an unstable and rapidly degraded protein, which represses unfolded protein response target genes (Ron and Walter 2007). The processing of XBP1 mRNA however causes a frameshift that leads to an isoform called spliced XBP1 (XBP1s), which exhibits a highly active transcriptional activation domain, leading to the induction of unfolded protein response genes by binding to cis-acting elements known as unfolded protein response element (UPRE) or ER stress response element II (ERSE-

II) (Hetz and Papa 2018; Walter and Ron 2011). Of note, the target genes of XBP1s may vary during different conditions, based on the ability of XBP1s to form heterodimers with other transcription factors, which however remains largely unexplored (Hetz and Papa 2018). XBP1 mRNA is targeted to the translocon in the ER membrane by binding of the SRP to a conserved hydrophobic domain of its nascent peptide chain during the early phase of translation, followed by classical SRP mediated translocation to the ER (Hetz and Papa 2018; Plumb et al. 2015). IRE1 directly interacts with the Sec61 translocon, where it comes in contact with the XBP1 mRNA (Plumb et al. 2015). A translation pausing sequence in the XBP1 mRNA ensures sufficient interaction with IRE1 for splicing before translation is continued (Kanda et al. 2016; Yanagitani et al. 2011). The cleaved fragments of the XBP1 mRNA are then ligated by the tRNA ligase RtcB, followed by completion of translation to generate XBP1s (Jurkin et al. 2014; Kosmaczewski et al. 2014; Lu et al. 2014). In addition to its regulation by post-transcriptional modification by IRE1-dependent splicing, transcript numbers of XBP1 mRNA also increase during ER stress, since the XBP1 gene locus is a target of the unfolded protein response, which further induces the activity of the IRE1-XBP1 signaling pathway (Ron and Walter 2007). Interestingly, XBP1 mRNA levels remain elevated even when ER stress resolves and IRE1 is inactivated. XBP1 mRNA then remains in its un-spliced precursor form, which inhibits the unfolded protein response, thereby eventually assisting in terminating signaling by spliced XBP1 through inhibitory heterodimerization or the competition for binding sites (Ron and Walter 2007; Yoshida et al. 2006). Despite its nucleolytic activity, IRE1 may have additional signaling functions through its interaction with other signaling pathways, which is not well characterized.

Two IRE1 isoforms, IRE1 alpha and beta, have been identified, both of which exert RIDD and XBP1 splicing activity (Maurel et al. 2014). While it has been reported that the XBP1 mRNA splicing activity of IRE1 alpha is stronger, compared to the stronger RIDD activity of IRE1 beta, most of the differences between both IRE1 isoforms and their implications for cellular physiology remain unexplored (Maurel et al. 2014). Importantly, RIDD and XBP1 splicing have been associated with opposite effects on cell fate (Han et al. 2009; Maurel et al. 2014). Whereas RIDD has a proapoptotic output, XBP1 splicing and the subsequent mediated gene program by XBP1s are associated with a pro-survival effect (Maurel et al. 2014). Still, basal RIDD activity is required for ER homeostasis, which highlights the importance of IRE1 even under physiological conditions for cellular function (Maurel et al. 2014).

1.4.2 Unfolded Protein Response - The PERK pathway

The second branch of the unfolded protein response is regulated by the type I transmembrane kinase PERK. PERK is phylogenetically related to IRE1, similar in structure, and also contains a luminal stress-sensing domain and a cytoplasmic protein kinase domain (Ron and Walter 2007). Like IRE1, oligomerization of PERK is mediated by the release of chaperones and the binding of misfolded proteins to its luminal domain, which results in its trans-autophosphorylation and activation (Carrara et al. 2015; Wang et al. 2018). Activated PERK then phosphorylates the alpha subunit of the translation initiation factor eIF2 (Hetz and Papa 2018). Normally, eIF2 associates with GTP and Met-tRNA to form the ternary complex, which is required for translation initiation. During translation initiation, eIF2-bound GTP is hydrolyzed to GDP. To promote a new round of translation initiation, the inactive eIF2-GDP is converted to the active eIF2-GTP by its guanine nucleotide exchange factor eIF2B (Jackson et al.

2010). However, eIF2 alpha phosphorylation stabilizes the eIF2-GDP-eIF2B complex and thereby hinders the exchange of GDP to GTP, ultimately resulting in the inhibition of protein synthesis and reduced load to the ER (Jackson et al. 2010; Walter and Ron 2011).

Even though this results in diminished translation of the majority of transcripts, several mRNAs can escape PERK induced translational attenuation. Among them is the mRNA encoding activating transcription factor 4 (ATF4). The 5′-untranslated region of ATF4 contains two upstream open reading frames (uORF). The proximal uORF1 of the ATF4 mRNA is a positive-acting element that facilitates ribosome scanning followed by re-initiation at a downstream coding region (Vattem and Wek 2004). In unstressed cells, in which high levels of GTP-loaded ternary complexes are present, ribosome scanning downstream of uORF1 reinitiates at the next coding region, which is uORF2 (Vattem and Wek 2004). Thereby ATF4 expression is largely suppressed by the inhibitory uORF2 during baseline conditions. During ER stress, when eIF2 alpha phosphorylation results in low levels of GTP-loaded ternary complexes, the time for the scanning ribosome to reinitiate at a downstream element of uORF1 is increased. This allows the ribosome to scan through the inhibiting uORF2 and instead reinitiate at the main ATF4-coding region, leading to increased expression of ATF4 during ER stress, even though general translation is reduced (Ron and Walter 2007; Vattem and Wek 2004). The potent transcription factor ATF4 then contributes to an antioxidant response, enhanced folding capacity, regulation of metabolism and induction of autophagy by its mediated gene response (Hetz and Papa 2018). Among the many genes induced by ATF4 are growth arrest and DNA damage–inducible 34 (GADD34) and C/EBP homologous protein (CHOP). GADD34 is a subunit of the protein phosphatase PP1, which antagonizes PERK by dephosphorylating eIF2 alpha, thereby

representing a negative feedback-loop of the PERK signaling pathway (Novoa et al. 2001). The transcription factor CHOP controls the expression of several apoptosis-related genes, including GADD34, and thereby controls cell death during prolonged ER stress, highlighting the protective function of modest or transient PERK activation, whereas strong or chronic PERK activation induces cell death (Walter and Ron 2011). It should be noted that ATF4 regulates the expression of many other genes besides GADD34 and CHOP, and that the PERK mediated phosphorylation of eIF2 alpha has a far more complex outcome than the increased expression of ATF4. While this and the other signaling pathways outlined in this summary are often described as the 'canonical' unfolded protein response, the full cellular response to ER stress is likely far more extensive and complex.

1.4.3 Unfolded Protein Response - The ATF6 pathway

The third branch of the unfolded protein response is transduced by the ER-resident transmembrane protein ATF6, which belongs to a group of transmembrane proteins that are part of the ATF/CREB family and contain a basic leucine zipper transcription factor, consisting of a basic DNA binding region next to an alpha-helical coiled coil region that can promote dimerization (Stauffer et al. 2020a). Members of this group are type II ER-transmembrane transcription factors that, similar to ATF6, become cleaved and thereby activated by site-1 and site-2 proteases in the Golgi apparatus. Among them are ATF6 beta (CREBL1), CREB3, CREB3L1 (OASIS), CREB3L2 (BBF2H7), CREB3L3 (CREBH) and CREB3L4 (CREB4), which are expressed in different tissues and whose functions remain largely unknown, even though some of them were suggested to have overlapping or opposing functions with ATF6 in the heart (Correll et al. 2019; Stauffer et al. 2020a; Thuerauf et al. 2004).

The canonical unfolded protein response is mediated by ATF6, which maintains proteostasis during ER stress by inducing an adaptive gene response (Haze et al. 1999). ATF6 remains inactive through oligomerization and binding of the chaperone GRP78 to its ER-luminal domain, which masks a Golgi localization sequence (Shen et al. 2002; Shen et al. 2005). ATF6 oligomerization is maintained by intermolecular disulfide bonds between cysteine residues in its luminal domain that are reduced during ER stress, which also promotes the dissociation of GRP78 from ATF6 by its binding to misfolded proteins. The reduction of ATF6 was recently shown to involve the two ER-resident protein disulfide isomerases PDIA5 and ERp18 (TXNDC12), however other protein disulfide isomerases may also be involved in this process (Higa et al. 2014; Oka et al. 2019). After monomerization and unmasking of its Golgi localization sequence, ATF6 is translocated to the Golgi apparatus, where it is cleaved by regulated intramembrane proteolysis of site-1 and site-2 proteases, releasing a 50kD fragment of ATF6 that freely translocates to the nucleus via a nuclear localization sequence (Blackwood et al. 2020). The transition to the Golgi apparatus has been proposed to involve a transient binding of ATF6 to the secreted calcium-binding protein thrombospondin 4 (Thbs4) (Lynch et al. 2012), even though the precise functions of Thbs4 for the induction of the unfolded protein response remains unknown. Once in the nucleus, the liberated N-terminal fragment, ATF6(N), acts as a potent transcription factor that maintains proteostasis by binding to ERSE and ERSE-II elements in the promoter regions of unfolded protein response genes, which include, among many other proteins, folding regulators and components of the ERAD pathway (Plate et al. 2019). Interestingly, the specific gene response that is ultimately induced by ATF6 is dependent on the stimulus that lead to ATF6 activation (Blackwood et al. 2020). This likely involves the dimerization of ATF6 with other transcription factors that become

activated during different conditions, however most of this is currently unknown (Blackwood et al. 2020).

1.4.4 Programmed Cell Death during Endoplasmic Reticulum Stress

While many of the pathways that become activated during ER stress transduce adaptive events that aid in the restoration of cellular proteostasis, some of them also promote cell death in order to eliminate cells that become irreversibly damaged (Figure 8) (Hetz and Papa 2018). While both protective and maladaptive effectors are activated in response to ER stress, it is thought that the relative ratios between protective and maladaptive events dictates the final cellular outcome (Urra et al. 2013). Even though the process in which the unfolded protein response transduces cell death is less well understood compared to its adaptive branches, several key pathways have emerged over the recent years. One of the best characterized ways in which cell death is triggered by ER stress is mediated by the ATF4 target gene CHOP. The transcription factor CHOP regulates the expression of several apoptosis-related genes, which include the upregulation of the death receptor DR5, the inhibition of BCL-2, and the induction of several other BCL-2 family members such as the pro-apoptotic proteins BIM, NOXA and PUMA (Hetz and Papa 2018; Urra et al. 2013). In addition, strong activation of ATF4 and CHOP induce high levels of the eIF2 alpha phosphatase GADD34. The resulting dephosphorylation of eIF2 alpha leads to increased amounts of protein synthesis, which increases protein misfolding, energy depletion, and the production of reactive oxygen species that directly promote cell death (Han et al. 2013). CHOP also directly regulates the generation of reactive oxygen species by affecting ER-localized oxidases and protein disulfide isomerases (Urra et al. 2013).

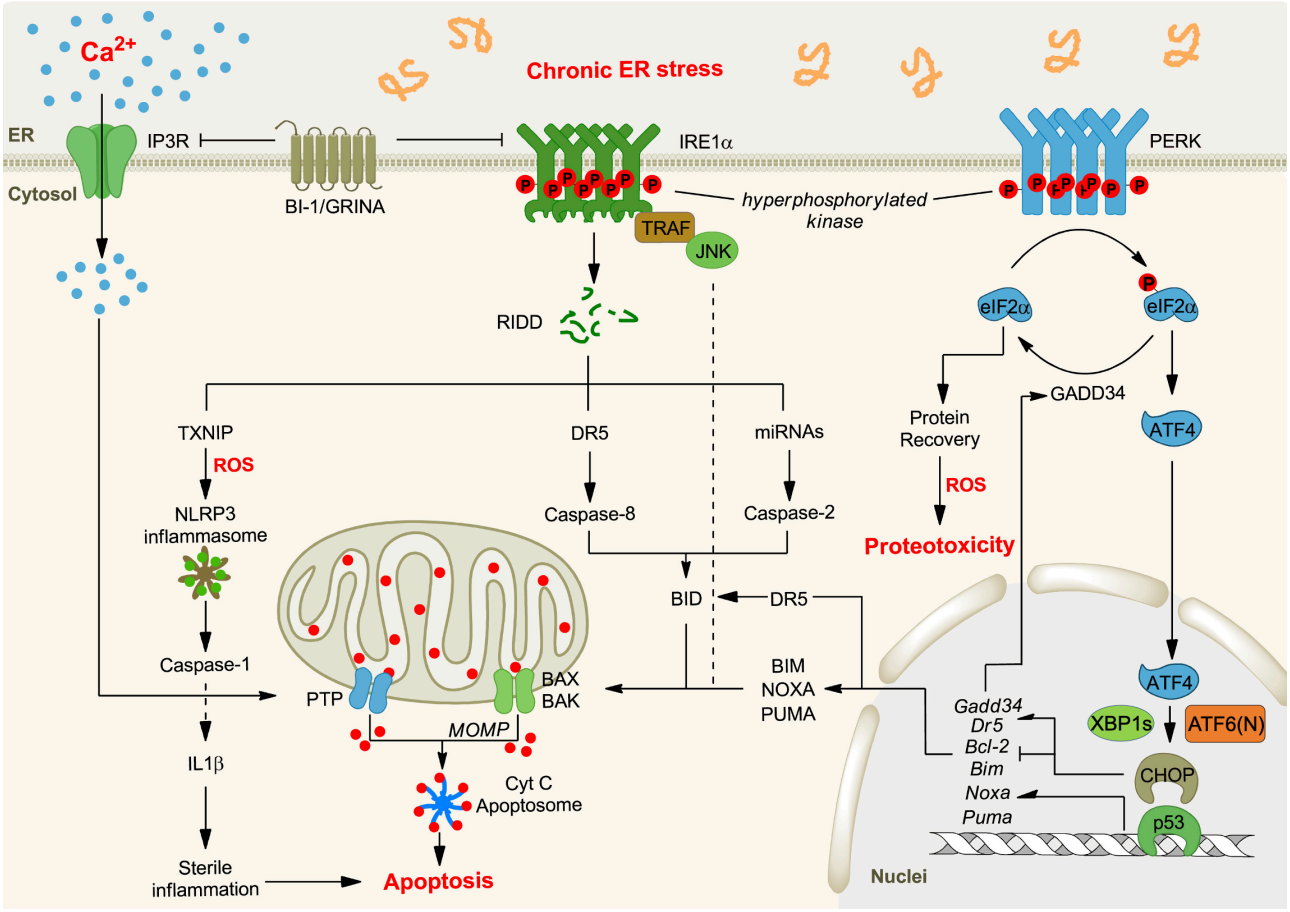

Figure 8 | Mechanisms of ER Stress-induced Apoptosis.

Apoptosis during ER stress is transduced by all three branches of the unfolded protein response. Central mechanisms include the release of calcium from the ER into the cytosol, regulation of the outer mitochondrial membrane permeability and the activation of specific caspases. Cell fate is ultimately determined by the relative ratios between adaptive and maladaptive pathways of the unfolded protein response. Adapted with permission from 'The Unfolded Protein Response and Cell Fate Control' (Hetz and Papa 2018).

In addition, CHOP was shown to activate the inositol-1,4,5-trisphosphate receptor (IP3R), which promotes the release of calcium from the ER, thereby increasing the cytoplasmic calcium content, resulting in the opening of the mitochondrial permeability transition pore and inducing apoptosis (Tsujimoto et al. 2006; Urra et al. 2013). Indeed, ablation of CHOP was sufficient to attenuate ER stress mediated apoptosis and cardiac dysfunction, highlighting its important role in the transduction of cell death in

response to ER stress (Fu Hai et al. 2010). Even though it was shown that the PERK signaling pathway transduces important cellular events that promote apoptosis in response to ER stress, inhibition of PERK increases cardiac dysfunction, likely due to the impairment of the many other adaptive elements that are regulated by PERK (Liu et al. 2014). Importantly, while CHOP activation is most often associated with the PERK pathway, it has been shown that CHOP is also a target gene of ATF6 and XBP1, showing that CHOP plays a general role in the regulation of cell death in the unfolded protein response (Iurlaro and Muñoz-Pinedo 2016).

IRE1 is also an important regulator of cell death in response to ER stress. While IRE1 transduces a large amount of protective functions, it can also induce apoptosis (Urra et al. 2013). This dual function of IRE1 is suggested to be regulated by the intensity and duration of ER stress (Han et al. 2009; Lin et al. 2007). Besides its splicing activity towards XBP1 mRNA, IRE1 degrades a subset of mRNAs via its endoribonuclease activity via RIDD. As outlined above, RIDD can promote cellular homeostasis by selectively degrading mRNAs that encode proteins which are targeted to the ER, where they would increase the protein load and potentially misfold (Hetz and Papa 2018). However, strong IRE1 activation can promote a massive decay of ER-localized mRNAs and microRNAs via RIDD, including crucial proteins such as chaperones and other protein-folding components, which can then worsen ER stress even further (Han et al. 2009; Hetz and Papa 2018; Hollien and Weissman 2006). Among these are also microRNAs that normally strongly repress pro-apoptotic targets, such as different caspases or the pro-oxidant protein TXNIP, whose subsequent upregulation activates the NLRP3 inflammasome that then promotes sterile inflammation and cell death (Lerner et al. 2012; Upton et al. 2012). In addition, IRE1 was shown to directly interact with many other proteins, that can transduce cell death in response to IRE1 activation

(Hetz and Papa 2018; Urra et al. 2013). Two relatively well characterized examples are the interaction with the adapter protein TRAF2, which activates the JNK and autophagy pathways (Castillo et al. 2011), and the binding to NCK which regulates the NF-κB pathway (Nguyen et al. 2004).

While it is also clear that ATF6 can induce cell death, the precise mechanisms and conditions for this ATF6-dependent signal transduction are mostly unknown (Iurlaro and Muñoz-Pinedo 2016). High activation of ATF6 induces the expression of CHOP, different caspases, and members of the BCL-2 family and transduces apoptosis through the mitochondrial apoptotic pathway (Huang et al. 2018; Nakanishi et al. 2005; Pagliarini et al. 2015; Yoshida et al. 2000). Other independent pathways that may include the protein WBP1 may also contribute to ATF6-mediated apoptosis (Morishima et al. 2011); however most of the mechanisms by which ATF6 regulates apoptosis are not known.

Taken together, all three branches of the canonical unfolded protein response regulate cell death through multiple pathways. Many of them ultimately control the expression of specific transcripts, such as members of the BCL-2 family, which collectively regulate the permeability of the outer mitochondrial membrane, a central nexus of the apoptosis pathway (Urra et al. 2013). In addition, some elements can directly control the activity of different caspases or other apoptosis-related signaling pathways (Hetz and Papa 2018). While maladaptive regulators of the unfolded protein response are activated together with its adaptive branches, it is generally thought that the relative ratios between adaptive and maladaptive elements determine the final cellular outcome, thereby leading to cell death when the adaptive responses are insufficient to resolve ER stress and the maladaptive elements prevail (Glembotski 2007).

1.4.5 The ATF6 Pathway in Cardiac Health and Disease

ATF6 has been implicated in both normal heart function and the pathophysiology of several cardiac diseases, where it is expressed in cardiomyocytes and cardiac fibroblast, and while not specifically investigated in the heart, also in other cardiac cell types such as endothelial cells and immune cells (Jin et al. 2016; Karali et al. 2014; Rao et al. 2014; Stauffer et al. 2020b). Here, ATF6 acts as a primary adaptive responder to ER stress by inducing a gene program that maintains proteostasis.

Transcript profiling of transgenic mice with a cardiomyocyte-restricted expression of a tamoxifen-activated form of ATF6 by microarray analysis or RNA sequencing showed that ATF6 regulates several hundred genes in the heart (Belmont et al. 2008; Blackwood et al. 2019b). While those genes include many that have been implicated in proteostasis, a large number of the ATF6 regulated genes are currently not associated with proteostasis, which could indicate that the function of ATF6 is much more complex than previously assumed. In contrast, a deletion of either ATF6 or its isoform ATF6 beta has no cardiac or other aberrant phenotype under baseline conditions in young mice (Correll et al. 2019). ATF6 deficiency however causes rod and cone dysfunction with increasing age, the only major phenotype known to occur in humans with mutations that attenuate the transcriptional activity of ATF6 (Kohl et al. 2015; Lee et al. 2020). However, a deletion of both genes, or a 3 of 4 allele combinatorial deletion, causes early embryonic lethality, suggesting that both genes play essential roles during development (Correll et al. 2019; Yamamoto et al. 2007). This indicates that the functions of ATF6 and ATF6 beta are at least partly overlapping and interchangeable (Correll et al. 2019). ATF6 insufficiency has also no effect on the baseline expression of the majority of tested unfolded protein response genes in the heart, suggesting that ATF6 is non-essential for their normal expression in the

postnatal heart (Jin et al. 2016). However, transgenic mice that express a dominant negative mutant of ATF6, that itself has no DNA-binding activity and dimerizes with endogenous ATF6 and eventually other ATF6 homologs to prevent binding to their target sites, is sufficient to reduce the expression of known ATF6 target genes under baseline conditions (Toko et al. 2010). These mice also develop ventricular dilatation and heart failure and have significantly impaired survival rates (Toko et al. 2010). While not fully proven, it is therefore currently thought that the combined function of ATF6 and ATF6 beta is necessary for the baseline expression of the unfolded protein response and the maintenance of cardiac function, whereas an insufficiency for one can be compensated by the other and eventually even by other homologs such as CREB3, CREB3L1 (OASIS), CREB3L2 (BBF2H7), CREB3L3 (CREBH) or CREB3L4. This hypothesis is supported by the finding that cardiac-specific transgenic mice expressing the transcriptionally-active N-terminus of either ATF6 or ATF6 beta induce overlapping gene sets which fall into the category of proteostasis and the unfolded protein response (Correll et al. 2019). Still, several functions of ATF6 and ATF6 beta in the heart are different and some reports even highlighted opposing functions of both isoforms on the induction of the unfolded protein response (Correll et al. 2019; Thuerauf et al. 2007; Thuerauf et al. 2004).

While ATF6 seems to be replaceable for the baseline expression of unfolded protein response genes, ATF6 has been reproducibly shown to be absolutely essential for the induction of a variety of proteostasis genes during ER stress (Jin et al. 2016). ATF6 is rapidly activated in response to a variety of cardiac pathologies, including ischemia, reperfusion, and pressure overload, where it enhances proteostasis through its gene program (Blackwood et al. 2019b; Doroudgar et al. 2009; Jin et al. 2016; Lynch et al. 2012; Toko et al. 2010). Indeed, activation of ATF6 has been consistently shown to

improve cardiac function in response to these pathologies, whereas ATF6 deficiency impaired myocardial function (Blackwood et al. 2019a; Blackwood et al. 2019b; Correll et al. 2019; Jin et al. 2016; Martindale et al. 2006; Toko et al. 2010). This adaptive function has been attributed to the induction of its downstream proteostasis target genes, which was validated by the isolated manipulation of several ATF6 target genes that also demonstrated protective functions in the heart (Arrieta et al. 2020; Belmont et al. 2010; Belmont et al. 2008; Bi et al. 2018; Doroudgar et al. 2015; Glembotski et al. 2012; Jin et al. 2016; Tadimalla et al. 2008; Vekich et al. 2012). Recent interest has also focused on the function of cardiac ATF6 target genes that are not associated with proteostasis, even though most of these aspects remain unexplored (Blackwood et al. 2020).

Taken together, in the heart, ATF6 functions as a stress-inducible transcription factor, whose activation appears to be protective in the context of different cardiac pathologies. While ATF6 deficiency can be mostly compensated in the healthy heart, ATF6 remains essential for cardiac function in response to stress. Here, it maintains myocardial function through transcriptional reprogramming, which includes many genes involved in proteostasis, but also other essential genes whose function in the context of ATF6 activation are mostly unknown.

1.5 The Proteostasis Network during Cardiac Aging

Protein homeostasis is essential to maintain cellular function. However, a significant decline of the capacity of the proteostasis network and the subsequent accumulation of misfolded proteins and intracellular damage is a hallmark of aging (Hipp et al. 2019; Kaushik and Cuervo 2015). Several age-related diseases were shown to be associated with protein misfolding (Labbadia and Morimoto 2015a). Increasing the capacity of the proteostasis network has therefore emerged as a promising strategy for the treatment or even prevention of age-associated disease caused by protein misfolding. Among several other pathways of the proteostasis network, the unfolded protein response was shown to decline during aging (Taylor 2016). The identification of key regulators of the unfolded protein response, that can be targeted to increase its adaptive branches without enhancing its maladaptive functions, could therefore lead to the development of novel therapeutic interventions for the treatment of different diseases, especially for aged patients. Despite a general consensus about the involvement of the decline of proteostasis in aging and age-associated diseases, only a limited number of studies examined the proteostasis network during cardiac aging. Here, especially the involvement of the unfolded protein response in cardiac postnatal development and aging remains incompletely characterized.

1.5.1 Proteostasis and Aging

The cellular capacity to buffer against protein misfolding in response to stress declines with a decreased activity of the proteostasis network (Labbadia and Morimoto 2015a). A large body of studies indicates that the activity of the proteostasis network becomes impaired during aging, which then results in the accumulation of misfolded proteins and the impairment of cellular function. By now, all branches of the cellular proteostasis

network have been shown to be affected to some degree by aging, including the heat shock response, the oxidative stress response, and the unfolded protein response (Kaushik and Cuervo 2015; Labbadia and Morimoto 2015a). Key elements of proteostasis are chaperones, the ubiquitin-proteasome system, and the lysosome-autophagy system, all of which have been shown to become impaired by age (Kaushik and Cuervo 2015).

Chaperones become less available during aging, which increases the probability of protein misfolding (Kaushik and Cuervo 2015). Impaired energetics, which can often be found during aging, based on a reduction of mitochondrial function and the dysregulation of cellular metabolism, can also further decrease the responsiveness of ATP-dependent chaperones (Kaushik and Cuervo 2015). Undesired protein modifications that accumulate in aged cells, such as advanced glycation end-products through non-enzymatic modifications on long-lived proteins, further interfere with chaperone function (Kaushik and Cuervo 2015). These modifications are normally recognized and reversed by different enzymes, however the expression of these enzymes is compromised with age (Kaushik and Cuervo 2015). In addition, metastable proteins which accumulate during aging can capture chaperones and thereby withdraw them from their desired site of action (Kaushik and Cuervo 2015). This general reduction in chaperone function is partly antagonized by specific small heat-shock proteins, which combine misfolded proteins into large aggregates, in which the toxic effects of misfolded proteins are reduced (Walther et al. 2015). While this can partly buffer the increased amount of protein misfolding in aged cells, this system may become overwhelmed at some point, ultimately contributing to cellular dysfunction.

Proteostasis is further compromised by a decline of proteasome activity (Saez and Vilchez 2014). This is mediated at least partly through a decreased expression and alteration of different proteasome subunits (Ferrington et al. 2005; Lee et al. 1999), the perturbed assembly of proteasomes (Vernace et al. 2007), and the inactivation of proteasomes by binding to protein aggregates (Grune et al. 2004; Saez and Vilchez 2014). Proteasomal dysfunction has been consistently observed in aged mammalian tissues, including muscle, and transgenic mice with decreased proteasomal activity that exhibit a shortened life span and develop age-related disease (Bulteau et al. 2002; Ferrington et al. 2005; Husom et al. 2004; Saez and Vilchez 2014; Tomaru et al. 2012). In contrast, increasing proteasomal activity extends longevity in different species (Saez and Vilchez 2014). While it is unclear if such results can be transferred from organismal models to humans, preliminary findings of increased proteasomal activity in long-lived humans support the hypothesis that proteasomal activity can also determine longevity in humans (Chondrogianni et al. 2000).

The lysosome-autophagy system has also been shown to become compromised with age (Escobar et al. 2019). Multiple studies reported a reduced expression of proteins which are required for autophagy in aged tissues, resulting in an overall decline of autophagy with age (Rubinsztein et al. 2011). Several longevity pathways regulate lifespan through the control of the expression of autophagy-related genes in different species, which may counteract triglyceride accumulation, mitochondrial dysfunction, muscle degeneration, and cardiac dysfunction (Lee et al. 2010; Masiero et al. 2009; Matecic et al. 2010; Tóth et al. 2008). Similar to other regulators of the proteostasis network, it was shown that the inhibition of autophagy results in a phenotype that is comparable to premature aging. Here, attenuation of the activity of autophagy results in the accumulation of dysfunctional organelles, protein aggregation, and ER stress

(Escobar et al. 2019; Rubinsztein et al. 2011). In contrast, activating autophagy delays aging and extends lifespan (Escobar et al. 2019; Rubinsztein et al. 2011).

Taken together, preclinical studies in invertebrates and mammals indicate that interventions that strengthen the proteostasis network can increase lifespan and health-span, and attenuate a variety of age-related diseases (Labbadia and Morimoto 2015a). However, while some of those studies were performed in mammals, the majority of those studies were performed in invertebrates and systemic analyses of the proteostasis network during mammalian aging are limited (Kaushik and Cuervo 2015). Similar to other pathways of the proteostasis network, activation of the unfolded protein response protects against protein misfolding and promotes longevity in yeast (*S. cerevisiae*), worms (*C. elegans*), and flies (*D. melanogaster*); however whether the unfolded protein response is also implicated in mammalian aging remains mostly unknown (Chen et al. 2009; Henis-Korenblit et al. 2010; Labunskyy et al. 2014; Matai et al. 2019; Sekiya et al. 2017; Shore et al. 2012).

1.5.2 The Unfolded Protein Response during Aging

The unfolded protein response of the ER is the major signaling pathway that is activated during ER-associated protein misfolding. Besides its protective function for the ER, the unfolded protein response was also shown to contribute to proteostasis in other subcellular compartments when activated (Jin et al. 2016). It thereby increases the overall cellular protein quality control capacity, highlighting its importance for cell survival in response to proteotoxic stress. As outlined above, the cellular response to misfolded proteins is compromised with age, which is thought to be mediated by a reduced capacity of the unfolded protein response (Brown and Naidoo 2012; Taylor

2016). Several studies suggested that key adaptive regulators of the unfolded protein response are significantly reduced during aging (Hussain and Ramaiah 2007; Naidoo et al. 2008; Paz Gavilán et al. 2006). It was also shown that their activation and function are compromised, further impairing a sufficient adaption to ER stress (Hussain and Ramaiah 2007; Taylor and Dillin 2013). In contrast, some maladaptive branches of the unfolded protein response were proposed to increase with age, while other studies showed decreased levels in some tissues (Estébanez et al. 2018; Hussain and Ramaiah 2007; Naidoo et al. 2008; Paz Gavilán et al. 2006). Importantly, preliminary data suggested, that some key protective proteins of the unfolded protein response do also become significantly compromised in the adult heart (Doroudgar et al. 2015). This appeared to involve their transcriptional downregulation, however further details and a systematic evaluation of the unfolded protein response in cardiac aging is currently missing (Doroudgar et al. 2015). While only shown in invertebrates, increasing the capacity of the unfolded protein response by activating or overexpressing some of its adaptive regulators is sufficient to promote longevity in yeast, *C. elegans*, and Drosophila (Chen et al. 2009; Henis-Korenblit et al. 2010; Labunskyy et al. 2014; Matai et al. 2019; Sekiya et al. 2017; Shore et al. 2012). A further decrease of the unfolded protein response however leads to premature aging and impaired lifespan, which indicates, that the low levels of unfolded protein response genes remain essential for proteostasis (Chadwick et al. 2020; Labunskyy et al. 2014). An age-dependent decline of proteostasis therefore appears to be at least partly mediated by a decreased activity of the unfolded protein response, making it a promising target for the treatment of age-associated disease caused by protein misfolding.

1.5.3 Evolutionary benefits of an age-dependent decline of proteostasis

It remains mostly obscure why a decline in proteostasis with age is such a common characteristic of most species. A strong response against protein misfolding would be beneficial by increased resistance to stress and therefore should have evolved throughout evolution. Initial reports indicated that some of the gradual impairment of protein homeostasis results from oxidative damage that accumulates in regulators of the proteostasis network (Brown and Naidoo 2012). However, recent evidence from invertebrates suggests that the downregulation of the proteostasis network during aging is not a random and gradual decline that proceeds with age, but rather a programmed event that already occurs during early adulthood and at least partly involves the reprogramming of the cellular gene program (Ben-Zvi et al. 2009; David et al. 2010; Labbadia and Morimoto 2014). In *C. elegans*, the decline of the proteostasis network, including the unfolded protein response, coincides with a timeframe that occurs shortly after sexual maturation and the beginning of the reproductive period (Labbadia and Morimoto 2015b; Taylor and Dillin 2013). While mostly hypothetical and not proven, it was further suggested that activation of stress pathways, such as those that sense and response to protein misfolding, may reduce fertility. Evolutionary pressure for optimal fecundity may therefore come with the expense of stress resistance of adult organisms that already reached the reproductive period (Labbadia and Morimoto 2015b). In addition, this may ensure that older animals do not compete for resources, which would prioritize reproduction and the younger generation in an environment where resources are limited, giving a possible explanation why a decrease of the proteostasis network with age was maintained throughout evolution (Labbadia and Morimoto 2015b).

1.5.4 Decline of Cardiac Protein Homeostasis during Aging

While the impairment of the proteostasis network has been extensively studied in cells and different model organisms, less is known about how aging affects proteostasis and protein misfolding in the heart. Accumulation of misfolded proteins has been described to occur regularly in aged hearts. One of the best characterized forms is amyloid deposition, which results from proteins that become structurally unstable with age and form misfolded intermediates that aggregate and precipitate as amyloid in different tissues, including the heart (Steenman and Lande 2017). About 25% of an elderly population aged 85 years or over showed ventricular amyloid deposition in a postmortem examination (Tanskanen et al. 2008). In comparison to ventricular amyloid deposition, atrial amyloidosis is more common, with a prevalence of approximately 95% in patients older than 80 years (Steiner 1987). The accumulation of protein aggregates has also been found in aged mouse hearts and their composition was found to be similar to protein aggregates that accumulate in response to hypertension (Ayyadevara et al. 2016). Similar to other tissues, the chaperone abundance, the activity of the ubiquitin-proteasome system, and the lysosome-autophagy system were found compromised in the aged heart, and enhancing their capacity decelerated cardiac aging (Abdellatif et al. 2018; Bulteau et al. 2002; Locke and Tanguay 1996; McLendon and Robbins 2015; Zhou et al. 2017).

While the accumulation of misfolded proteins has been observed in the aged heart and in several heart diseases whose prevalence increases with age, it remains to be clearly demonstrated that protein misfolding is an essential contributor to the development and progression of cardiac dysfunction (Singh and Robbins 2018). As outlined above, a large number of studies consistently showed that the manipulation of protein quality control pathways affects myocardial function, making it likely that misfolded proteins

are at least partly involved in the regulation of cardiac function and disease. However, a different mechanism that does not involve misfolded proteins, such as the regulation or degradation of specific effector proteins, cannot be ruled out. Additionally, even though it was demonstrated that massive protein misfolding can directly induce heart failure (Pattison et al. 2008; Rubin and Maurer 2020; Sanbe et al. 2004; Wang et al. 2001), it is not known when or to what degree protein misfolding occurs in most cardiac diseases or cardiac aging and if those amounts are indeed sufficient to directly impair myocardial function. Also, the misfolded protein species that is responsible for cardiac damage is unknown, even though emerging evidence indicates that it is not the insoluble protein aggregates or amyloid plaques but rather its soluble oligomeric precursor that causes cellular toxicity (McLendon and Robbins 2015).

1.6 Rationale of the Study

As outlined in the previous chapters, numerous studies suggest that impaired proteostasis and protein misfolding contribute to cardiac disease development. Improving proteostasis may therefore be a promising strategy for the treatment of heart disease, especially in aged patients where the proteostasis network may be particularly compromised. However, many key aspects remain unaddressed. Since previous studies have focused on the failing heart, it is currently incompletely characterized if ER stress occurs at earlier stages of disease, or if it solely occurs in the failing heart. Further, the activation and function of the proteostasis network in response to pathologic stimuli to the heart and how this is affected by age is incompletely characterized. This study examines some of those aspects for the unfolded protein response and implications for cardiac hypertrophy, a common risk factor for cardiac dysfunction, that is associated with increased protein processing. A specific focus is put on the ATF6 gene program, which was described as a nexus of protein quality control that initiates a large number of adaptive effects in response to protein misfolding. Specifically, the following points are addressed in this study:

1. How is the expression and function of the unfolded protein response in the heart affected by age?
2. Does an impairment of the ATF6 pathway compromise the cardiac responsiveness to endoplasmic reticulum stress?
3. Does increased protein synthesis during hypertrophic growth lead to activation of the unfolded protein response?
4. Is cardiac hypertrophy regulated by ATF6?
5. What are the consequences of ATF6 deficiency for cardiac function?

1.7 Limitations

Most of the experiments of this study were performed in mice and isolated cardiomyocytes of mice and rat. Despite a close phylogenetic relationship between rodents and human, findings in experimental settings in rodents do not necessarily translate to humans. This can have multiple reasons, such as differences in rodent physiology, human specific effects, drug interactions, a heterogenous collective of patients, comorbidities, lack of efficacy in a chronic disease state and many more. While some of the results which indicate that certain ATF6 target genes decline in the adult heart showed a similar trend in a small publicly available gene expression database of heart samples from humans of different age, larger studies are needed before any assertions of the unfolded protein response can be made. This study used tunicamycin, a specific inhibitor of N-linked glycosylation that blocks the first step of glycoprotein synthesis and thereby induces protein misfolding, for the induction of ER stress and the adrenergic agonists phenylephrine and isoproterenol for the induction of cardiomyocyte hypertrophy *in vitro*. *In vivo*, cardiac hypertrophy was induced by the implantation of isoproterenol-loaded osmotic pumps. While all techniques are established and widely used models for ER stress, cardiac hypertrophy, and heart failure, it is important to note that none of these models is capable of capturing the full complexity of human disease. Even though some existing data points to the general involvement of protein misfolding in human cardiac disease, this study does not allow any definite conclusions about proteostasis, the unfolded protein response, or the ATF6 pathway in humans. It should be seen as preliminary data, which once these results have been confirmed by others, eventually even with different model systems, may encourage human translational studies, if sufficient safety conditions can be guaranteed.

2 Materials

The materials section is partly based on the preprint article ‘Age-related decline of the unfolded protein response in the heart promotes protein misfolding and cardiac pathology’ (Hofmann et al. 2021).

Reagent or Resource	Source	Identifier
Antibodies		
Mouse monoclonal anti-Puromycin, clone 12D10	Sigma-Aldrich	Cat#MABE343; RRID: AB_2566826
Mouse monoclonal anti-KDEL	ENZO Life Sciences	Cat#10C3; RRID: AB_10618036
Rabbit polyclonal anti-ATF6	Proteintech	Cat#24169-1-AP; RRID: AB_2876891
Mouse monoclonal anti-β-Actin	Santa Cruz Biotechnology	Cat#sc-47778; RRID: AB_626632
Mouse monoclonal anti-GAPDH (G-9)	Santa Cruz Biotechnology	Cat#sc-365062; RRID: AB_10847862
Mouse monoclonal anti-α-Actinin (Sarcomeric)	Sigma-Aldrich	Cat#A7811; RRID: AB_476766
Donkey polyclonal Fluorescein (FITC)-conjugated AffiniPure Donkey Anti-Mouse IgG	Jackson Immuno Research	Cat#715-095-151; RRID: AB_2335588
Virus strains		
AAV9-Control	(Jin et al., 2017)	N/A
Adenovirus dnATF6α	(Thuerauf et al., 2001)	N/A
Chemicals		
Ponceau BS	Sigma-Aldrich	Cat#B6008
Fibronectin bovine plasma	Sigma-Aldrich	Cat#F1141
DMEM/F-12, HEPES	Thermo Fisher Scientific	Cat#11330032
Medium 199	Sigma-Aldrich	Cat#M7528
DPBS, no calcium, no magnesium	Thermo Fisher Scientific	Cat#14190144
Penicillin-Streptomycin-Glutamine (100X)	Thermo Fisher Scientific	Cat#10378016
Laminin	Sigma-Aldrich	Cat#L2020
HiPerFect Transfection Reagent	QIAGEN	Cat#301704

PF-429242 dihydrochloride	Sigma-Aldrich	Cat#SML0667
(R)-(−)-Phenylephrine hydrochloride	Sigma-Aldrich	Cat#P6126
(−)-Isoproterenol -hydrochlorid	Sigma-Aldrich	Cat#I6504
Propidium Iodide	Thermo Fisher Scientific	Cat#P21493
Hoechst 33342, Trihydrochloride, Trihydrate	Thermo Fisher Scientific	Cat#H21492
Tunicamycin	Sigma-Aldrich	Cat#T7765
Protease inhibitor cOmplete ULTRA	Roche	Cat#5892791001
PhosSTOP	Sigma-Aldrich	Cat#04906837001
4x Laemmli Sample Buffer	Bio-Rad	Cat#1610747
2-Mercaptoethanol	Sigma-Aldrich	Cat#M6250
ALLN	Sigma-Aldrich	Cat#208719
Commercial assays		
RNeasy Mini Kit	QIAGEN	Cat#74104
Quick-RNA MiniPrep Kit	Zymo Research	Cat#R1055
DC Protein Assay Kit II	Bio-Rad	Cat#5000112
Superscript III First-Strand Synthesis System	Invitrogen	Cat#18080051
Maxima SYBR Green/ROX qPCR Master Mix	Thermo Fisher Scientific	Cat#K0221
Deposited data		
Raw and analyzed data	(Hofmann et al. 2021)	Data supplements
Mouse reference genome GRCm39, Ensembl release 102	Ensembl	http://www.ensembl.org/Mus_musculus/Info/Index
Cardiomyocyte-specific RNA-Seq and ribosome profiling gene expression data from hearts after TAC 3 hours, 2 days and 2 weeks	(Doroudgar et al., 2019)	SRA: PRJNA484227 https://www.ncbi.nlm.nih.gov/sra/?term=PRJNA484227
ATF6 and XBP1s target genes	(Shoulders et al., 2013)	Data supplements
PERK target genes	(Lu et al., 2004)	Data supplements
Experimental animal models		
Rat: WISTAR, HanRj:WI Rattus norvegicus	Janvier Labs	Cat#13792727; RRID: RGD_13792727
Mouse: C57BL/6JRj	Janvier Labs	MGI Cat# 2670020; RRID:MGI:2670020
Mouse: ATF6α KO	(Wu et al., 2007)	N/A
Oligonucleotides		
Rat ATF6α Stealth siRNA: GCUCUCUUUGUUGUUGCUUAGUGGA	Thermo Fisher	ID#RSS315363

Rat siRNA Negative Control	Thermo Fisher	Cat#12935300
Real-time PCR primers		
Mouse-Atf6-F: ATGGCCATGCTGGTCTATG	This paper	N/A
Mouse-Atf6-R: CTGGTTGGGAAAGACATCTTCTA	This paper	N/A
Mouse-Atp2a2-F: CCAGAGAGATGCCTGCTTAAA	This paper	N/A
Mouse-Atp2a2-R: CACGTTGGATGAGATGAGGTAG	This paper	N/A
Mouse-β-Actin-F: GACGGCCAGGTCATCACTAT	This paper	N/A
Mouse-β-Actin-R: GTACTTGCGCTCAGGAGGAG	This paper	N/A
Mouse-Col1a1-F: GAAGCACGTCTGGTTTGGA	This paper	N/A
Mouse-Col1a1-R: ACTCGAACGGGAATCCATC	This paper	N/A
Mouse-Hsp90b1-F: TCGTCAGAGCTGATGATGAAGT	This paper	N/A
Mouse-Hsp90b1-R: GCGTTTAACCCATCCAACTGAAT	This paper	N/A
Mouse-Hspa5-F: CACGTCCAACCCCGAGAA	This paper	N/A
Mouse-Hspa5-R: ATTCCAAGTGCGTCCGATG	This paper	N/A
Mouse-Manf-F: TGGGTGCGTTCTTCGACAT	This paper	N/A
Mouse-Manf-R: GACGGTTGCTGGATCATTGAT	This paper	N/A
Mouse-Myh7-F: TGCCCGATGACAAAGAAGAG	This paper	N/A
Mouse-Myh7-R: AAGAGGCCCGAGTAGGTATAG	This paper	N/A
Mouse-Nppa-F: GAGAGAGAGAAAGAAACCAGAGTG	This paper	N/A
Mouse-Nppa-R: CTCATCTTCTACCGGCATCTTC	This paper	N/A
Mouse-Nppb-F: GTCAGTCGTTTGGGCTGTAA	This paper	N/A
Mouse-Nppb-R: GCAAGTTTGTGCTCCAAGATAAG	This paper	N/A
Mouse-Pdia6-F: TGCCACCATGAATCAGGTTCT	This paper	N/A
Mouse-Pdia6-R: TCGTCCGACCACCATCATAGT	This paper	N/A
Mouse-Syvn1-F: CCAACATCTCCTGGCTCTTCCA	This paper	N/A
Mouse-Syvn1-R: CAGGATGCTGTGATAAGCGTGG	This paper	N/A
Rat-Atf6-F: CTTCCTCCAGTTGCTCCATC	This paper	N/A
Rat-Atf6-R: CAACTCCTCAGGAACGTGCT	This paper	N/A
Rat-Gapdh-F: GACAAACGTCTTCGGGAATTG	This paper	N/A

Rat-Gapdh-R: CTCTTTAAGGGCAGGGAGTATC	This paper	N/A
Rat-Hsp90b1-F: AAGCATCTGATTACCTTGAATTGGAT	This paper	N/A
Rat-Hsp90b1-R: CTCCTCCACAGTCTCAGTCTTGCT	This paper	N/A
Rat-Hspa5-F: CACGTCCAACCCGGAGAA	This paper	N/A
Rat-Hspa5-R: GTAGCCTGCGTGAACCTTA	This paper	N/A
Rat-Xbp1-F: ACGAGAGAAAACTCATGGGC	This paper	N/A
Rat-Xbp1-R: ACAGGGTCCAACTTGTCCAG	This paper	N/A
Software and algorithms		
FIJI (ImageJ)	(Rueden et al., 2017; Schindelin et al., 2012)	https://fiji.sc
Prism v7.0	GraphPad	https://www.graphpad.com/scientific-software/prism/
Adobe Illustrator	Adobe	https://www.adobe.com/products/illustrator.html
R	R Foundation	https://www.r-project.org
R studio	R studio	https://rstudio.com/
Flexbar v3.0.315	(Roehr et al., 2017)	https://github.com/seqan/flexbar
Bowtie2 v2.3.0	(Langmead and Salzberg, 2012)	http://bowtie-bio.sourceforge.net/bowtie2/index.shtml
STAR aligner, v2.5.3a17	(Dobin et al., 2013)	https://github.com/alexdobin/STAR
Rsubread v1.24.218	(Liao et al., 2019)	https://bioconductor.org/packages/release/bioc/html/Rsubread.html
edgeR v3.32.1	(Robinson et al., 2010)	https://bioconductor.org/packages/release/bioc/html/edgeR.html
DAVID v6.8	(Dennis et al., 2003; Huang et al., 2009)	https://david.ncifcrf.gov
Other		
ALZET mini-osmotic pump (Model 1007D)	ALZET	Cat#0000290
Immobilon-P Membrane	Merck Millipore	Cat#IPVH00010

3 Methods

The methods section is partly based on the preprint article 'Age-related decline of the unfolded protein response in the heart promotes protein misfolding and cardiac pathology' (Hofmann et al. 2021).

Laboratory animals

Data associated with all animal studies reported in this article has been reviewed and approved by the institutional animal care and use committee and conforms to the guide for the care and use of laboratory animals published by the National Research Council. All experiments were performed in 7 day, 10-week and 52-week-old male mice unless otherwise indicated. WT mice used for experiments in which no comparison to ATF6 KO mice was performed were purchased from Jackson Laboratory (Jackson Stock No: 005304). Mice carrying a global deletion of the ATF6α isoform, hereinafter referred to as ATF6, were provided by the Glembotski laboratory (Jin et al. 2016; Wu et al. 2007). In agreement with previous reports, ATF6 deletion did not affect mouse development (Blackwood et al. 2019b; Jin et al. 2016; Wu et al. 2007). In addition, no gender differences were found. Due to these observations, and in an attempt to decrease the total number of mice needed to adequately power the study, only male mice were used. All animals were fed ad libitum and were housed in a temperature- and humidity-controlled facility with a 12-h light-dark cycle. In the experiments where Puromycin was used to determine protein synthesis rate *in vivo*, 40mg/kg of Puromycin diluted in PBS was given via intraperitoneal injection.

Cultured cardiomyocytes

Isolation of neonatal rat ventricular cardiomyocytes was performed as previously described (Jin et al. 2016). Cells were isolated from one to two-day old WISTA rats

(cat# 13792727, WISTAR HanRj:WI, Janvier Labs) via enzymatic digestion and purified by Percoll density gradient centrifugation. Cardiomyocytes were then plated at a density of 0.5 X 10^6 cells per well on 34.8 mm plastic plates that had been pre-treated with 5 µg/ml fibronectin (cat# F1141, Sigma-Aldrich) in serum free DMEM/F12 medium (cat# 11330032, Thermo Fisher Scientific) for one hour and then cultured in DMEM/F12 1:1, containing 10% fetal bovine serum, 100 units/mL of penicillin, 100µg/mL streptomycin and 292 µg/ml glutamine (cat# 10378016, Thermo Fisher Scientific). After 24h, media was changed to DMEM/F12 1:1 supplemented with BSA (1 mg/ml), 100 units/mL of penicillin, 100µg/mL streptomycin and 292 µg/ml glutamine or when neonatal cardiomyocytes were directly compared to adult cardiomyocytes to DMEM/F12 1:1, containing only 100 units/mL of penicillin, 100µg/mL streptomycin and 292 µg/ml glutamine for 24h after which the cells were subjected to the respective treatments. Adult rat ventricular myocytes were isolated from 6-week old male WISTA rats (WISTAR RjHan:WI, Janvier Labs) via enzymatic digestion as previously described (Jin et al. 2016; Völkers et al. 2011). Hearts were rapidly excised and perfused with a rate of 8 mL/min in a Langendorff apparatus. After excision, hearts were initially perfused with calcium-free medium (ACM) (pH 7.2) consisting of (in mM) 5.4 KCl, 3.5 MgSO4, 0.05 pyruvate, 20 NaHCO3, 11 glucose, 20 HEPES, 23.5 glutamate, 4.87 acetate, 10 EDTA, 0.5 phenol red, 15 butanedionemonoxime (BDM), 20 creatinine, 15 creatine phosphate (CrP), 15 taurine and 27 units/mL insulin under continuous equilibrium with 95% O2 and 5% CO2. After 5 min the perfusion was switched to ACM plus collagenase (0.5 U/mL) for 20 – 30 min. Finally, perfusion was changed to low Na+, high sucrose Tyrode solution containing (in mM) 52.5 NaCl, 4.8 KCl, 1.19 KH2PO4, 1.2 MgSO4, 11.1 glucose, 145 sucrose, 10 taurine, 10 HEPES, 0.2 CaCl2 for 15 min. Thereafter left ventricles of digested hearts were cut into small pieces and subjected to gentle agitation to allow for dissociation of cells. Consequently,

cells were resuspended in ACM without BDM in which 2 mM extracellular calcium was gradually reintroduced at 25 °C. Adult cardiomyocytes were cultured on laminin coated culture dishes. Cells were plated in Medium 199 (cat# M7528, Sigma-Aldrich) supplemented with 100 units/mL of penicillin, 100µg/mL streptomycin and 10µg/mL Laminin (cat# L2020, Sigma-Aldrich). After one hour media was changed to M199 media supplemented with 100 units/mL of penicillin, 100µg/mL streptomycin. Cells were subjected to the respective treatments after 24 hours. To induce ER stress *in vitro*, 10 µg/mL tunicamycin (TM) was added to the cell media for 24h in the indicated experiments. Other concentrations that were used are described in the respective figures.

siRNA transfection

Neonatal rat ventricular myocytes were plated at a density of 0.5 X 10^6 cells per well on fibronectin coated 34.8 mm plates and cultured in Dulbecco´s modified Eagle´s medium (DMEM)/F12 1:1 (cat# 11330-032, Thermo Fisher Scientific), containing 10% fetal bovine serum, 100 units/mL of penicillin, 100µg/mL streptomycin and 292 µg/ml glutamine for 24h. One day after, media was changed to DMEM/F12 1:1 containing 0.5% fetal bovine serum, 120 nM of siRNA and 0.625% HiPerFect (cat# 301704, QIAGEN) and no antibiotics. HiPerFect transfection reagent was used to transfect cells with small interfering (si) RNA oligoribonucleotides targeted to rat ATF6 (assay ID# RSS315363, Stealth siRNA, Thermo Fisher). A non-targeting sequence (cat# 12935300, Thermo Fisher) was used as a control siRNA. Cells were incubated with the siRNA for 16 hours. Then, medium was changed to DMEM/F12 1:1 supplemented with BSA (1 mg/ml), 100 units/mL of penicillin, 100µg/mL streptomycin and 292 µg/ml glutamine. Respective treatments were initiated after 48 hours.

Adenovirus generation and transfection

Plasmid vector construction and recombinant adenovirus generation encoding AAV9-control and dominant-negative ATF6α (dnATF6) has been described previously (Thuerauf et al. 2001; Wang et al. 2000). Transduction was performed by incubating cultures overnight with the appropriate adenovirus at a multiplicity of infection (MOI, number infectious particles per cell) of five. On the next day media was changed to DMEM/F12 1:1 supplemented with BSA (1 mg/ml), 100 units/mL of penicillin, 100µg/mL streptomycin and 292 µg/ml glutamine. After 24 hours, desired treatments were initiated.

Cultured cell area

Phase-contrast microscopy pictures were taken from five different fields per culture (n=3 individual cell cultures for each treatment). Cell area was determined using FIJI (Rueden et al. 2017; Schindelin et al. 2012). The number of measured cells can be found in the respective figure legends. For cultured myocytes cell area, myocytes were seeded at a density of 0.5 X 10^6 cells per well on fibronectin coated 34.8 mm plates maintained in Dulbecco´s modified Eagle´s medium (DMEM)/F12 1:1, containing 10% fetal bovine serum, 100 units/mL of penicillin, 100µg/mL streptomycin and 292 µg/ml glutamine for 24h. After 24h media was changed to DMEM/F12 1:1 supplemented with BSA (1 mg/ml), 100 units/mL of penicillin, 100µg/mL streptomycin and 292 µg/ml glutamine. After an additional 24 hours, cells were pretreated with either DMSO or 50µM of PF-429242 dihydrochloride (cat# SML0667, Sigma-Aldrich), diluted in DMSO, for 30 minutes and then treated with Dulbecco´s phosphate buffered saline (PBS) (cat# 14190-144, Thermo Fisher Scientific), (R)-(-)-phenylephrine hydrochloride (50µM) (cat# P6126, Sigma-Aldrich) or isoproterenol (10µM) diluted in PBS, for 24h. For siRNA and virus transfection cells were treated as described above.

Immunofluorescence

Cardiomyocytes were isolated as described above. Cardiomyocytes were then plated on glass chamber slides that had been pre-treated with 25 µg/ml fibronectin for one hour. After the respective treatments, the slides were washed twice in PBS and then fixed with 4% PFA for 20 minutes. Slides were washed three times for 5-10 minutes in PBS and then incubated for 10 minutes in permeabilization buffer consisting of PBS, 0.2% Triton X-100 and 0.1M Glycine. Then slides were washed once with PBS and then incubated with blocking buffer containing 10% horse serum and 0.2% Triton X-100 in PBS for one hour. Next, slides were incubated overnight at 4°C with primary antibody diluted in blocking buffer. The primary antibody used was anti-α-Actinin, Sarcomeric (cat# A7811, Sigma-Aldrich; 1:100). On the next day slides were washed three times for 5-10 minutes in PBS and then incubated with secondary antibody in blocking buffer for one hour. The secondary antibody used was Fluorescein (FITC)-conjugated AffiniPure Donkey Anti-Mouse IgG (cat# 715-095-151, Jackson Immuno Research; 1:100). The slides were then washed three times for 5-10 minutes in PBS and incubated in a 1:500 solution of 1mM TO-PRO-3 iodide (cat# T3605, Thermo Fisher Scientific) diluted in PBS for 10 minutes. Then slides were washed twice in PBS for 10 minutes and covered with VECTASHIELD Antifade Mounting Medium (cat# H-1000, Vector Laboratories) and a glass plate and visualized by microscopy. Images were obtained using a Leica DMi8 confocal laser scanning microscope.

Cell viability

For quantification of viability cells were subjected to the respective treatments. Then, 1 µg/mL of propidium iodide (cat# P21493, Thermo Fisher Scientific) and 5 µg/mL of Hoechst 33342, trihydrochloride, trihydrate (cat# H21492, Thermo Fisher Scientific) was added to the culture media. After 10 minutes fluorescent images of random

positions of the cell culture area were taken using a ZEISS Axio Vert.A1 microscope. Propidium iodide positive and negative cells were quantified with FIJI (Rueden et al. 2017; Schindelin et al. 2012).

Isoproterenol model of cardiac hypertrophy

Male WT and ATF6 KO mice at 10 weeks of age were randomly assigned to the experimental groups. To induce cardiac hypertrophy, mice were subjected to either Lactated Ringer´s solution or 30mg/kg/day Isoproterenol (cat# I6504, Sigma-Aldrich) treatment via ALZET mini-osmotic pump implants (Model 1007D, cat# 0000290) for seven days. For osmotic pump implantation, mice were anesthetized with isoflurane. Pumps were inserted subcutaneously through a small incision at the lower back. Mice received daily intraperitoneal injections of 1µl/g of 0.1 mg/ml Buprenorphine solution, diluted in phosphate-buffered saline at time of surgery and up to 2d after surgery.

TAC surgery

Animals were randomly assigned to the experimental groups. TAC was performed as previously described (Blackwood et al. 2019b). Briefly, adult male mice were anesthetized using a 2% isofluorane/O2 mixture and intubated. Mice were treated with buprenorphine (0.1 mg/kg IP) and a partial trans-sternal thoracotomy performed using aseptic technique. An approximately 1.5 cm vertical left parasternal skin incision was made, underlying pectoralis muscle retracted, and the chest cavity entered through the fourth intercostal space. Using hooked retractors, adjacent ribs were retracted to expose the heart and aortic arch. The aorta was isolated from annexed tissue, and the artery partially ligated between the innominate and left common carotid arteries with 6-0 silk. The calibrated constriction of the aorta was performed by placing a dull 27-gauge needle to the side of the artery, the ligature tied firmly to both the needle and

the artery, and, subsequently, the needle was removed leaving a calibrated stenosis of the aorta. Sham operated mice were exposed to the same procedure, except that the aorta was not constricted. The thoracic cavity was closed and the animals were allowed to recover. Animals were injected once with buprenorphine (0.1 mg/kg IP) about 12 h after recovery in order to reduce any post-operative discomfort. In case any animals displayed signs of pain or distress after this period, additional doses of buprenorphine were administered as needed. Sham-operated mice were euthanized at time points matching to TAC surgery time points.

Echocardiography

Echocardiography was carried out on anesthetized mice using a Visualsonics Vevo 2100 high-resolution echocardiograph (Tsujita et al. 2005). Anesthesia was administered via a facial mask and maintained by a minimum dose of isoflurane (1.0–2.0%). Echocardiography was performed at a heart rate of 450-550 bpm.

Preparation of tissue lysates

Mice were sacrificed and different tissues were rapidly excised, washed in PBS and snap frozen in liquid nitrogen. Different tissues were homogenized using a tissue homogenizer in 5 volumes of ice-cold polysome buffer containing 20mM Tris pH 7.4, 10mM MgCl, 200mM KCl and 1% Trition X-100. For protein analysis via immunoblotting, initial lysates were further diluted with 9 volumes of RIPA buffer containing 20mM Tris-HCl (pH 7.4), 150mM NaCl, 1% Triton X-100, 0.1% SDS, 0,5% Sodium deoxycholate, protease inhibitor cOmplete ULTRA (cat# 05892791001, Roche) and phosphatase inhibitor PhosSTOP (cat# 04906837001, Sigma-Aldrich). RNA was isolated from tissue lysates using the RNeasy Mini Kit (cat# 74104, Qiagen).

Immunoblotting

Cultured cells and mouse tissues were lysed in RIPA Buffer consisting of 50mM Tris pH 7.5, 150mM NaCl, 1% Triton X-100 and 1% SDS, which was supplemented with protease inhibitor cOmplete ULTRA (cat# 05892791001, Roche) phosphatase inhibitor PhosSTOP (cat# 04906837001, Roche). Lysates were cleared by centrifugation at 4°C for 10 minutes at 20.000 rcf. Lysate protein concentration was determined using DC Protein Assay Kit II (cat# 5000112, Bio-Rad). Equivalent amounts of protein, usually 20-30 µg, were brought up to similar volume, mixed with Laemmli Sample Buffer (Bio-Rad; 161-0747) and 2-Mercapoethanol (cat# M6250, Sigma-Aldrich) and boiled at 95°C for 5 minutes. Samples were separated on SDS-PAGE gels and transferred to Immobilon-P transfer membranes (cat# IPVH00010, Merck Millipore). The following antibodies were used to probe the membranes: GAPDH (cat# G-9, sc-365062, Santa Cruz Biotechnology; 1:20,000), β-Actin (cat# C4, sc-47778, Santa Cruz Biotechnology; 1:20,000), KDEL (cat# 10C3, ADI-SPA-827, ENZO Life Sciences; 1:2,000-5,000), ATF6 (cat# 24169-1-AP, Proteintech; 1:1,000), Puromycin (cat# MABE343, Merck Millipore; 1:2,000-1:10,000). Ponceau solution was prepared with Ponceau BS (cat# B6008, Sigma Aldrich).

Quantitative Real Time PCR

Total RNA was isolated from cultured cardiomyocytes using the Quick-RNA MiniPrep Kit (cat# R1055, Zymo Research) and from tissue using the RNeasy Mini Kit (cat# 74104, Qiagen). cDNA was generated by reverse transcription using Superscript III First-Strand Synthesis System (Invitrogen; 18080-051). Quantitative Real Time PCR was performed with Maxima SYBR Green/ROX qPCR Master Mix (Thermo Fisher cat# K0222) in a StepOnePlus RT-PCR System (Thermo Fisher).

Xbp1 splicing

XBP1 splicing was assessed with Real Time PCR using the following primers: FW ACGAGAGAAAACTCATGGGC; Rev ACAGGGTCCAACTTGTCCAG. cDNA was run on a 2% agarose gel at 130V for one hour and viewed by UV illumination.

Sequencing data analysis

Transcript profiling of ATF6 KO mice was performed as previously described. Briefly, total RNA was isolated from mouse left ventricular extracts and RNA sequencing was carried out on Illumina Nextseq at CellNetworks Deep Sequencing Core Facility at Heidelberg University. Sequencing adapter residues and low-quality bases were removed from raw sequencing reads prior to all other analysis steps using Flexbar version 3.0.315 (Roehr et al. 2017). Subsequently, reads mapping to known ribosomal RNA species were excluded from further analyses using Bowtie2 version 2.3.0 (Langmead and Salzberg 2012) with a custom rRNA index and only keeping non-aligning reads. Principal read mapping against the mouse reference genome (GRCm39, Ensembl release 102) was performed with the STAR aligner, version 2.5.3a17 (Dobin et al. 2013). The read-to-transcript assignment was carried out using the R package Rsubread version 1.24.218 (Liao et al. 2019) and the ENSMBL gene annotation GRCm39, Ensembl release 102. The resulting count table was further processed with the edgeR R package19 (Robinson et al. 2010) to construct the list of differentially expressed genes. RNA-Seq and ribosome profiling data of TAC 3h, 2d and 2wk relative to time-matched Sham mice was obtained from the previously published dataset (Doroudgar et al. 2019). Significantly regulated genes were defined as FDR <0.05. ATF6 and XBP1s target genes were identified from Shoulders et al. (Shoulders et al. 2013). Due to incorrectly reported q-values in the available gene list from Shoulders et al., novel q-values were derived from the reversed log10 scores of

Benjamini-Hochberg. PERK-selective target genes were identified from Lu et al. (Lu et al. 2004). PERK-selective target genes were defined as genes induced both >2 fold in AP20187 treated eIF2a (S/S) Fv2E-PERK cells at 8h and >2 fold in TM treated WT cells at 6 hours. 'Unfolded protein response genes' were defined as the merged gene entries from the GO categories GO:0006986 (response to unfolded protein), GO:0030968 (endoplasmic reticulum unfolded protein response) and GO:0034976 (response to endoplasmic reticulum stress).

Gene Ontology analysis

GO term enrichment analysis was performed as previously described. Briefly, genes with FDR <0.05 were considered for further analysis. GOTERM_BP_DIRECT in DAVID v6.8 (Dennis et al. 2003; Huang et al. 2009) was used with the subset of expressed protein-coding genes as background set. Only enriched GO terms with at least five significantly changed genes were kept for further analysis and ranked by p-value. Top enriched terms were retained and visualized with a custom plotting routine showing enrichment p-value.

Quantification and statistical analysis

Statistical analysis was performed using GraphPad Prism 7.0 (Graphpad Software Inc; www.graphpad.com) or R (R Foundation; https://www.r-project.org). Data values are mean ± standard error of the mean (SEM). For statistical analysis one-way ANOVA with Turkey post-hoc analysis was used. When only two conditions where compared, unpaired two tailed t-test was used. $p < 0.05$ was defined as significant difference. Details of the statistical analyses of the sequencing data can be found in the method details. Biological replicate numbers for each figure can be found in the accompanying figure legend.

4 Results

4.1 Age-dependent Decline of Protein Synthesis and the Unfolded Protein Response in Mice

The proteostasis network and its change during postnatal development and aging has been extensively studied in invertebrates where aging is associated with a decline of protein homeostasis (Kikis et al. 2010). However, systematic analysis of the proteostasis network in mammalians are limited. Specifically, the regulation of the unfolded protein response during mammalian aging is incompletely understood. To evaluate the unfolded protein response and its association with the rate of protein synthesis during mammalian aging, protein synthesis and the expression of several essential unfolded protein response genes were assessed in different organs, including heart, skeletal muscle, brain, kidney, and liver in neonatal (one day old), young-adult (10 weeks old), and middle aged (52 weeks old) mice. The organs were grouped into low mitotic activity (heart, skeletal muscle and brain) and high mitotic activity tissues (kidney and liver). Protein synthesis rate was assessed by using the aminonucleoside antibiotic puromycin, which incorporates into elongating peptide chains via the formation of a peptide bond (Nathans 1964). When used in very low concentration that do not inhibit protein synthesis, puromycin-labeled peptides reflect the rate of synthesized proteins during the time of incubation with the compound (Schmidt et al. 2009). To measure the rate of protein synthesis *in vivo*, mice were subjected to intraperitoneal puromycin injection (40 µM/kg), followed by the isolation of the respective organs after thirty minutes. Puromycin-labeled peptides were then detected in tissue lysates by immunoblotting using an anti-puromycin antibody. Protein synthesis decreased in all organs with age (Figure 9). While a significant decline of protein synthesis occurred from neonate to adult mice, no further reduction was

observed from adult to aged mice. Importantly, the reduction of protein synthesis was much more pronounced in tissues with low mitotic activity (heart, skeletal muscle and brain) compared to tissues which maintain mitotic activity (kidney and liver), where only a slight decrease of protein synthesis was found.

Next, the expression of the canonical hallmarks of the unfolded protein response, chaperones 78 kDa glucose-regulated protein (GRP78) and GRP94, and protein disulfide-isomerase A6 (PDIA6), were assessed in neonatal, young adult, and middle-aged mouse tissues.

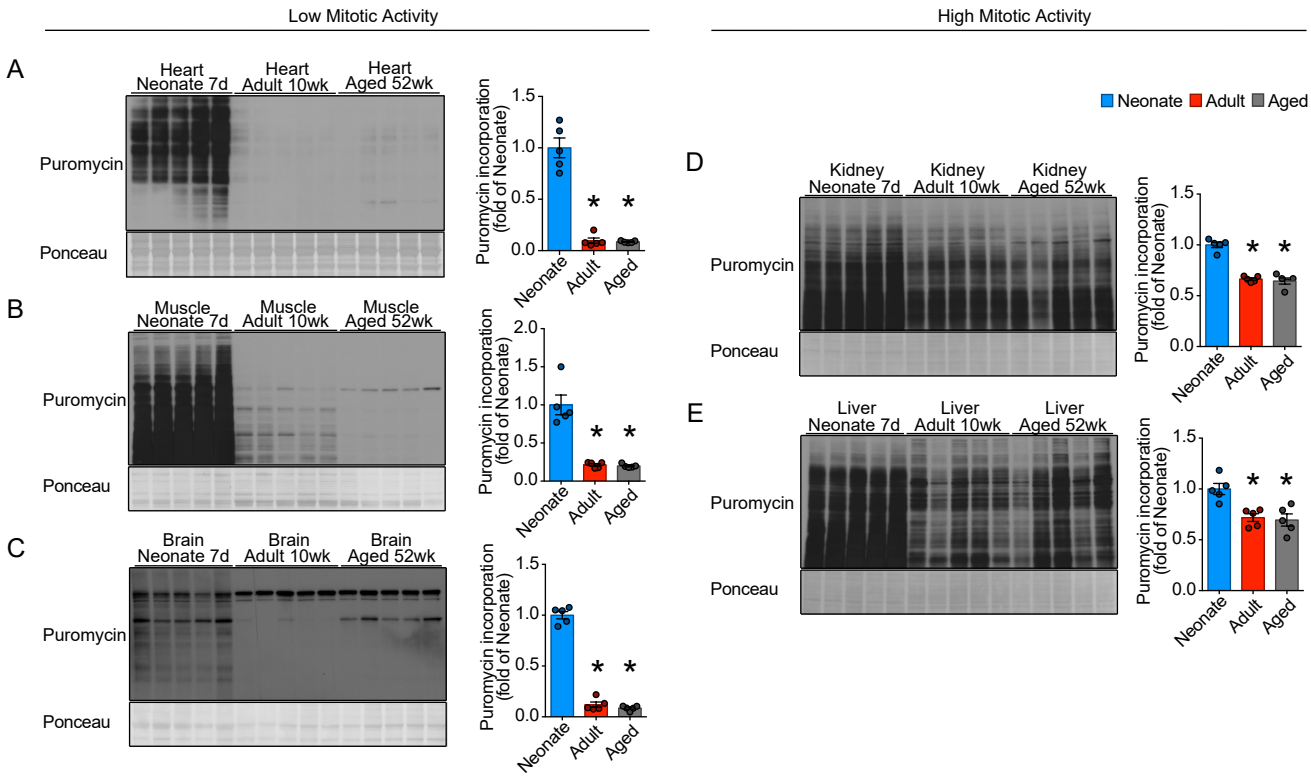

Figure 9 | Extensive Downregulation of Protein Synthesis in Tissues with Low Mitotic Activity during Mammalian Adulthood.

Immunoblots of Puromycin and respective quantifications for the low-mitotic tissues heart (A), skeletal muscle (B), brain (C) and the mitotic tissues kidney (D) and liver (E). * indicates $p<0.05$ from neonate. Figure 9 was adapted from 'Age-related decline of the unfolded protein response in the heart promotes protein misfolding and cardiac pathology' (Hofmann et al. 2021).

Similar to the observed age-dependent decline of protein synthesis, the expression of the unfolded protein response gene products declined with age, especially from neonate to adult mice. Only a slight further decrease of some of the evaluated proteins could be observed from adult to aged mice in some, but not all tissues (Figure 10). The expression of the unfolded protein response gene products was especially reduced in tissues with low mitotic activity. However, significant protein- and organs-specific differences could be observed. Interestingly, the correlation between protein synthesis and the expression of the unfolded protein response genes was highly significant across all samples (Figure 11). While this correlation does not prove a direct relation between protein synthesis and the unfolded protein response, it may indicate that the unfolded protein response is regulated in a way coordinate with the baseline cellular protein synthesis activity of the tissue or vice versa. Since changes of the proteostasis network during postnatal aging of the heart are incompletely understood, the following experiments focused primarily on the regulation of the unfolded protein response in the heart.

Figure 10 | Reduced Age-dependent Expression of Unfolded Protein Response Genes in Mice.

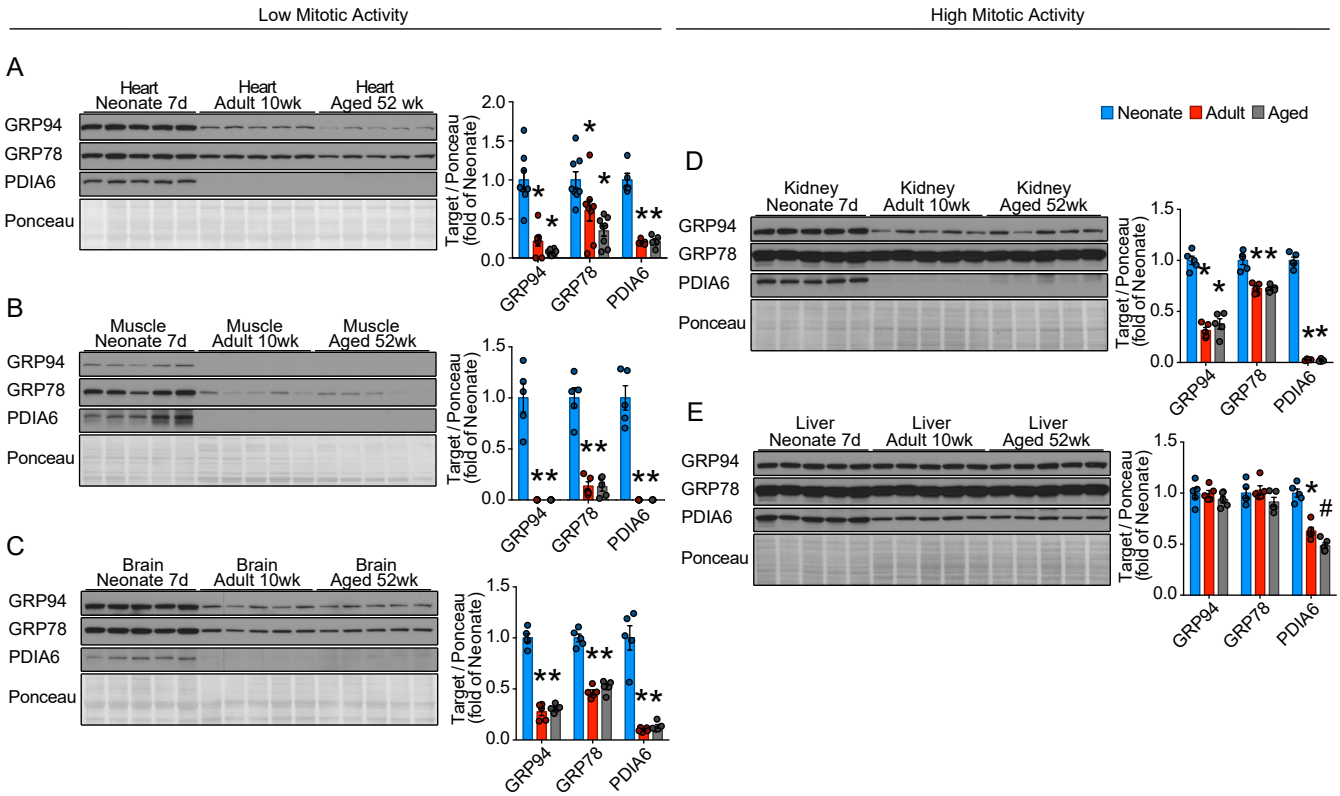

Figure 10 | Reduced Age-dependent Expression of Unfolded Protein Response Genes in Mice.

Immunoblots and respective quantifications of the unfolded protein response gene products GRP94, GRP78, and PDIA6 for the low-mitotic tissues heart (A), skeletal muscle (B), brain (C) and the mitotic tissues kidney (D) and liver (E). * indicates p<0.05 from neonate; # indicates p<0.05 from adult. Figure 10 was adapted from 'Age-related decline of the unfolded protein response in the heart promotes protein misfolding and cardiac pathology' (Hofmann et al. 2021).

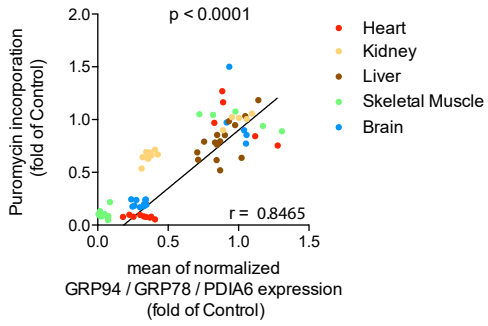

Figure 11 | Correlation of Protein Synthesis and Unfolded Protein Response *in vivo*.

Scatter plot showing the correlation between puromycin incorporation and the mean of the normalized expression of GRP94, GRP78, and PDIA6. Colors for each organ are shown on the right. r was calculated with GraphPad Prism v7.0. Figure 11 was adapted from 'Age-related decline of the unfolded protein response in the heart promotes protein misfolding and cardiac pathology' (Hofmann et al. 2021).

To further assess that the findings which were observed in mice are relevant for human pathophysiology, the expression of several unfolded protein response genes was retrospectively analyzed in a publicly available RNA-sequencing dataset of healthy human hearts across different ages from newborn to late adulthood (Cardoso-Moreira et al. 2019). In agreement with the results obtained in mice, a trend for decreased

expression of several unfolded protein response genes from young adulthood in human hearts was observed (Figure 12). However, these initial results should be interpreted with caution, since the dataset contained very low numbers of samples for each age group (n = 1-3). The results indicated that mammalian low-mitotic organs are more affected by a decline in baseline protein synthesis and unfolded protein response compared to mitotic organs. While cardiomyocytes make up the majority of the cardiac mass, about 70% of the cells of the heart are non-myocytes, such as endothelial cells or fibroblasts (Litviňuková et al. 2020; Pinto et al. 2016). Those highly mitotic cells may have masked an even more pronounced decline of the unfolded protein response in cardiomyocytes from the left ventricular lysates (heart).

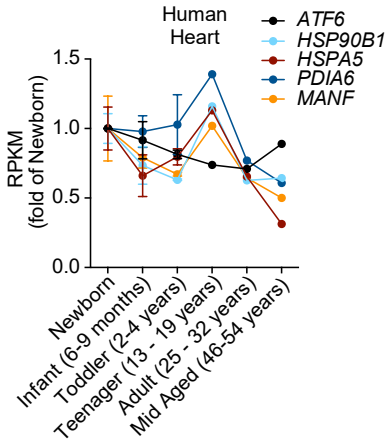

Figure 12 | Baseline Unfolded Protein Response in Healthy Human Hearts from Newborn to Adulthood.

Normalized RPKM values of the respective genes for human RNA sequencing data of the indicated age groups; newborn n=2, infant n=3, toddler n=2, teenager n=1, young adult n=1, older mid-aged n=1. Figure 12 was adapted from 'Age-related decline of the unfolded protein response in the heart promotes protein misfolding and cardiac pathology' (Hofmann et al. 2021).

Thus, to characterize the unfolded protein response in cardiomyocytes during postnatal development and aging, cardiomyocytes from neonatal and adult rats were isolated and analyzed. Similar to the results obtained from left ventricular lysates, both

the rate of protein synthesis, as well as the baseline unfolded protein response were reduced in adult cardiomyocytes. However, especially the decline of the unfolded protein response was much more pronounced, falling to nearly undetectable levels in adult cardiomyocytes for some of the tested unfolded protein response gene products (Figure 13).

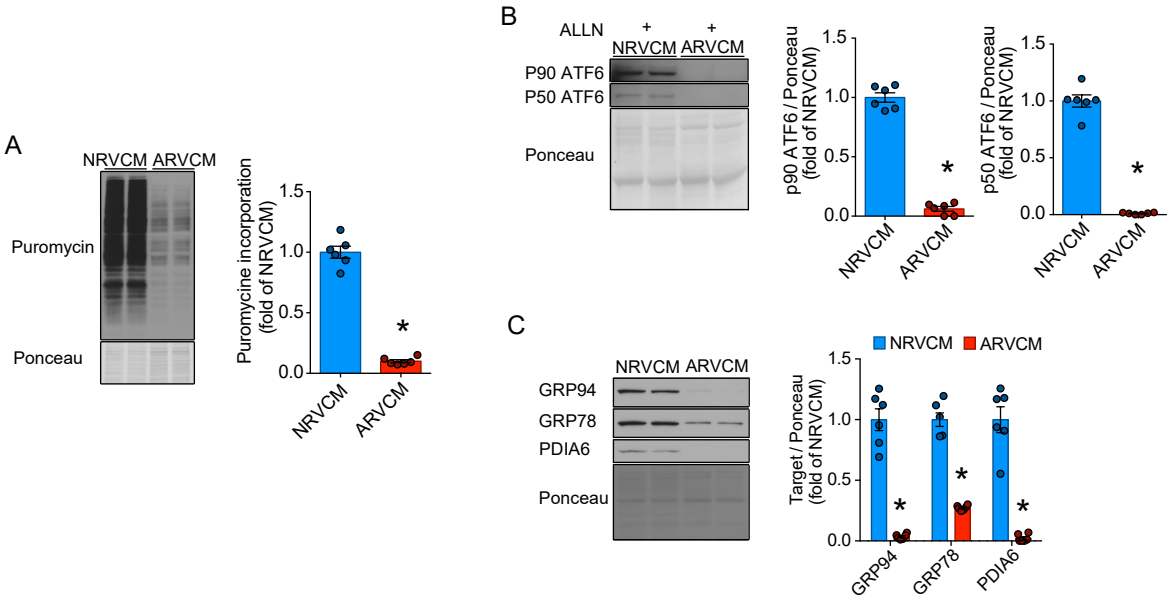

Figure 13 | Protein Synthesis Rate and Unfolded Protein Response in Neonatal and Adult isolated Cardiomyocytes.

(A) Puromycin immunoblot and respective quantification of neonatal and adult cardiomyocytes under baseline conditions. (B) p90 and p50 ATF6 immunoblots and respective quantification of neonatal and adult cardiomyocytes under baseline conditions. (C) Immunoblots and respective quantifications for GRP94, GRP78, and PDIA6 of neonatal and adult cardiomyocytes under baseline conditions. * indicates $p<0.05$ from control. Figure 13 was adapted from 'Age-related decline of the unfolded protein response in the heart promotes protein misfolding and cardiac pathology' (Hofmann et al. 2021).

A decreased baseline expression of some unfolded protein response genes does not necessarily translate into pathophysiological consequences, especially since this reduced expression was observed to be associated with a decline in protein synthesis rate of adult cardiomyocytes. If adult cardiomyocytes are capable of a sufficient

upregulation of their proteostasis network in response to proteotoxic stress, the low baseline expression of unfolded protein response genes may come without any maladaptive consequences. To examine the expression of the unfolded protein response during proteotoxic stress, isolated neonatal and adult rat ventricular cardiomyocytes were treated with tunicamycin (TM), an inhibitor of N-linked glycosylation that blocks glycoprotein synthesis and thereby induces protein misfolding. Tunicamycin induced a robust upregulation of the examined unfolded protein response gene products in both neonatal and adult cardiomyocytes (Figure 14A). While the fold change of their expression was comparable in neonatal and adult cardiomyocytes, the total expression of the unfolded protein response gene products in adult cardiomyocytes remained well below the level of neonatal cardiomyocytes. This was associated with reduced survival of adult cardiomyocytes in response to TM treatment, compared to neonatal cardiomyocytes (Figure 14B). While this observation does not prove that the reduced expression of the unfolded protein response itself is directly accountable for the increased cell death during proteotoxic stress, it however suggests that it may be at least partly involved in this process.

Figure 14 | Reduced Responsiveness of Adult Cardiomyocytes to Proteotoxic Stress.

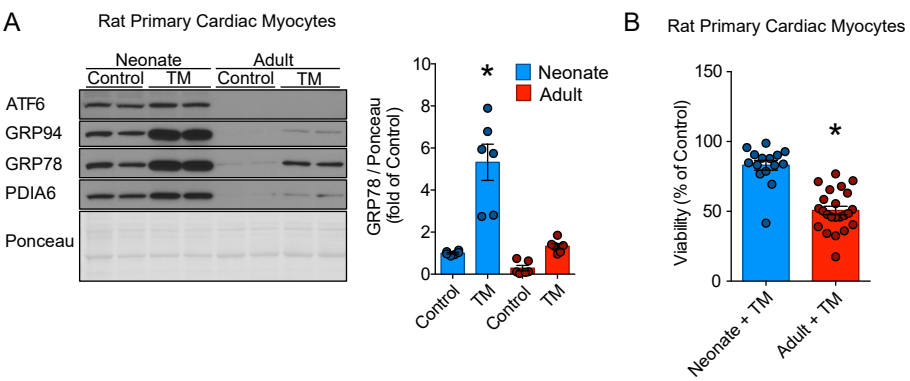

Figure 14 | Reduced Responsiveness of Adult Cardiomyocytes to Proteotoxic Stress.

(A) Immunoblots and quantifications for ATF6, GRP94, GRP78, and PDIA6 of neonatal and adult rat primary cardiomyocytes treated with vehicle (DMSO; control) or TM for 24h. (B) Relative viability of neonatal and adult rat cardiomyocytes after 24h of 20µg/mL TM treatment. Values are normalized to the viability of vehicle (DMSO) treated cells of the same experiment. Each dot represents the viability of all cells in a random 10× magnified cell culture view. Data are representative of three independent experiments. * indicates $p<0.05$ from neonate control in (A) and $p<0.05$ from neonate + TM in (B). Figure 14 was adapted from 'Age-related decline of the unfolded protein response in the heart promotes protein misfolding and cardiac pathology' (Hofmann et al. 2021).

4.2 Loss of ATF6 has only Minor Effects on the Unfolded Protein Response at Baseline *in vivo*

The unfolded protein response is executed by at least three transmembrane proteins inside the ER; inositol requiring protein 1 (IRE1), protein kinase RNA-like ER kinase (PERK), and activating transcription factor 6 (ATF6) (Hetz and Papa 2018). A strong reduction of ATF6 expression, with almost undetectable levels of transcriptionally active p50 ATF6, was found in adult cardiomyocytes (Figure 13B), which is why this study focused the following experiments on the ATF6 branch of the unfolded protein response.

The consequence of ATF6 deficiency, such as it may occur in the aging heart, on global cardiac gene expression has not been analyzed before. Thus, transcript profiling via mRNA sequencing was performed on ATF6 knockout (KO) mice and WT mice. ATF6 KO was confirmed by PCR (Figure 15A). The generation of ATF6 KO mice has been described before (Wu et al. 2007) and similar to the previous study, ATF6 KO mice developed normally throughout adulthood and exhibit no obvious cardiac phenotype, indicating that ATF6 is not essential for normal cardiac development and

function under non-stressed conditions (Jin et al. 2016). RNA sequencing revealed that genes regulated in ATF6 KO hearts enrich for several GO categories, including 'oxidation-reduction process', 'response to endoplasmic reticulum stress' and 'regulation of cell growth' (Figure 15B). However, a detailed analysis of the unfolded protein response and changes in gene expression of previously described target genes of the three canonical branches ATF6, PERK, and IRE1 (XBP1s) revealed that only a few unfolded protein response genes are actually significantly regulated at baseline in mouse hearts (Figure 15C and 15D).

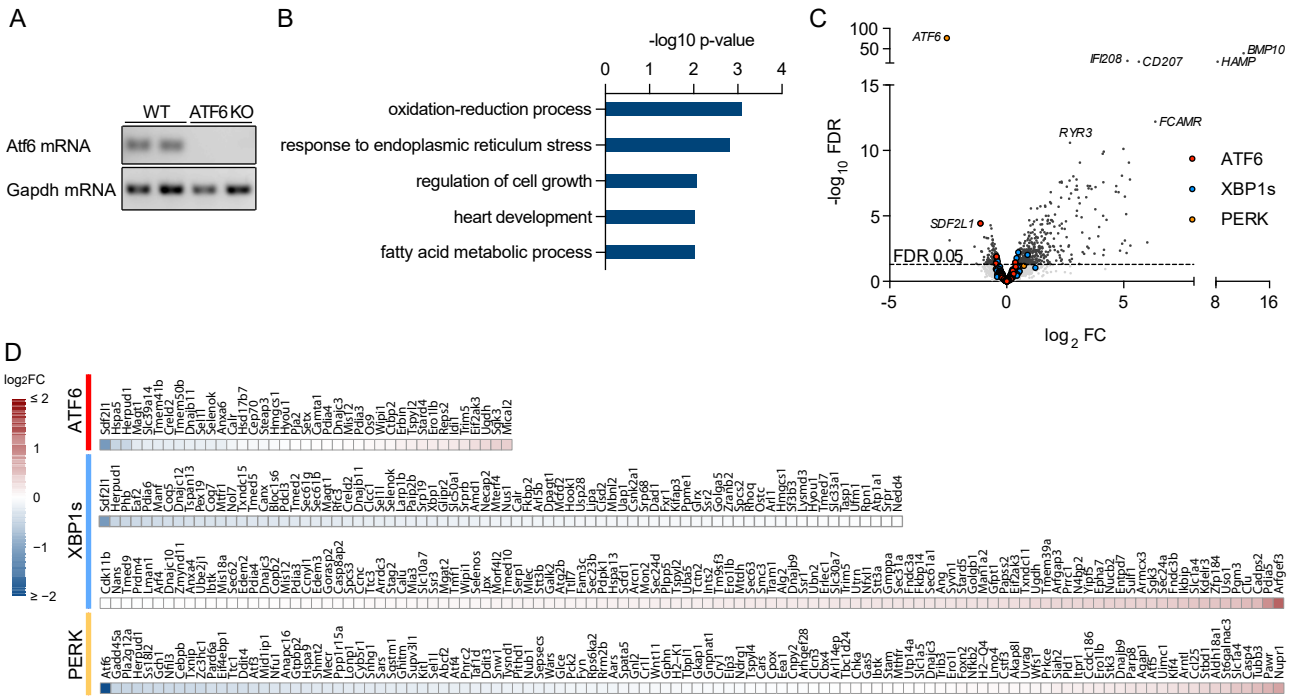

Figure 15 | mRNA Sequencing of ATF6 KO Mouse Hearts.

(A) ATF6 PCR of WT and ATF6 KO mice showing the successful knock-out of ATF6. (B) Enrichment of gene ontology terms (biological process) of significantly changed genes. (C) Volcano blots of transcriptional changes measured by RNA sequencing in adult ATF6 KO mice compared to WT mice. The highlighted colors indicate ATF6 (red), XBP1s (blue), or PERK (yellow) target genes. The horizontal dotted line indicates an FDR of 0.05. Genes above the line are considered significant (FDR < 0.05). 4 WT and 3 ATF6 KO adult mice were used for

the analysis. (D) Heat map showing the regulation of all ATF6 (red), XBP1s (blue) or PERK (yellow) target genes in ATF6 KO mice. Figure 15 was adapted from 'Age-related decline of the unfolded protein response in the heart promotes protein misfolding and cardiac pathology' (Hofmann et al. 2021).

ATF6 target genes are regulated via the binding of the transcriptional active 50kD N-terminal fragment of ATF6 to ERSE and ERSE-II elements in their respective promoter regions (Kokame et al. 2001; Yamamoto et al. 2004). Other transcriptionally active proteins are known to bind to the same elements as ATF6(N), which might compensate ATF6 deficiency (Correll et al. 2019; Thuerauf et al. 2004; Yamamoto et al. 2004). Among those are ATF6 beta and spliced XBP1. Indeed, rapid splicing of XBP1 could be observed when ATF6 activation was pharmacologically inhibited with the PF-429242 (Figure 16), a reversible, competitive inhibitor of sterol regulatory element-binding protein (SREBP) site 1 protease, which is required for the generation of the transcriptional active 50kD N-terminal fragment of ATF6 (Glembotski 2014). This indicates that cardiomyocytes respond to the inhibition of ATF6 activation with compensatory XBP1 splicing. While further mechanisms of compensation for ATF6 insufficiency were not investigated, it seems likely that cardiomyocytes can compensate a loss of ATF6 via the activation of other transcription factors that bind to ERSE and ERSE-II elements. It was therefore concluded that ATF6 is only required for the expression of a few unfolded protein response genes at baseline and is in general non-essential for the unfolded protein response in unstressed cardiomyocytes.

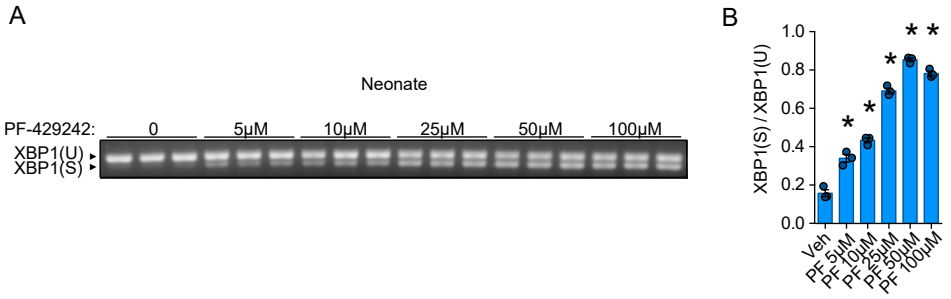

Figure 16 | XBP1 Splicing in Response to Acute ATF6 Inhibition.

(A) RT-PCR using primers that recognize the unspliced and spliced isoform of XBP1 with the respective quantification (B). Neonatal cardiomyocytes were treated with indicated doses of the ATF6 inhibitor PF-429242 for 24 hours. * indicates $p<0.05$ from control. Figure 16 was adapted from 'Age-related decline of the unfolded protein response in the heart promotes protein misfolding and cardiac pathology' (Hofmann et al. 2021).

4.3 Re-Induction of the ATF6 Branch of the Unfolded Protein Response during Adult Cardiomyocyte Hypertrophy

It was shown that cardiac protein synthesis and activation of the unfolded protein response, including the ATF6 branch, are compromised in adult mice. However, the *in vitro* model that was used to induce protein misfolding and ER stress via pharmacological inhibition of protein glycosylation might be insufficiently translatable to pathophysiological cardiac conditions in which protein misfolding occurs. One such condition that is commonly observed in the clinic is cardiac hypertrophy, in which the increased amount of protein synthesis drives cardiomyocyte growth and challenges the protein homeostasis environment (Heineke and Molkentin 2006). Importantly, large accumulations of misfolded proteins have been previously described in hypertrophic human hearts, at least in its failing stage (Sanbe et al. 2004). It was therefore hypothesized that the ATF6-mediated unfolded protein response is activated in

cardiomyocytes during phases of increased protein synthesis to protect against proteotoxic stress of increased protein load on the endoplasmic reticulum.

Chronic stimulation of adrenergic receptors of cardiomyocytes is known to initiate cardiomyocyte hypertrophy (Heineke and Molkentin 2006). Isolated neonatal cardiomyocytes were therefore subjected to the adrenergic receptor agonists phenylephrine (PE) and isoproterenol (ISO), which consistently induced cardiomyocyte hypertrophy and increased protein synthesis, measured by puromycin incorporation (Figure 17). However, neonatal cardiomyocyte hypertrophy was not associated with ATF6 activation or induction of total ATF6 protein levels (Figure 18A).

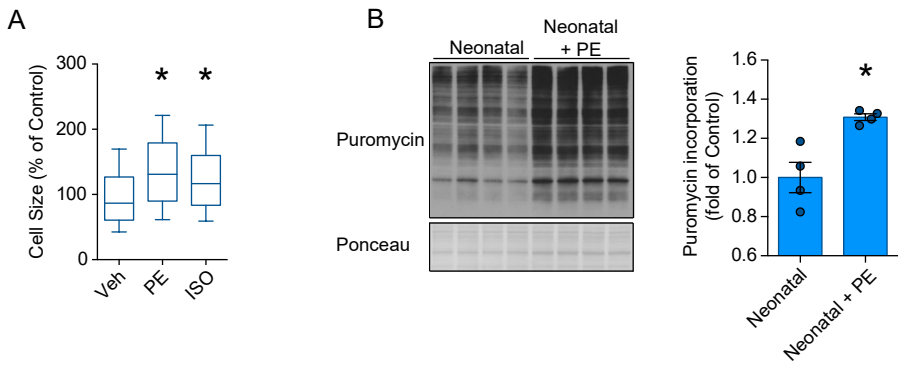

Figure 17 | Hypertrophic Growth Response of isolated Neonatal Cardiomyocytes subjected to Adrenergic Receptor Agonists.

(A) Cell surface area measurements of neonatal cardiomyocytes in response to PBS (Vehicle; Veh), phenylephrine (PE), or isoproterenol (ISO) for 24h. At least 800 cells were measured in total per condition in three independent experiments. (B) Immunoblot for Puromycin and respective quantification of vehicle or PE-treated neonatal cardiomyocytes. Cells were lysed 24h after treatment. * indicates $p<0.05$ from control.

In accordance with the absence of ATF6 activation, neonatal cardiomyocyte hypertrophy did also not lead to increased expression of canonical ATF6 targets both on the mRNA and protein level (Figure 18B and 18C). These results indicate that

neonatal cardiomyocytes are capable of hypertrophic growth without suffering from significant amounts of ER stress and protein misfolding that would require an increased expression of protein homeostasis genes. This does not exclude that more severe forms of cardiomyocyte hypertrophy can cause ER stress and protein misfolding in neonatal cardiomyocytes, though the results clearly indicate that such a phenotype was not occurring in the *in vitro* experiment setup used for this study.

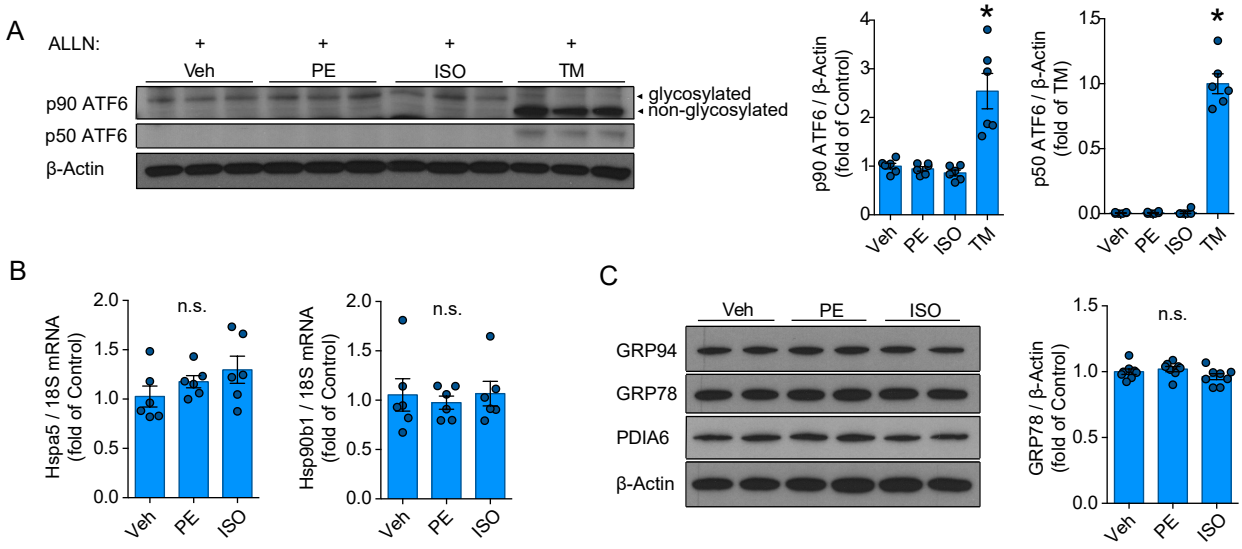

Figure 18 | Absence of ATF6 Activation and Unfolded Protein Response Induction during Neonatal Cardiomyocyte Hypertrophy.

(A) Full-length (p90) and active (p50) ATF6 immunoblots and respective quantifications of neonatal cardiomyocytes after 24h vehicle, PE, ISO, or TM treatment. Due to the rapid degradation of ATF6, all samples were treated with the protease inhibitor ALLN for 3 hours prior to lysing the cells. The two visible bands of p90 ATF6 represent its glycosylated and non-glycosylated forms after treatment with the glycosylation inhibitor TM. (B) mRNA levels of Hspa5 or Hsp90b1 after 24h of PE or ISO treatment normalized to 18S mRNA. (C) Immunoblots and respective quantification of GRP94, GRP78, and PDIA6 in neonatal cardiomyocytes treated with Veh, PE, or ISO for 24h, normalized to β-Actin protein levels. * indicates $p<0.05$ from all other samples.

A previous study highlighted the possibility of transient unfolded protein response induction in the absence of ER stress within minutes after growth factor stimulation in endothelial cells (Karali et al. 2014). To examine if such a rapid, but transient unfolded protein response activation occurs in cardiomyocytes, which could have been missed with the 24h treatment regime, XBP1 splicing was quantified in isolated neonatal cardiomyocytes 0.5h, 1h, and 3h after PE or ISO treatment. XBP1 splicing was used as a readout for unfolded protein response activation in this setup, because XBP1 splicing was previously described as a rapid and sensitive readout of ER stress (Yoshida et al. 2001). No XBP1 splicing could be observed at any of the tested treatment timepoints in neonatal cardiomyocytes (Figure 19A). Similarly, no XBP1 splicing occurred at 24h when cardiomyocyte hypertrophy is consistently observed (Figure 19B). The correct execution of the experiments was controlled with 24h of tunicamycin treatment as a positive control (Figure 19A, 19B and 19C).

Figure 19

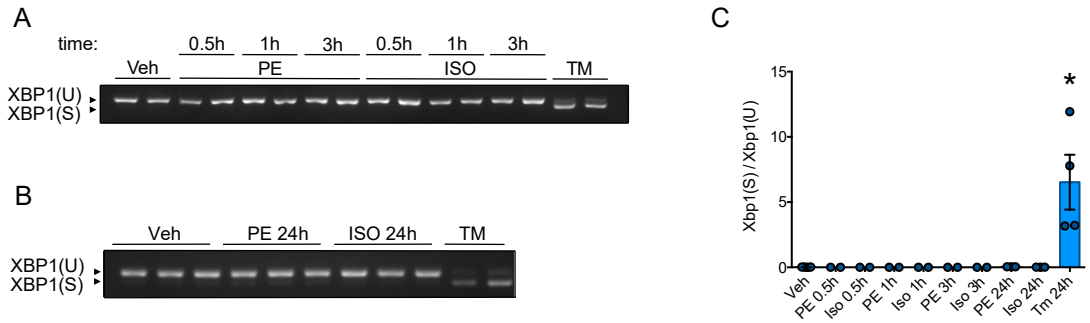

Figure 19 | Absence of XBP1 Splicing in Response to Adrenergic Stimulation in Neonatal Cardiomyocytes.

(A) and (B) XBP1 splicing of neonatal cardiomyocytes treated with vehicle, PE or ISO for the indicated timepoints. The vehicle timepoint matches the longest treatment of each panel. A 24h TM treatment was used as a positive control. Treatments were conducted in a way that all cells of the same experiment were lysed at the same time. (C) Quantification of all treatment timepoints. * indicates p<0.05 from control.

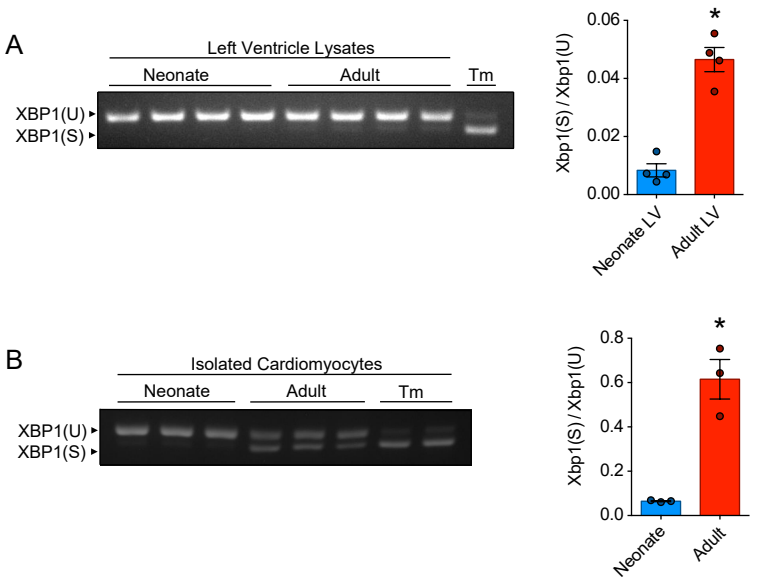

Figure 20 | XBP1 Splicing in the Unstressed Adult Heart.

(A) PCR for XBP1 splicing of left ventricular lysates from neonatal and adult hearts. A 24h TM treatment was used as a positive control. (B) PCR for XBP1 splicing of untreated isolated neonatal and adult rat cardiomyocytes. A 24h TM treatment was used as a positive control. * indicates p<0.05 from neonate.

In contrast to the absence of XBP1 splicing in neonatal cardiomyocytes at baseline or during hypertrophic growth, significant amounts of XBP1 splicing were observed in adult cardiomyocytes even at baseline (Figure 20). Similarly, XBP1 splicing was detectable in left ventricular lysates from adult hearts at baseline, compared to almost no detectable spliced XBP1 in neonatal left ventricular lysates (Figure 20). While the exact cause and consequence of the observed XBP1 splicing in adult hearts remains unknown, it is reasonable to assume that the low expression of the unfolded protein response in the adult mouse heart might cause mild ER stress even at baseline.

Based on the impaired responsiveness and increased susceptibility of adult cardiomyocytes to proteotoxic stress, it was hypothesized that contrary to neonatal cardiomyocytes, adult cardiomyocytes experience ER stress during phases of increased protein load to the endoplasmic reticulum when they undergo hypertrophic growth. Similar to the previous experiments, adult cardiomyocytes were treated with the adrenergic receptor agonists PE and ISO, as well as TM as a positive control. Both PE and ISO induced mild adult cardiomyocyte hypertrophy (Figure 21A), which was associated with increased expression of ATF6 (Figure 21B and 21C). Due to the low expression and rapid degradation of the transcriptionally active cleaved N-terminal fragment of ATF6, it was not possible to detect p50 ATF6 in adult cardiomyocytes. Nevertheless, transcriptional activity of ATF6 appears to be induced in response to adrenergic stimulation, due to a dose-dependent expression of ATF6 target genes both on the mRNA (Figure 21D) and protein level (Figure 21E and 21F).

To compare the unfolded protein response induction during hypertrophic growth of isolated adult cardiomyocytes with that observed in the experimental model of ER stress using pharmacological treatment with TM, adult cardiomyocytes were treated with increasing doses of TM for twenty-four hours, similar to the treatment timepoint

used in the hypertrophy model. Even the lowest concentration of TM (100nM) induced a higher unfolded protein response than the highest concentrations of adrenergic receptor agonists (Figure 22), indicating that if the unfolded protein response activation in adult cardiomyocytes in response to adrenergic stimulation is due the ER stress from hypertrophic growth, the amount of protein misfolding is likely much lower than that observed after TM treatment.

It should be noted that the expression of several unfolded protein response genes is dependent on the concentration of serum in the culture media (Figure 23A and 23B). A direct comparison between neonatal and adult cardiomyocytes for the expression of these genes is therefore only possible when the same media serum conditions are used for all cells. A direct comparison of neonatal and adult cardiomyocytes verified the decreased baseline expression of unfolded protein response genes in adult cardiomyocytes. It also confirmed the absence of their induction only in neonatal cardiomyocytes during hypertrophic growth stimulation, and the inability of adult cardiomyocytes to upregulate the unfolded protein response genes to levels similar to that of neonatal cardiomyocytes (Figure 23C).

Figure 21 | Activation of the ATF6-mediated Unfolded Protein Response in Adult Cardiomyocytes in Response to Adrenergic Stimulation-induced Hypertrophy.

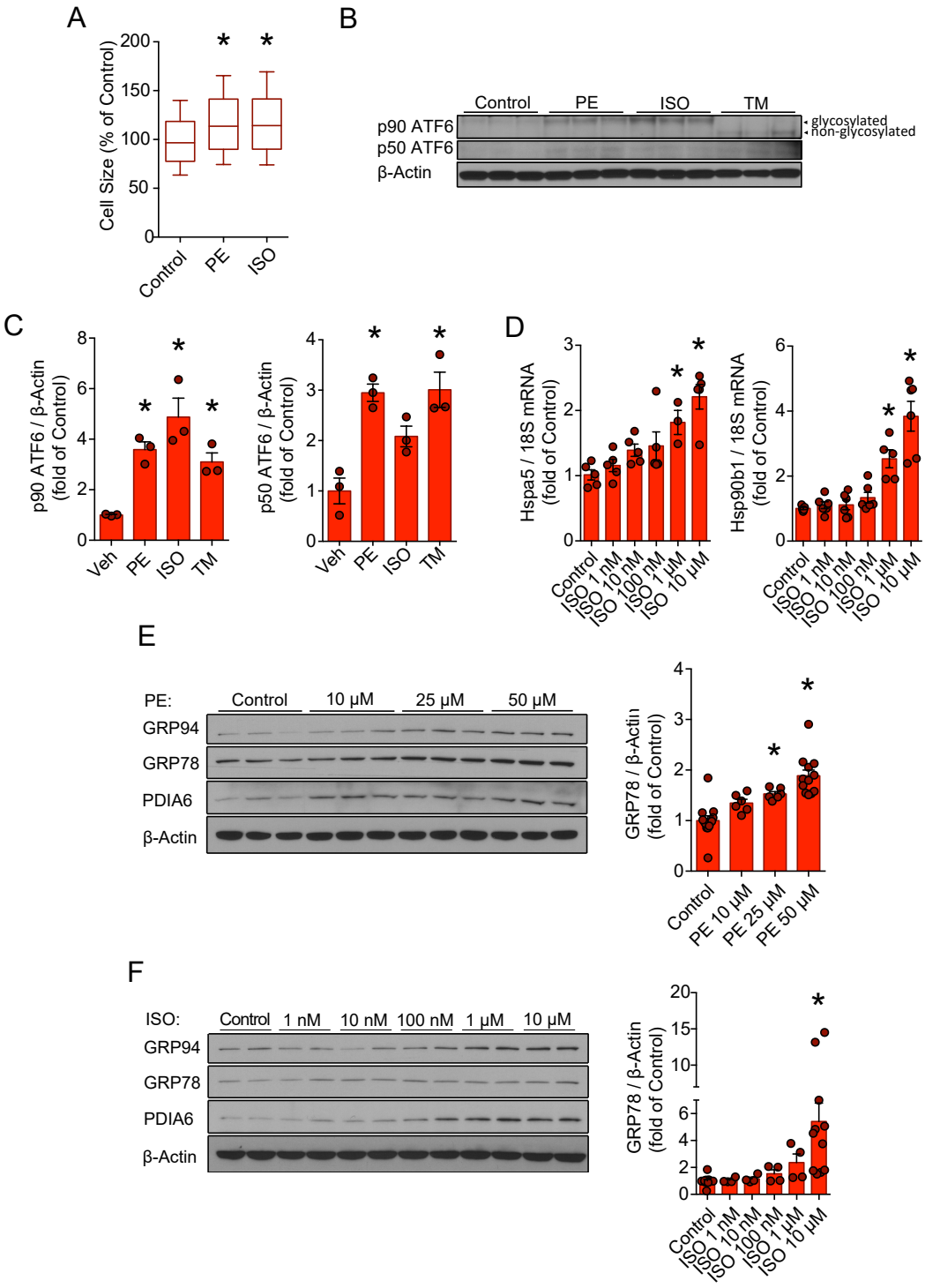

Figure 21 | Activation of the ATF6-mediated Unfolded Protein Response in Adult Cardiomyocytes in Response to Adrenergic Stimulation-induced Hypertrophy.

(A) Cell surface area measurements of adult cardiomyocytes in response to PBS (Veh), phenylephrine (PE), or isoproterenol (ISO) for 24h. At least 400 cells were measures in total per condition in three independent experiments. (B) p90 and p50 ATF6 immunoblots and respective quantifications (C) of adult cardiomyocytes after 24h vehicle, PE, ISO, or TM treatment. The two visible bands of p90 ATF6 represent its glycosylated and non-glycosylated form after treatment with the glycosylation inhibitor TM. (D) mRNA levels of Hspa5 or Hsp90b1 after 24h treatment of adult cardiomyocytes with increasing PE or ISO dosages normalized to 18S mRNA. (E and F) Immunoblots and respective quantifications of GRP94, GRP78, and PDIA6 in adult cardiomyocytes treated with increasing dosages of Veh, PE, or ISO for 24h, normalized to β-Actin protein levels. Figure 21 was adapted from 'Age-related decline of the unfolded protein response in the heart promotes protein misfolding and cardiac pathology' (Hofmann et al. 2021).

Figure 22 | Induction of the Unfolded Protein Response in Adult Cardiomyocytes in Response to Endoplasmic Reticulum Stress induced by Tunicamycin Treatment.

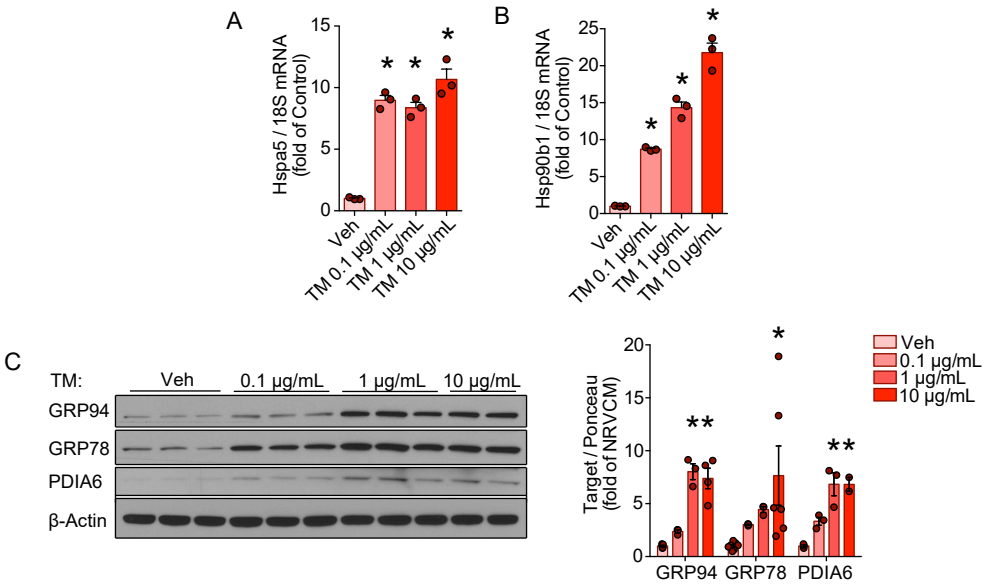

Figure 22 | Activation of the Unfolded Protein Response in Adult Cardiomyocytes in Response to Endoplasmic Reticulum Stress induced by Tunicamycin Treatment.

(A and B) Hspa5 and Hsp90b1 levels in adult cardiomyocytes treated with indicated doses of TM for 24h. (C) Immunoblot and respective quantifications of GRP94, GRP78, and PDIA6 of adult cardiomyocytes treated with indicated doses of TM for 24h. * indicates p<0.05 from control. Figure 22 was adapted from 'Age-related decline of the unfolded protein response in the heart promotes protein misfolding and cardiac pathology' (Hofmann et al. 2021).

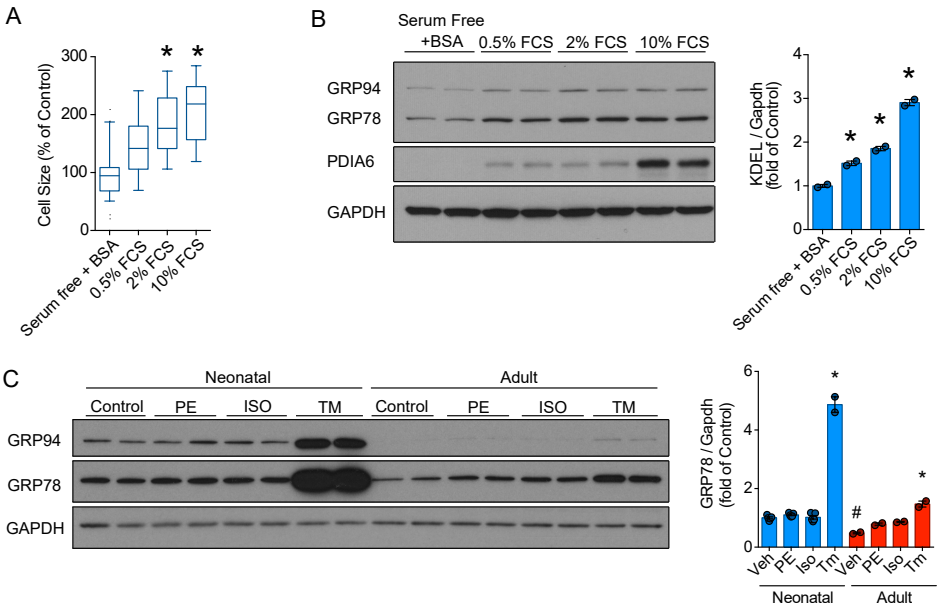

Figure 23 | Comparison of the Unfolded Protein Response Activation during Neonatal and Adult Cardiomyocyte Hypertrophy.

(A) Cell surface area measurements of adult cardiomyocytes in response to serum free media, supplemented with BSA, or increasing dosages of fetal calf serum. At least 25 cells were measured for each condition. (B) Immunoblot and respective quantifications of GRP94, GRP78, and PDIA6 of neonatal cardiomyocytes cultured in indicated dosages of serum. (C) Immunoblot and respective quantifications of GRP94 and GRP78 of neonatal and adult cardiomyocytes treated with PE, ISO or TM for 24h. * indicates p<0.05 from all other samples. # indicates p<0.05 to neonatal vehicle.

To confirm that the results from isolated cardiomyocytes *in vitro* are translatable to an *in vivo* model of increased cardiac protein synthesis and cardiac hypertrophy, left ventricular lysates of mice that underwent transverse aortic constriction (TAC) surgery were used to quantify protein levels of the ATF6 target genes GRP94, GRP78, and PDIA6 (Figure 24). TAC surgery is a model of pressure overload-induced cardiac hypertrophy, in which a suture around the aortic arch is used to induce aortic stenosis, resulting in cardiac hypertrophy (deAlmeida et al. 2010; Rockman et al. 1991). Hearts were isolated three hours and two days after surgery. Increased protein synthesis is robustly detectable at two days post-surgery, whereas the three-hour timepoints was used to exclude unspecific effects from the invasiveness of the surgery or anesthesia. Significantly increased protein levels of the ATF6 targets were detectable at two days post-surgery when increased protein synthesis and hypertrophic growth is observable, whereas no regulation of the proteins was seen at three hours post-surgery (Figure 24), indicating that the increased expression of the ATF6 target genes is primarily associated with the hypertrophic growth response after TAC surgery.

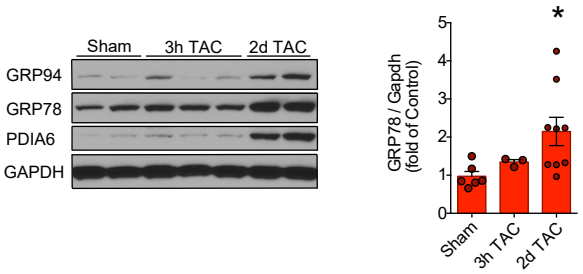

Figure 24 | Unfolded Protein Response induction in the Adult Mouse Heart after Transverse Aortic Constriction.

Immunoblots and respective quantification of GRP94, GRP78, and PDIA6 of left ventricular lysates from mice 3h or 2d after TAC surgery. Sham mice were sacrificed after 2d. * indicates $p<0.05$ from Sham. Figure 24 was adapted from 'Age-related decline of the unfolded protein response in the heart promotes protein misfolding and cardiac pathology' (Hofmann et al. 2021).

These results were further validated in an additional unbiased sequencing screen for transcriptional and post-transcriptional gene regulation after TAC surgery. To this end, publicly available RNA sequencing, cardiomyocyte-specific ribosome profiling, and quantitative mass spectrometry-based proteomics datasets generated from the left ventricle of mice that were subjected to sham or TAC surgery were retrospectively analyzed (Doroudgar et al. 2019). Among the top regulated GO categories, the terms 'Protein folding' and 'Response to ER stress' could be found in the two-day post TAC surgery group (Figure 25), indicating that among the significantly regulated genes in response to TAC surgery, those that function in protein homeostasis and the unfolded protein response are significantly enriched. In addition, many unfolded protein response genes were found to be regulated both on the transcriptional and translational level at two days after TAC surgery (Figure 26).

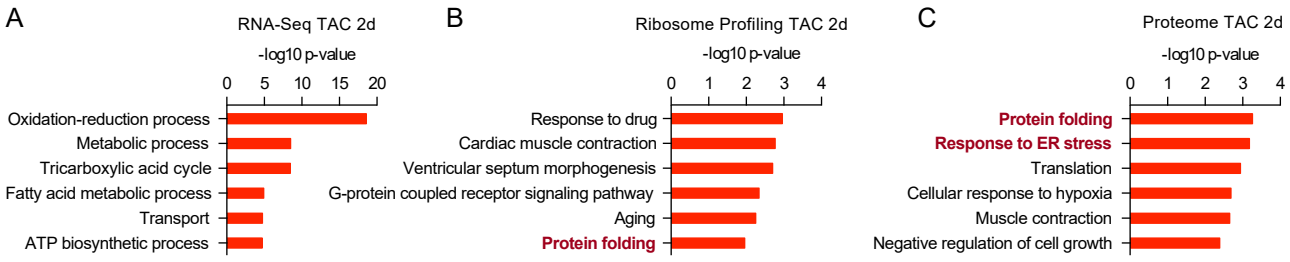

Figure 25 | Enrichment of the Regulation of Proteostasis-associated Genes in Response to Transverse Aortic Constriction Surgery.

Enrichment of gene ontology terms (biological process) of RNA-Seq (A), ribosome profiling (B), and quantitative mass spectrometry-based proteomics (C) 2d post-TAC or sham surgery. RNA-Seq and ribosome profiling libraries were derived from left ventricular lysates of Ribo-Tag mice. Proteome data is based on isolated cardiomyocytes from similarly treated mice. Figure 25 was adapted from ‘Age-related decline of the unfolded protein response in the heart promotes protein misfolding and cardiac pathology’ (Hofmann et al. 2021).

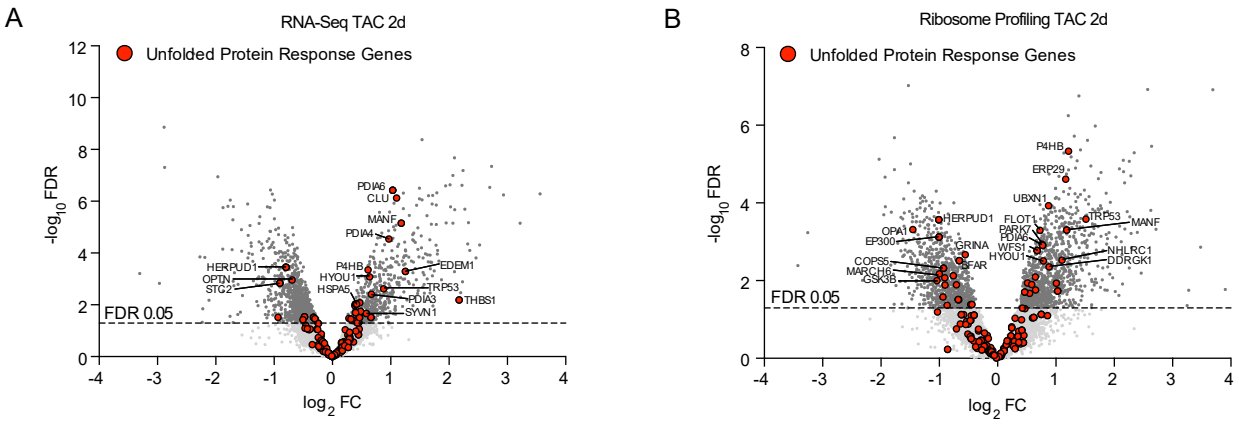

Figure 26 | Unfolded Protein Response Induction in the Adult Mouse Heart after Transverse Aortic Constriction.

Transcriptional (A) or translational (B) regulation of unfolded protein response genes 2d after TAC surgery. Transcripts were considered significant when false discovery rate (FDR) was <0.05. Figure 26 was adapted from 'Age-related decline of the unfolded protein response in the heart promotes protein misfolding and cardiac pathology' (Hofmann et al. 2021).

An in-depth analysis of the gene targets of the three major branches of the unfolded protein response, ATF6, IRE1 (XBP1s), and PERK revealed that all three branches are activated after TAC surgery, with a mild regulation at three hours, a peak of the number of regulated genes at two days, followed by a reduction of regulated genes at two weeks, both on the transcriptional and translational levels (Figure 27 and Figure 28). Taken together, the results indicate that upon hypertrophic growth of adult cardiomyocytes, which is associated with increased protein load to the endoplasmic reticulum, the unfolded protein response, including the ATF6 branch, is activated. This results in the upregulation of gene networks that maintain protein quality control, which might be necessary to enable adult cardiomyocyte growth. In contrast to adult cardiomyocytes, hypertrophic growth of neonatal cardiomyocytes is not necessarily associated with the activation of the unfolded protein response, eventually due to their

higher baseline expression of protein quality control elements, which then might protect from ER stress at the tested experimental conditions.

Figure 27 | Transcriptional Unfolded Protein Response Induction in Response to Transverse Aortic Constriction in the Adult Heart.

(A, B and C) Volcano plots of transcriptional changes after 3h, 2d or 2wk TAC surgery in mice compared to time-matched sham controls. The highlighted colors indicate ATF6 (red), XBP1s (blue), or PERK (yellow) target genes. The horizontal dotted line indicates an FDR of 0.05. Genes above the line are considered significant (FDR < 0.05). (D) Enrichment of gene ontology terms (biological process) of significantly changed ATF6 (red), XBP1s (blue), or PERK (yellow) target genes 2d after TAC surgery. (F) Heat map showing the transcriptional regulation of all ATF6 (red), XBP1s (blue), or PERK (yellow) target genes 2d after TAC surgery. Figure 27 was adapted from 'Age-related decline of the unfolded protein response in the heart promotes protein misfolding and cardiac pathology' (Hofmann et al. 2021).

Figure 28 | Translational Unfolded Protein Response Induction in Response to Transverse Aortic Constriction in the Adult Heart.

(A, B and C) Volcano plots of translational changes after 3h, 2d, or 2wk TAC surgery in mice compared to time-matched sham controls. The highlighted colors indicate ATF6 (red), XBP1s (blue), or PERK (yellow) target genes. The horizontal dotted line indicates an FDR of 0.05. Genes above the line are considered significant (FDR < 0.05). (D) Enrichment of gene ontology terms (biological process) of significantly changed ATF6 (red), XBP1s (blue), or PERK (yellow) target genes 2d after TAC surgery. (F) Heat map showing the translational regulation of all ATF6 (red), XBP1s, (blue) or PERK (yellow) target genes 2d after TAC surgery. Figure 28 was adapted from 'Age-related decline of the unfolded protein response in the heart promotes protein misfolding and cardiac pathology' (Hofmann et al. 2021).

Figure 27 | Transcriptional Unfolded Protein Response Induction in Response to Transverse Aortic Constriction in the Adult Heart.

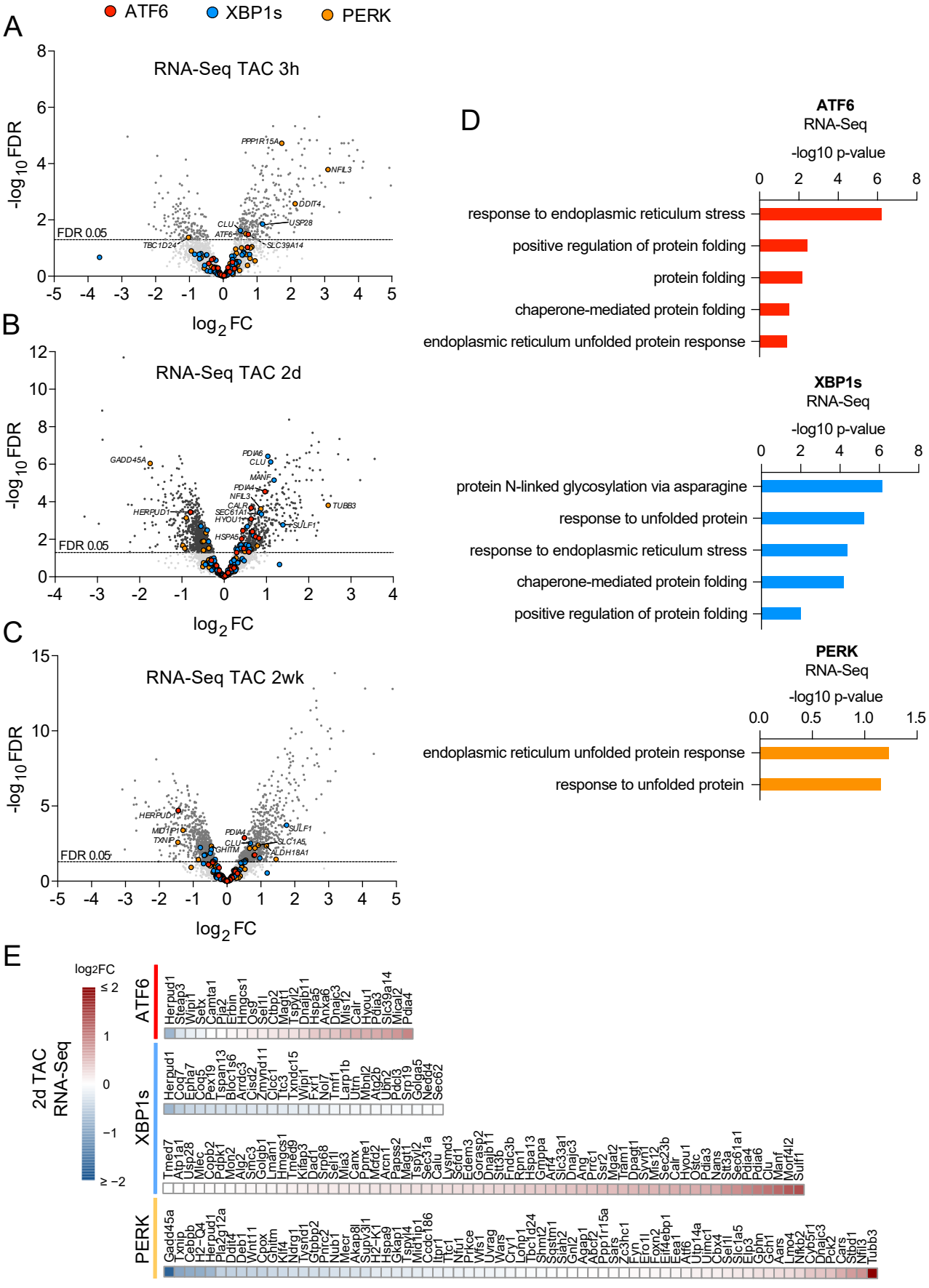

Figure 28 | Translational Unfolded Protein Response Induction in Response to Transverse Aortic Constriction in the Adult Heart.

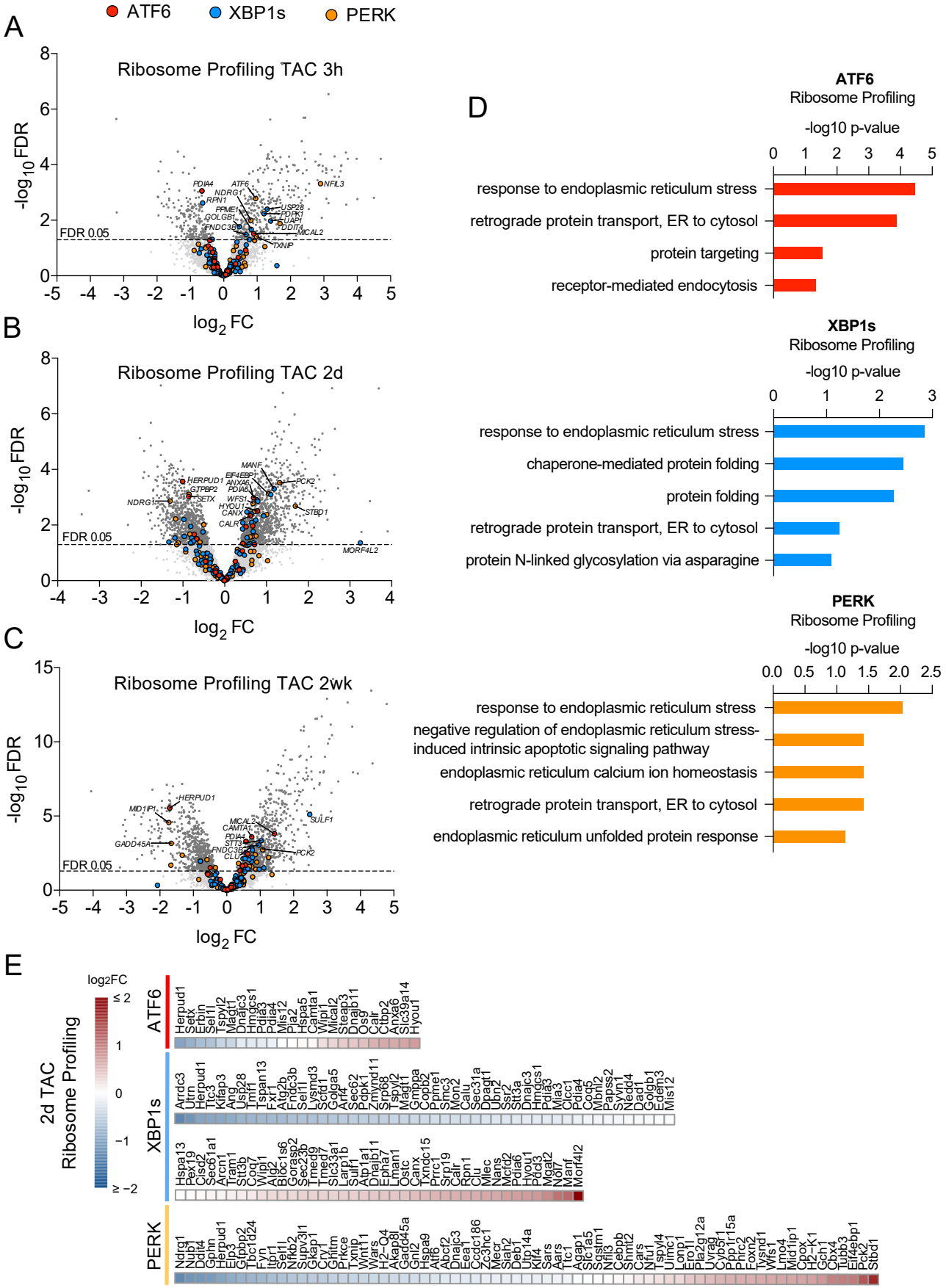

4.4 Insufficient ATF6 Activation Impairs the Myocardial Hypertrophic Growth Response during Cardiac Stress

To investigate the functional role of ATF6 during cardiomyocyte hypertrophy, isolated neonatal cardiomyocytes were subjected to siRNA-mediated knock-down of ATF6 followed by adrenergic stimulation with PE to induce hypertrophic growth. siRNA-mediated knock-down of ATF6 resulted in an approximately 90% reduction of ATF6 gene expression (Figure 29A). ATF6 knock-down did not affect cell size at baseline, however ATF6 deficiency led to an attenuated growth response when cardiomyocytes were treated with PE (Figure 29B).

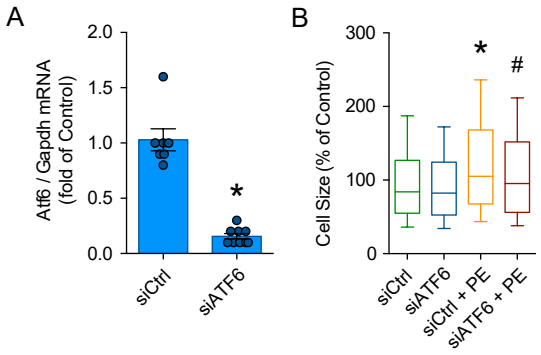

Figure 29 | Attenuated Hypertrophic Growth Response of ATF6 deficient Neonatal Cardiomyocytes.

(A) ATF6 mRNA levels after siRNA mediated knock-down in neonatal cardiomyocytes. (B) Cell surface area measurements of neonatal cardiomyocytes after siRNA-mediated ATF6 knock-down in response to PE for 24h. Figure 29 was adapted from 'Age-related decline of the unfolded protein response in the heart promotes protein misfolding and cardiac pathology' (Hofmann et al. 2021).

Next, adult wild-type and ATF6 knock-out mice were subjected to implantation of ISO loaded ALZET osmotic mini pumps, a common model of cardiac hypertrophy *in vivo* (Chang et al. 2018). As described above, ATF6 KO mice did not show a significant cardiac growth phenotype at baseline (Figure 30A). In contrast to WT mice, which showed cardiac hypertrophy at seven days after chronic ISO infusion, ATF6 KO mice presented with only a mild, significantly reduced cardiac growth response (Figure 30A). Similar to the *in vitro* data of adult cardiomyocytes, cardiac hypertrophy was associated with the induction of several unfolded protein response genes in adult WT mice, which was almost completely absent in ATF6 KO mice (Figure 30B). The *in vivo* model does not lead to cardiac dysfunction in WT mice at seven days, a timepoint that remains fully compensatory despite the robust hypertrophic phenotype (Figure 30C). Contrary, ATF6 KO mice showed reduced cardiac function at seven days of chronic ISO infusion, measured by transthoracic echocardiography (Figure 30C, Table 2). In line with this observation, the fetal gene program including Nppa, Nppb, Myh7, Col1a1, and Atp2a2 was only significantly upregulated in ATF6 KO mice, whereas those genes were not yet significantly changed in WT mice, suggesting the occurrence of heart failure in ATF6 KO mice at this timepoint (Figure 30D). To investigate if the impaired growth response of ATF6 deficient cardiomyocytes is due to the absence of the ATF6-dependent gene program or due to other currently unknown functions of ATF6, two different *in vitro* models were used to specifically inhibit the transcriptional activity of the N-terminal fragment of ATF6 in cardiomyocytes.

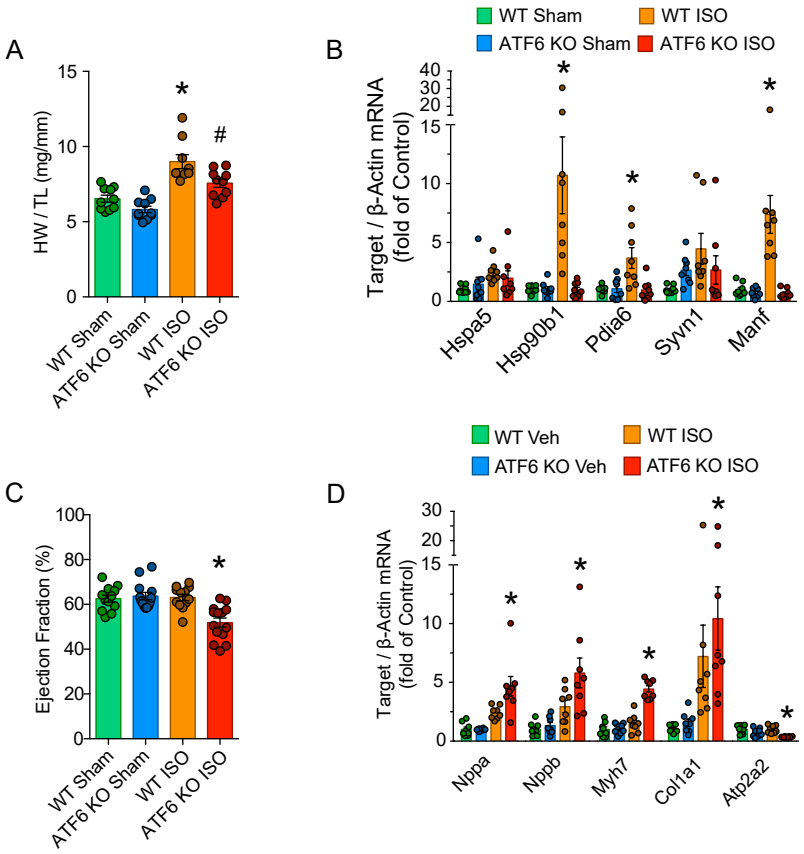

Figure 30 | Impairment of the Adaptive Hypertrophic Growth Response in ATF6 Knock-out Mice.

(A) Heart weight (HW) to body weight (BW) ratio of WT and ATF6 KO mice subjected to sham or ISO pump implantation for seven days. (B) mRNA levels of respective unfolded protein response genes normalized to β-actin of WT and ATF6 KO mice subjected to sham or ISO pump implantation at seven days. (C) Ejection fraction of WT and ATF6 KO mice subjected to sham or ISO pump implantation at seven days. (D) mRNA levels of respective maladaptive remodeling genes normalized to β-Actin of mice subjected to sham or ISO pump implantation at seven days. * indicates $p<0.05$ from all other conditions; # indicates $p<0.05$ from WT ISO. ATF6 KO ISO is not significantly different from WT ISO for Col1a1. ATF6 KO ISO is not significantly different from ATF6 KO Veh for Atp2a2. Figure 30 was adapted from 'Age-related decline of the unfolded protein response in the heart promotes protein misfolding and cardiac pathology' (Hofmann et al. 2021). qPCRs of Figure 30B and Figure 30D were performed by Erik A. Blackwood, a coauthor of the study (Hofmann et al. 2021).

Table 2: 7-day Isoproterenol Echocardiographic Parameters for WT and ATF6 KO Mice

	WT Sham (n=12)	ATF6 KO Sham (n=13)	WT ISO (n=12)	ATF6 KO ISO (n=14)
FS (%)	33.20 ± 1.09	34.03 ± 1.28	33.76 ± 1.01	26.24 ± 1.25[1,2]
EF (%)	62.56 ± 1.55	63.69 ± 1.65	63.09 ± 1.44	51.85 ± 2.05[1,2]
LVEDV (µl)	55.56 ± 3.16	50.70 ± 2.09	67.57 ± 3.09[1]	62.25 ± 2.98[1]
LVESV (µl)	21.14 ± 1.88	18.57 ± 1.28	26.17 ± 1.75	30.20 ± 2.20[1]
LVIDD (mm)	3.57 ± 0.08	3.43 ± 0.05	3.86 ± 0.08	3.76 ± 0.08[1]
LVIDS (mm)	2.51 ± 0.07	2.37 ± 0.08	2.59 ± 0.06	2.75 ± 0.10[1]
LVPW;d (mm)	0.79 ± 0.05	0.72 ± 0.03	0.98 ± 0.02[1]	0.90 ± 0.04[1]
LVPW;s (mm)	1.16 ± 0.07	1.08 ± 0.04	1.39 ± 0.04	1.23 ± 0.05
LVAW;d (mm)	0.89 ± 0.06	0.86 ± 0.04	1.12 ± 0.08	0.99 ± 0.06
LVAW;s (mm)	1.28 ± 0.06	1.17 ± 0.04	1.54 ± 0.08[1]	1.35 ± 0.07
LV mass (mg)	106.84 ± 7.36	90.22 ± 3.84	158.55 ± 11.67[1]	134.53 ± 8.12[1]
HR (bpm)	480.67 ± 4.27	489.85 ± 4.01	493.58 ± 3.06	488.43 ± 2.60
SV (µl)	34.42 ± 1.58	32.13 ± 1.19	41.73 ± 2.20[1]	32.01 ± 1.73[2]
CO (ml/min)	16.50 ± 0.69	15.73 ± 0.59	20.61 ± 1.10[1]	15.26 ± 0.99[2]

FS = fractional shortening
EF = ejection fraction
LVEDV = left ventricular end diastolic volume
LVESV = left ventricular end siastolic volume
LVIDD = left ventricular inner diameter in diastole
LVIDS = left ventricular inner diameter in systole
LVPW;d = left ventricular posterior wall thickness in diastole
LVPW;s = left ventricular posterior wall thickness in systole
LVAW;d = left ventricular anterior wall thickness in diastole
LVAW;s = left ventricular anterior wall thickness in systole
LV mass = left ventricular mass (calculated)
HR = heart rate in beats per minute
SV = stroke volume
CO = cardiac output

Statistical analyses used one-way ANOVA with Turkey post-hoc analysis.
[1] = $p < 0.05$ different from respective Sham
[2] = ATF6 KO ISO $p < 0.05$ different from WT ISO

Table 2 was adapted from 'Age-related decline of the unfolded protein response in the heart promotes protein misfolding and cardiac pathology' (Hofmann et al. 2021).

ATF6 is cleaved and thereby activated by site-1 and site-2 proteases in the Golgi apparatus, which leads to the release of the transcriptional active 50kD N-terminal fragment of ATF6 (Glembotski 2014). The site-1 protease inhibitor PF-429242 inhibits ATF6 cleavage, thereby hindering transcriptional activity of ATF6 (Hay et al. 2007; Lebeau et al. 2018). PF-429242 did not affect cardiomyocyte cell size at baseline. However, PE-mediated hypertrophic growth was completely absent in neonatal cardiomyocytes which were treated with PF-429242 (Figure 31A and 31B). To exclude off-target effects that might have occurred from inhibiting other functions of site-1 protease, a dominant-negative form of ATF6, dnATF6, was expressed via adenoviral-mediated transfection of neonatal cardiomyocytes. dnATF6 exhibits a DNA-binding domain but lacks its transcriptional activation domain, thereby inhibiting ATF6-mediated gene induction by blocking ATF6 binding sides in cardiomyocytes (Doroudgar et al. 2009). Similar to PF-429242, expression of dnATF6 did not affect cell size at baseline. Cardiomyocyte growth was largely inhibited in cardiomyocytes expressing dnATF6 (Figure 31C), which supports the hypothesis that the induction of the ATF6-mediated gene program is essential for cardiomyocytes hypertrophy.

Figure 31 | Necessity of Transcriptional Activity of ATF6 for Cardiomyocyte Hypertrophy.

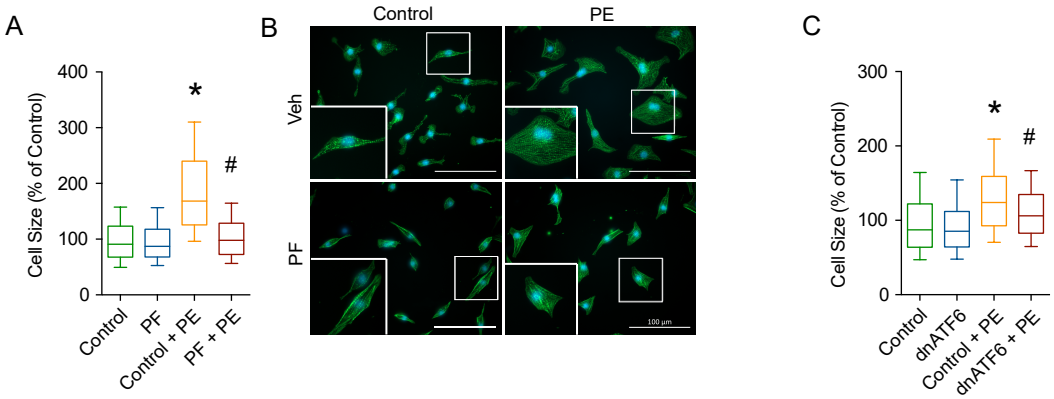

Figure 31 | Necessity of Transcriptional Activity of ATF6 for Cardiomyocyte Hypertrophy.

(A) Cell surface area measurements and representative immunofluorescence images (B) of neonatal cardiomyocytes after PF-429242 treatment in response to PE for 24h. (C) Cell surface area measurements of neonatal cardiomyocytes after dnATF6 treatment in response to PE for 24h. At least 400 cells were counted in total per condition in three independent experiments for (A) and (C). * indicates $p<0.05$ from Control; # indicates $p<0.05$ from Control + PE. Figure 31 was adapted from 'Age-related decline of the unfolded protein response in the heart promotes protein misfolding and cardiac pathology' (Hofmann et al. 2021).

5 Discussion

This discussion is partly based on the preprint article 'Age-related decline of the unfolded protein response in the heart promotes protein misfolding and cardiac pathology' (Hofmann et al. 2021).

5.1 Reduced Protein Synthesis and Unfolded Protein Response Expression in Adult Mammalian Tissues with low Mitotic Activity

Impairment of protein homeostasis is a general hallmark of aging. It is associated with several age-related disease during which the intra- or extracellular accumulation of misfolded proteins can be commonly observed, especially during phases of stress. Interventions that strengthen the proteostasis network were shown to extend the lifespan of invertebrates and vertebrates, including mammals, by suppressing age-related disease (Eisenberg et al. 2016; Harrison et al. 2009; Kaushik and Cuervo 2015; Labbadia and Morimoto 2014). One of several signaling pathways which maintains protein homeostasis is the unfolded protein response, which is activated in response to endoplasmic reticulum-associated protein misfolding (Hetz and Papa 2018). Among

several of its important functions is the increase of the capacity of protein folding, degradation, and cellular redox status, especially inside the endoplasmic reticulum (Hetz and Papa 2018). Previous studies showed that enhanced activity of the unfolded protein response increases longevity in yeast, *C. elegans*, and Drosophila (Burkewitz et al. 2020; Chen et al. 2009; Henis-Korenblit et al. 2010; Kaushik and Cuervo 2015; Labunskyy et al. 2014; Matai et al. 2019; Sekiya et al. 2017; Shore et al. 2012). While the majority of those studies were performed in invertebrates, studies that systematically examine the unfolded protein response in mammalian aging are currently limited. This study aimed to investigate the expression and activity of the unfolded protein response during postnatal development and aging in rodents, with a specific emphasis on the functional relevance for the heart.

Current studies in *C. elegans* suggest that the collapse of the proteostasis network is a programmed event which occurs during early adulthood (Ben-Zvi et al. 2009; David et al. 2010; Labbadia and Morimoto 2015b). In order to reduce the number of animals needed for statistical power, this study limited its analysis to up to three different age groups which capture the transition from neonate to young and late adulthood. Specifically, neonatal (7 days), young adult (10 weeks), and middle-aged (52 weeks) mice as well as neonatal (1-2 days) and young adult (6 weeks) rats were used for the study. Comparable to the reports in *C. elegans*, expression and activity of the unfolded protein response, as well as the overall rate of protein synthesis, reduced dramatically in young adult rodents, whereas only a slight additional reduction was observed from young adulthood to aged animals. While a reduced unfolded protein response was observed in all evaluated organs (brain, heart, skeletal muscle, liver and kidney), this decrease was especially prominent in tissues with low mitotic activity. Explanations for the evolutionary benefit of such a general impairment of the cellular proteostasis capacity remain hypothetical but currently involve the elimination of older animals for

a prioritization of the younger generation in an environment with limited resources, as well as the reduction of energy consumption for the synthesis of proteostasis regulators in old cells in which high rates of protein synthesis, which are necessary for rapid cellular differentiation early in life and during cell division, become non-essential as cells enter senescence (Labbadia and Morimoto 2015a; Labbadia and Morimoto 2015b).

This study finds evidence for the latter due to the observation that tissues which maintain high levels of cellular division maintain both high rates of protein synthesis and high levels of the unfolded protein response. Similarly, the rate of protein synthesis correlated highly with the expression of several unfolded protein response genes across all organs and age groups in mice. Whether the reduction of protein synthesis or the reduced expression of the unfolded response occurs first and then drives the downregulation of the other pathway was not addressed in this study, however evidence for both exists in the literature. A recent study found that proteome homeostasis in hematopoietic stem cells is maintained through the attenuation of protein synthesis (Hidalgo San Jose et al. 2020). Vice versa, the levels of the unfolded protein response is known to respond to the amount of protein synthesis (Ozcan et al. 2008). Nevertheless, this study finds evidence for a direct relationship between the rate of protein synthesis and the expression of the unfolded protein response in mammals *in vivo*, which seems to undergo major regulatory changes during postnatal development and aging in all examined organs, especially in tissues with low mitotic activity such as the heart.

5.2 Impaired Responsiveness of the ATF6-mediated Unfolded Protein Response to Proteotoxic Stress in Adult Cardiomyocytes

The observed reduced baseline expression of protein quality control genes is not necessarily pathogenic if the proteostasis environment can be sufficiently upregulated in phases of proteotoxic stress. Studies in *C. elegans*, however, showed that an appropriate activation of the heat shock response or the unfolded protein response is compromised after early adulthood (Ben-Zvi et al. 2009; Taylor and Dillin 2013). This study found that even though adult cardiomyocytes are capable of partly activating the unfolded protein response during phases of proteotoxic stress, both the total and relative increases of the unfolded protein response genes regulated by the ATF6 pathway were largely compromised in adult cardiomyocytes compared to neonatal cardiomyocytes. This was associated with reduced cellular survival.

ATF6 was previously shown to be essential for the induction of several unfolded protein response genes during proteotoxic stress *in vitro* and *in vivo* (Jin et al. 2016). It is therefore reasonable to speculate that the loss of ATF6 activity is at least partly responsible for the phenotype that was observed in adult cardiomyocytes. It should however be noted that the evaluation of cardiac gene expression in ATF6 deficient mice did not reveal a significant impact on the expression of the majority of unfolded protein response genes at baseline. ATF6 therefore seems to primarily act as a stress transcription factor that can become activated by different upstream events in the adult heart, albeit to lower levels than during younger age. The increased levels of spliced XBP1 in both isolated adult cardiomyocytes as well as in left ventricular lysates even at baseline might indicate that the reduced levels of the unfolded protein response in the adult heart might directly cause endoplasmic reticulum stress. However, whether XBP1 splicing indeed indicates endoplasmic reticulum stress or occurs due to other

reasons, and if this is mediated in any way by the decreased levels of ATF6 in the adult heart, remains unresolved.

5.3 Insufficient ATF6 Activation Inhibits the Myocardial Hypertrophic Growth Response and Impairs Cardiac Function during Stress

This study found an association between the rate of protein synthesis and the expression of the unfolded protein response, which might be at least partly mediated by ATF6. Cardiac hypertrophy is a commonly observed phenotype that occurs in response to myocardial stress. It is facilitated by increases in the rate of protein synthesis which then drives hypertrophic growth of cardiomyocytes. Disproportional increases of protein synthesis are known to cause endoplasmic reticulum stress (Ozcan et al. 2008). It was therefore evaluated if increases in the rate of protein synthesis cause endoplasmic reticulum stress during cardiomyocyte hypertrophy, which might occur especially in the adult heart where the unfolded protein response is attenuated. Different model systems of increased protein synthesis and cardiomyocyte hypertrophy failed to activate ATF6 or induce the upregulation of several unfolded protein response genes in neonatal cardiomyocytes. The expression of the unfolded protein response is high in neonatal myocytes at baseline. This study observed 30% increase of protein synthesis in one of the two model systems used to induce cardiomyocyte hypertrophy in neonatal cells. Cell size increased by approximately 30% in the neonatal model systems used. The high baseline unfolded protein response in neonatal cardiomyocytes might be sufficient to maintain proteostasis during those conditions, which is why the unfolded protein response might have remained unchanged during neonatal cardiomyocyte hypertrophy. It should be noted that other studies previously reported an activation of the unfolded protein response in isolated

neonatal cardiomyocytes in response to insulin (Blackwood et al. 2019b), phenylephrine (Blackwood et al. 2019b; Zhang et al. 2019) or isoproterenol and angiotensin II treatments (Chen et al. 2017), even though some inconsistencies can be found in one of the studies (Zhang et al. 2019). One of the studies reported the increase of cell size in their experimental setup, in which a starving protocol combined with a longer treatment time results in an almost 3-fold increase of cardiomyocytes size. Of note, these results could not be repeated when the respective treatment protocol was followed. While it was not possible to confirm these results, it is still reasonable to hypothesize that very strong growth stimuli that result in large changes of the rate of protein synthesis, can cause endoplasmic reticulum stress and activation of the unfolded protein response also in neonatal cardiomyocytes.

Contrary to neonatal cardiomyocytes, all model systems used to induce cardiomyocyte hypertrophy in adult cells *in vitro* and *in vivo* caused a rapid and treatment intensity-dependent activation of the unfolded protein response. The experiments of this study indicated that the activation of the unfolded protein response does not sufficiently counteract endoplasmic reticulum stress and cell deaths in adult cardiomyocytes in response to artificially induced proteotoxic stress. However, the amount of proteotoxic stress caused by the increase of protein synthesis is likely much less compared to the experiments where tunicamycin was used to induce protein misfolding by inhibiting protein glycosylation. Whether the induction of the unfolded protein response is also insufficient to protect from proteotoxic stress during adult cardiomyocyte hypertrophy is therefore unknown. Further experiments are needed to clarify if the reduced unfolded protein response in adult and aged rodents is of pathophysiological relevance in disease relevant animal models.

To specifically evaluate the role of ATF6 for adult cardiac hypertrophy and function, ATF6 deficient isolated cardiomyocytes and mice were subjected to chronic adrenergic stimulation, a common model to induce hypertrophic growth. ATF6 deficiency resulted in an impaired growth response and a reduction of cardiac function *in vivo*. This was associated with the inability of the heart to activate the unfolded protein response, which indicates a direct relationship between the unfolded protein response and cardiac function during cardiac hypertrophy. Indeed, specific inhibition of the transcriptional activity of ATF6 was sufficient to impair the cardiomyocyte growth response, highlighting the importance of the ATF6-mediated gene program, which includes a large number of genes that maintain cellular proteostasis, for cardiac hypertrophy. Other ATF6 target genes that do not function in protein homeostasis might also be involved in this process, as recently suggested (Blackwood et al. 2019b).

6 Summary

The integrity of the proteome is essential for optimal cardiac function. Proteome integrity is maintained by the proteostasis network, which regulates cellular protein synthesis, folding, and degradation. An insufficient capacity of the proteostasis network results in the accumulation of toxic misfolded proteins, which impairs cellular function and can promote cell death. The integrity of the cardiac proteome is challenged during phases of stress, where cells augment the capacity of the proteostasis network to prevent protein misfolding. This is mediated by several adaptive mechanisms such as the induction of chaperones or the increased degradation of misfolded proteins. One essential element of the proteostasis network is the unfolded protein response, which maintains protein homeostasis of the endoplasmic reticulum. The canonical unfolded protein response is mediated by three sensors of protein misfolding, including activating transcription factor 6, which has been suggested to act as a nexus of adaptive responses that maintain cellular proteostasis. Importantly, previous studies reported a decline of the cellular proteostasis network and its ability to sufficiently respond to stress with age. Whether such a decline also occurs in the mammalian heart and if it leaves the heart vulnerable to protein misfolding in response to stress remains unknown. This study investigates how the expression and activity of the unfolded protein response in the heart changes with age. It further examines how a deficiency of the activating transcription factor 6 pathway impacts the activation of the unfolded protein response and cardiac function in response to chronic adrenergic stimulation, a common risk factor for cardiac dysfunction that promotes the development of cardiac hypertrophy through the stimulation of protein synthesis.

This study found that the expression of the unfolded protein response decreases in adult mice, especially in postmitotic tissues. An in-depth analysis of the unfolded protein response in the heart and isolated cardiomyocytes revealed that this is accompanied by an impaired responsiveness to proteotoxic stress, resulting in decreased viability of adult cardiomyocytes in comparison to neonatal cardiomyocytes, which might be at least partly mediated by a decreased activity of the activating transcription factor 6 pathway. Further experiments revealed that hypertrophic cell growth causes the activation of the unfolded protein response in adult but not neonatal cardiomyocytes, eventually due to endoplasmic reticulum stress caused by increased protein synthesis in adult cells in which the baseline expression of proteostasis elements is low. The activity of activating transcription factor 6 was then shown to be essential for hypertrophic growth of cardiomyocytes. Importantly, a deficiency for activating transcription factor 6 resulted in an impaired unfolded protein response and reduced hypertrophic growth and cardiac dysfunction in mouse hearts in response to pressure overload and chronic adrenergic stimulation. Taken together, this study suggests that the induction of activating transcription factor 6 and its gene program protects against cardiac dysfunction in response to stimuli that promote hypertrophic growth in the adult heart. While not fully examined, it also suggests that the decreased capacity of the unfolded protein response in the adult heart makes it more susceptible to proteotoxic stress induced by adult cardiac hypertrophic growth.

7 Zusammenfassung

Die Integrität des Proteoms ist essentiell für eine optimale kardiale Funktion. Diese wird durch das Proteostase-Netzwerk gewahrt, welches Proteinsynthese, -faltung und -abbau reguliert. Eine unzureichende Kapazität des Proteostase-Netzwerks führt zu einer Ansammlung von schädlichen fehlgefalteten Proteinen, welche die zelluläre Funktion einschränken und zum Zelltod führen können. Die Integrität des kardialen Proteoms wird durch zellulären Stress beeinträchtigt. Um Proteinfehlfaltungen zu vermeiden reagieren kardiale Zellen hierauf mit einer Steigerung der Kapazität ihres Proteostase-Netzwerks. Dies wird durch verschiedene adaptive Mechanismen, wie die Induktion von Chaperonen, oder den vermehrten Abbau von fehlgefalteten Proteinen vermittelt. Ein essentielles Element des Proteostase-Netzwerks ist hierbei der „Unfolded Protein Response“, welcher die Proteostase im endoplasmatischen Retikulum reguliert. Der Unfolded Protein Response wird durch mindestens drei, sich teilweise überlappende, Signalwege reguliert, welche durch Sensoren für Proteinfehlfaltung vermittelt werden. Hierzu zählt „Activating Transcription Factor 6“, welcher als ein Nexus für adaptive und Proteostase wahrende Mechanismen wirkt. Vorherige Studien konnten eine Verminderung des Proteostase-Netzwerks und seiner Fähigkeit hinreichend auf Stress zu reagieren mit steigendem Alter nachweisen. Ob eine derartige Abnahme auch im Herzen von Säugetieren auftritt und ob es dieses anfällig gegenüber Proteinfehlfaltung während kardialem Stress macht, ist weitestgehend unbekannt. Diese Studie untersucht, wie sich die Expression und Aktivität des Unfolded Protein Response im Herzen mit zunehmendem Alter ändert. Weiterhin untersucht sie, wie sich ein Mangel des Activating Transcription Factor 6 auf die kardiale Funktion in Reaktion auf chronische adrenerge Stimulation auswirkt, einem kardialen Risikofaktor, welcher die Entwicklung einer kardialen Hypertrophie durch Steigerung der Proteinsynthese fördert.

Die vorliegende Studie zeigt, dass sich die Expression des Unfolded Protein Response in erwachsenen Mäusen im Vergleich zu Neonaten vor allem in postmitotischen Geweben ausgeprägt reduziert. Eine ausführliche Analyse des Unfolded Protein Response im Herzen und isolierten Kardiomyozyten zeigte, dass dies von einer verminderten Reaktion auf proteotoxischen Stress begleitet wird, was zu einem vermindertem Zellüberleben von adulten Kardiomyozyten im Vergleich zu neonatalen Kardiomyozyten führt. Weiterführende Experimente zeigten, dass hypertrophes Zellwachstum zu einer Aktivierung des Unfolded Protein Response in adulten, jedoch nicht neonatalen Kardiomyozyten führt. Dies wird möglicherweise durch „Endoplasmic Reticulum Stress“ in adulten Kardiomyozyten, in denen die basale Expression von Proteostase Elementen gering ist, als Reaktion auf die gesteigerte Proteinsynthese vermittelt. Es wurde weiterhin gezeigt, dass die Aktivität des Activating Transcription Factor 6 essentiell für funktionelles hypertrophes Wachstum von Kardiomyozyten ist. Ein Defizit für Activating Transcription Factor 6 führt hierbei zu einem eingeschränkten Unfolded Protein Response, reduziertes hypertrophes Wachstum und kardiale Dysfunktion in Maus Herzen in Reaktion auf chronische adrenerge Stimulation. Zusammengefasst deuten die Ergebnisse dieser Studie darauf hin, dass in adulten Herzen das Protein Activating Transcription Factor 6 und sein vermitteltes Genprogramm gegen kardiale Dysfunktion in Reaktion auf Stimuli, welche hypertrophes Wachstum fördern, schützt. Auch wenn nicht vollständig untersucht, deuten die Ergebnisse dieser Studie ebenfalls an, dass die verminderte Kapazität des Unfolded Protein Response in erwachsenen Herzen diese anfälliger gegenüber proteotoxischem Stress macht, der durch adulte kardiale Hypertrophie verursacht wird.

8 References

Abdellatif, M., Sedej, S., Carmona-Gutierrez, D., Madeo, F. and Kroemer, G. (2018). **Autophagy in Cardiovascular Aging**. Circulation Research *123*, 803-824, doi: 10.1161/CIRCRESAHA.118.312208.

Albakri, A. (2018). **Heart failure with reduced ejection fraction: A review of clinical status and meta-analyses of diagnosis by 3D echocardiography and natriuretic peptides-guided heart failure therapy**. Trends in Research *1*, doi: DOI: 10.15761/TR.1000122.

Arensdorf, A. M., Diedrichs, D. and Rutkowski, D. T. (2013). **Regulation of the transcriptome by ER stress: non-canonical mechanisms and physiological consequences**. Frontiers in genetics *4*, 256-256, doi: 10.3389/fgene.2013.00256.

Aro, A. L. and Chugh, S. S. (2016). **Clinical Diagnosis of Electrical Versus Anatomic Left Ventricular Hypertrophy: Prognostic and Therapeutic Implications**. Circulation. Arrhythmia and electrophysiology *9*, e003629-e003629, doi: 10.1161/CIRCEP.115.003629.

Arrieta, A., Blackwood, E. A., Stauffer, W. T., Santo Domingo, M., Bilal, A. S., Thuerauf, D. J., Pentoney, A. N., Aivati, C., Sarakki, A. V., Doroudgar, S. and Glembotski, C. C. (2020). **Mesencephalic astrocyte–derived neurotrophic factor is an ER-resident chaperone that protects against reductive stress in the heart**. Journal of Biological Chemistry *295*, 7566-7583, doi: https://doi.org/10.1074/jbc.RA120.013345.

Artham, S. M., Lavie, C. J., Milani, R. V., Patel, D. A., Verma, A. and Ventura, H. O. (2009). **Clinical Impact of Left Ventricular Hypertrophy and Implications for Regression**. Progress in Cardiovascular Diseases *52*, 153-167, doi: https://doi.org/10.1016/j.pcad.2009.05.002.

Aviram, N., Ast, T., Costa, E. A., Arakel, E. C., Chuartzman, S. G., Jan, C. H., Haßdenteufel, S., Dudek, J., Jung, M., Schorr, S., Zimmermann, R., Schwappach, B., Weissman, J. S. and Schuldiner, M. (2016). **The SND proteins constitute an alternative targeting route to the endoplasmic reticulum**. Nature *540*, 134-138, doi: 10.1038/nature20169
http://www.nature.com/nature/journal/v540/n7631/abs/nature20169.html#supplementary-information.

Ayyadevara, S., Mercanti, F., Wang, X., Mackintosh Samuel, G., Tackett Alan, J., Prayaga Sastry, V. S., Romeo, F., Shmookler Reis Robert, J. and Mehta Jawahar, L. (2016). **Age- and Hypertension-Associated Protein Aggregates in Mouse Heart Have Similar Proteomic Profiles**. Hypertension *67*, 1006-1013, doi: 10.1161/HYPERTENSIONAHA.115.06849.

Balch, W. E., Morimoto, R. I., Dillin, A. and Kelly, J. W. (2008). **Adapting Proteostasis for Disease Intervention**. Science *319*, 916, doi: 10.1126/science.1141448.

Balmforth, C., Simpson, J., Shen, L., Jhund, P. S., Lefkowitz, M., Rizkala, A. R., Rouleau, J. L., Shi, V., Solomon, S. D., Swedberg, K., Zile, M. R., Packer, M. and McMurray, J. J. V.

(2019). **Outcomes and Effect of Treatment According to Etiology in HFrEF**. JACC: Heart Failure *7*, 457, doi: 10.1016/j.jchf.2019.02.015.

Bang, C. N., Soliman, E. Z., Simpson, L. M., Davis, B. R., Devereux, R. B., Okin, P. M. and and for the, A. C. R. G. (2017). **Electrocardiographic Left Ventricular Hypertrophy Predicts Cardiovascular Morbidity and Mortality in Hypertensive Patients: The ALLHAT Study**. American Journal of Hypertension *30*, 914-922, doi: 10.1093/ajh/hpx067.

Belmont, P. J., Chen, W. J., San Pedro, M. N., Thuerauf, D. J., Lowe, N. G., Gude, N., Hilton, B., Wolkowicz, R., Sussman, M. A. and Glembotski, C. C. (2010). **Roles for ER-associated Degradation (ERAD) and the Novel ER Stress Response Gene, Derlin-3, in the Ischemic Heart**. Circulation Research *106*, 307-316, doi: 10.1161/CIRCRESAHA.109.203901.

Belmont, P. J., Tadimalla, A., Chen, W. J., Martindale, J. J., Thuerauf, D. J., Marcinko, M., Gude, N., Sussman, M. A. and Glembotski, C. C. (2008). **Coordination of Growth and Endoplasmic Reticulum Stress Signaling by Regulator of Calcineurin 1 (RCAN1), a Novel ATF6-inducible Gene**. Journal of Biological Chemistry *283*, 14012-14021, doi: 10.1074/jbc.M709776200.

Ben-Zvi, A., Miller, E. A. and Morimoto, R. I. (2009). **Collapse of proteostasis represents an early molecular event in Caenorhabditis elegans aging**. Proceedings of the National Academy of Sciences of the United States of America *106*, 14914-14919, doi: 10.1073/pnas.0902882106.

Bertolotti, A., Zhang, Y., Hendershot, L. M., Harding, H. P. and Ron, D. (2000). **Dynamic interaction of BiP and ER stress transducers in the unfolded-protein response**. Nature Cell Biology *2*, 326-332, doi: 10.1038/35014014.

Bhuiyan, M. S., Pattison, J. S., Osinska, H., James, J., Gulick, J., McLendon, P. M., Hill, J. A., Sadoshima, J. and Robbins, J. (2013). **Enhanced autophagy ameliorates cardiac proteinopathy**. The Journal of clinical investigation *123*, 5284-5297, doi: 10.1172/JCI70877.

Bi, X., Zhang, G., Wang, X., Nguyen, C., May Herman, I., Li, X., Al-Hashimi Ali, A., Austin Richard, C., Gillette Thomas, G., Fu, G., Wang Zhao, V. and Hill Joseph, A. (2018). **Endoplasmic Reticulum Chaperone GRP78 Protects Heart From Ischemia/Reperfusion Injury Through Akt Activation**. Circulation Research *122*, 1545-1554, doi: 10.1161/CIRCRESAHA.117.312641.

Blackwood, A. E., Bilal, S. A., Stauffer, T. W., Arrieta, A. and Glembotski, C. C. (2020). **Designing Novel Therapies to Mend Broken Hearts: ATF6 and Cardiac Proteostasis**. Cells *9*, doi: 10.3390/cells9030602.

Blackwood, E. A., Azizi, K., Thuerauf, D. J., Paxman, R. J., Plate, L., Kelly, J. W., Wiseman, R. L. and Glembotski, C. C. (2019a). **Pharmacologic ATF6 activation confers global**

protection in widespread disease models by reprograming cellular proteostasis. Nature Communications *10*, 187, doi: 10.1038/s41467-018-08129-2.

Blackwood, E. A., Hofmann, C., Santo Domingo, M., Bilal Alina, S., Sarakki, A., Stauffer, W., Arrieta, A., Thuerauf Donna, J., Kolkhorst Fred, W., Müller Oliver, J., Jakobi, T., Dieterich, C., Katus Hugo, A., Doroudgar, S. and Glembotski Christopher, C. (2019b). **ATF6 Regulates Cardiac Hypertrophy by Transcriptional Induction of the mTORC1 Activator, Rheb**. Circulation Research *124*, 79-93, doi: 10.1161/CIRCRESAHA.118.313854.

Bottini, P. B., Carr, A. A., Prisant, L. M., Flickinger, F. W., Allison, J. D. and Gottdiener, J. S. (1995). **Magnetic resonance imaging compared to echocardiography to assess left ventricular mass in the hypertensive patient***. American Journal of Hypertension *8*, 221-228, doi: 10.1016/0895-7061(94)00178-E.

Brouwers, F. P., de Boer, R. A., van der Harst, P., Voors, A. A., Gansevoort, R. T., Bakker, S. J., Hillege, H. L., van Veldhuisen, D. J. and van Gilst, W. H. (2013). **Incidence and epidemiology of new onset heart failure with preserved vs. reduced ejection fraction in a community-based cohort: 11-year follow-up of PREVEND**. European Heart Journal *34*, 1424-1431, doi: 10.1093/eurheartj/eht066.

Brown, M. K. and Naidoo, N. (2012). **The endoplasmic reticulum stress response in aging and age-related diseases**. Frontiers in physiology *3*, 263-263, doi: 10.3389/fphys.2012.00263.

Bulteau, A.-L., Szweda, L. I. and Friguet, B. (2002). **Age-Dependent Declines in Proteasome Activity in the Heart**. Archives of Biochemistry and Biophysics *397*, 298-304, doi: https://doi.org/10.1006/abbi.2001.2663.

Burchfield, S., Xie, M. and Hill Joseph, A. (2013). **Pathological Ventricular Remodeling**. Circulation *128*, 388-400, doi: 10.1161/CIRCULATIONAHA.113.001878.

Burkewitz, K., Feng, G., Dutta, S., Kelley, C. A., Steinbaugh, M., Cram, E. J. and Mair, W. B. (2020). **Atf-6 Regulates Lifespan through ER-Mitochondrial Calcium Homeostasis**. Cell Reports *32*, 108125, doi: https://doi.org/10.1016/j.celrep.2020.108125.

Cardoso-Moreira, M., Halbert, J., Valloton, D., Velten, B., Chen, C., Shao, Y., Liechti, A., Ascenção, K., Rummel, C., Ovchinnikova, S., Mazin, P. V., Xenarios, I., Harshman, K., Mort, M., Cooper, D. N., Sandi, C., Soares, M. J., Ferreira, P. G., Afonso, S., Carneiro, M., Turner, J. M. A., VandeBerg, J. L., Fallahshahroudi, A., Jensen, P., Behr, R., Lisgo, S., Lindsay, S., Khaitovich, P., Huber, W., Baker, J., Anders, S., Zhang, Y. E. and Kaessmann, H. (2019). **Gene expression across mammalian organ development**. Nature *571*, 505-509, doi: 10.1038/s41586-019-1338-5.

Carrara, M., Prischi, F., Nowak, P. R. and Ali, M. M. U. (2015). **Crystal structures reveal transient PERK luminal domain tetramerization in endoplasmic reticulum stress signaling**. The EMBO Journal *34*, 1589-1600, doi: 10.15252/embj.201489183.

Castillo, K., Rojas-Rivera, D., Lisbona, F., Caballero, B., Nassif, M., Court, F. A., Schuck, S., Ibar, C., Walter, P., Sierralta, J., Glavic, A. and Hetz, C. (2011). **BAX inhibitor-1 regulates autophagy by controlling the IRE1α branch of the unfolded protein response**. The EMBO Journal *30*, 4465-4478, doi: 10.1038/emboj.2011.318.

Chadwick, S. R., Fazio, E. N., Etedali-Zadeh, P., Genereaux, J., Duennwald, M. L. and Lajoie, P. (2020). **A functional unfolded protein response is required for chronological aging in Saccharomyces cerevisiae**. Current Genetics *66*, 263-277, doi: 10.1007/s00294-019-01019-0.

Chang, S. C., Ren, S., Rau, C. D. and Wang, J. J. (2018). **Isoproterenol-Induced Heart Failure Mouse Model Using Osmotic Pump Implantation**. Methods in molecular biology (Clifton, N.J.) *1816*, 207-220, doi: 10.1007/978-1-4939-8597-5_16.

Chen, D., Thomas, E. L. and Kapahi, P. (2009). **HIF-1 Modulates Dietary Restriction-Mediated Lifespan Extension via IRE-1 in Caenorhabditis elegans**. PLOS Genetics *5*, e1000486, doi: 10.1371/journal.pgen.1000486.

Chen, L., Zhao, M., Li, J., Wang, Y., Bao, Q., Wu, S., Deng, X., Tang, X., Wu, W. and Liu, X. (2017). **Critical role of X-box binding protein 1 in NADPH oxidase 4-triggered cardiac hypertrophy is mediated by receptor interacting protein kinase 1**. Cell cycle (Georgetown, Tex.) *16*, 348-359, doi: 10.1080/15384101.2016.1260210.

Chondrogianni, N., Petropoulos, I., Franceschi, C., Friguet, B. and Gonos, E. S. (2000). **Fibroblast cultures from healthy centenarians have an active proteasome**. Experimental Gerontology *35*, 721-728, doi: https://doi.org/10.1016/S0531-5565(00)00137-6.

Cleland, J. G. F., Lyon, A. R., McDonagh, T. and McMurray, J. J. V. (2020). **The year in cardiology: heart failure: The year in cardiology 2019**. European Heart Journal *41*, 1232-1248, doi: 10.1093/eurheartj/ehz949.

Cohn, J. N., Ferrari, R. and Sharpe, N. (2000). **Cardiac remodeling—concepts and clinical implications: a consensus paper from an international forum on cardiac remodeling**. Journal of the American College of Cardiology *35*, 569-582, doi: https://doi.org/10.1016/S0735-1097(99)00630-0.

Correll, R. N., Grimes, K. M., Prasad, V., Lynch, J. M., Khalil, H. and Molkentin, J. D. (2019). **Overlapping and differential functions of ATF6α versus ATF6β in the mouse heart**. Scientific Reports *9*, 2059, doi: 10.1038/s41598-019-39515-5.

Cowie, M. R., Mosterd, A., Wood, D. A., Deckers, J. W., Poole-Wilson, P. A., Sutton, G. C. and Grobbee, D. E. (1997). **The epidemiology of heart failure**. European Heart Journal *18*, 208-225, doi: 10.1093/oxfordjournals.eurheartj.a015223.

Cuspidi, C., Sala, C., Negri, F., Mancia, G., Morganti, A. and on behalf of the Italian Society of, H. (2012). **Prevalence of left-ventricular hypertrophy in hypertension: an updated**

review of echocardiographic studies. Journal of Human Hypertension *26*, 343-349, doi: 10.1038/jhh.2011.104.

Dandel, M., Knosalla, C. and Hetzer, R. (2014). **Contribution of ventricular assist devices to the recovery of failing hearts: a review and the Berlin Heart Center Experience**. European Journal of Heart Failure *16*, 248-263, doi: 10.1002/ejhf.18.

David, D. C., Ollikainen, N., Trinidad, J. C., Cary, M. P., Burlingame, A. L. and Kenyon, C. (2010). **Widespread protein aggregation as an inherent part of aging in C. elegans**. PLoS biology *8*, e1000450-e1000450, doi: 10.1371/journal.pbio.1000450.

deAlmeida, A. C., van Oort, R. J. and Wehrens, X. H. T. (2010). **Transverse aortic constriction in mice**. Journal of visualized experiments : JoVE, 1729, doi: 10.3791/1729.

Dennis, G., Sherman, B. T., Hosack, D. A., Yang, J., Gao, W., Lane, H. C. and Lempicki, R. A. (2003). **DAVID: Database for Annotation, Visualization, and Integrated Discovery**. Genome Biology *4*, R60, doi: 10.1186/gb-2003-4-9-r60.

Dobin, A., Davis, C. A., Schlesinger, F., Drenkow, J., Zaleski, C., Jha, S., Batut, P., Chaisson, M. and Gingeras, T. R. (2013). **STAR: ultrafast universal RNA-seq aligner**. Bioinformatics *29*, 15-21, doi: 10.1093/bioinformatics/bts635.

Dorn (2007). **The Fuzzy Logic of Physiological Cardiac Hypertrophy**. Hypertension *49*, 962-970, doi: 10.1161/HYPERTENSIONAHA.106.079426.

Doroudgar, S. and Glembotski, C. C. (2013). **New concepts of endoplasmic reticulum function in the heart: programmed to conserve**. J Mol Cell Cardiol *55*, 85-91, doi: 10.1016/j.yjmcc.2012.10.006.

Doroudgar, S., Hofmann, C., Boileau, E., Malone, B., Riechert, E., Gorska Agnieszka, A., Jakobi, T., Sandmann, C., Jürgensen, L., Kmietczyk, V., Malovrh, E., Burghaus, J., Rettel, M., Stein, F., Younesi, F., Friedrich Ulrike, A., Mauz, V., Backs, J., Kramer, G., Katus Hugo, A., Dieterich, C. and Völkers, M. (2019). **Monitoring Cell-Type–Specific Gene Expression Using Ribosome Profiling In Vivo During Cardiac Hemodynamic Stress**. Circulation Research *125*, 431-448, doi: 10.1161/CIRCRESAHA.119.314817.

Doroudgar, S., Thuerauf, D. J., Marcinko, M. C., Belmont, P. J. and Glembotski, C. C. (2009). **Ischemia activates the ATF6 branch of the endoplasmic reticulum stress response**. The Journal of biological chemistry *284*, 29735-29745, doi: 10.1074/jbc.M109.018036.

Doroudgar, S., Völkers, M., Thuerauf, D. J., Khan, M., Mohsin, S., Respress, J. L., Wang, W., Gude, N., Müller, O. J., Wehrens, X. H. T., Sussman, M. A. and Glembotski, C. C. (2015). **Hrd1 and ER-Associated Protein Degradation, ERAD, Are Critical Elements of the Adaptive ER Stress Response in Cardiac Myocytes**. Circulation Research *117*, 536-546, doi: 10.1161/circresaha.115.306993.

Drazner, H., Dries Daniel, L., Peshock Ronald, M., Cooper Richard, S., Klassen, C., Kazi, F., Willett, D. and Victor Ronald, G. (2005). **Left Ventricular Hypertrophy Is More Prevalent in Blacks Than Whites in the General Population**. Hypertension *46*, 124-129, doi: 10.1161/01.HYP.0000169972.96201.8e.

Eisenberg, T., Abdellatif, M., Schroeder, S., Primessnig, U., Stekovic, S., Pendl, T., Harger, A., Schipke, J., Zimmermann, A., Schmidt, A., Tong, M., Ruckenstuhl, C., Dammbrueck, C., Gross, A. S., Herbst, V., Magnes, C., Trausinger, G., Narath, S., Meinitzer, A., Hu, Z., Kirsch, A., Eller, K., Carmona-Gutierrez, D., Büttner, S., Pietrocola, F., Knittelfelder, O., Schrepfer, E., Rockenfeller, P., Simonini, C., Rahn, A., Horsch, M., Moreth, K., Beckers, J., Fuchs, H., Gailus-Durner, V., Neff, F., Janik, D., Rathkolb, B., Rozman, J., de Angelis, M. H., Moustafa, T., Haemmerle, G., Mayr, M., Willeit, P., von Frieling-Salewsky, M., Pieske, B., Scorrano, L., Pieber, T., Pechlaner, R., Willeit, J., Sigrist, S. J., Linke, W. A., Mühlfeld, C., Sadoshima, J., Dengjel, J., Kiechl, S., Kroemer, G., Sedej, S. and Madeo, F. (2016). **Cardioprotection and lifespan extension by the natural polyamine spermidine**. Nature Medicine *22*, 1428-1438, doi: 10.1038/nm.4222.

Escobar, K. A., Cole, N. H., Mermier, C. M. and VanDusseldorp, T. A. (2019). **Autophagy and aging: Maintaining the proteome through exercise and caloric restriction**. Aging Cell *18*, e12876, doi: 10.1111/acel.12876.

Estébanez, B., de Paz, J. A., Cuevas, M. J. and González-Gallego, J. (2018). **Endoplasmic Reticulum Unfolded Protein Response, Aging and Exercise: An Update**. Frontiers in physiology *9*, 1744-1744, doi: 10.3389/fphys.2018.01744.

Ferrington, D. A., Husom, A. D. and Thompson, L. V. (2005). **Altered proteasome structure, function, and oxidation in aged muscle**. The FASEB Journal *19*, 644-646, doi: 10.1096/fj.04-2578fje.

Fu Hai, Y., Okada, K.-i., Liao, Y., Tsukamoto, O., Isomura, T., Asai, M., Sawada, T., Okuda, K., Asano, Y., Sanada, S., Asanuma, H., Asakura, M., Takashima, S., Komuro, I., Kitakaze, M. and Minamino, T. (2010). **Ablation of C/EBP Homologous Protein Attenuates Endoplasmic Reticulum–Mediated Apoptosis and Cardiac Dysfunction Induced by Pressure Overload**. Circulation *122*, 361-369, doi: 10.1161/CIRCULATIONAHA.109.917914.

Gerber, Y., Weston, S. A., Redfield, M. M., Chamberlain, A. M., Manemann, S. M., Jiang, R., Killian, J. M. and Roger, V. L. (2015). **A Contemporary Appraisal of the Heart Failure Epidemic in Olmsted County, Minnesota, 2000 to 2010**. JAMA Internal Medicine *175*, 996-1004, doi: 10.1001/jamainternmed.2015.0924.

Glembotski, C. C. (2007). **Endoplasmic Reticulum Stress in the Heart**. Circulation Research *101*, 975-984, doi: 10.1161/circresaha.107.161273.

Glembotski, C. C. (2014). **Roles for ATF6 and the sarco/endoplasmic reticulum protein quality control system in the heart**. Journal of molecular and cellular cardiology *71*, 11-15, doi: 10.1016/j.yjmcc.2013.09.018.

Glembotski, C. C., Thuerauf, D. J., Huang, C., Vekich, J. A., Gottlieb, R. A. and Doroudgar, S. (2012). **Mesencephalic Astrocyte-derived Neurotrophic Factor Protects the Heart from Ischemic Damage and Is Selectively Secreted upon Sarco/endoplasmic Reticulum Calcium Depletion**. Journal of Biological Chemistry *287*, 25893-25904, doi: 10.1074/jbc.M112.356345.

Greber, B. J. and Ban, N. (2016). **Structure and Function of the Mitochondrial Ribosome**. Annual Review of Biochemistry *85*, 103-132, doi: 10.1146/annurev-biochem-060815-014343.

Grossman, W., Jones, D. and McLaurin, L. P. (1975). **Wall stress and patterns of hypertrophy in the human left ventricle**. The Journal of Clinical Investigation *56*, 56-64, doi: 10.1172/JCI108079.

Grothues, F., Smith, G. C., Moon, J. C. C., Bellenger, N. G., Collins, P., Klein, H. U. and Pennell, D. J. (2002). **Comparison of interstudy reproducibility of cardiovascular magnetic resonance with two-dimensional echocardiography in normal subjects and in patients with heart failure or left ventricular hypertrophy**. The American Journal of Cardiology *90*, 29-34, doi: https://doi.org/10.1016/S0002-9149(02)02381-0.

Gruebele, M., Dave, K. and Sukenik, S. (2016). **Globular Protein Folding In Vitro and In Vivo**. Annual Review of Biophysics *45*, 233-251, doi: 10.1146/annurev-biophys-062215-011236.

Grune, T., Jung, T., Merker, K. and Davies, K. J. A. (2004). **Decreased proteolysis caused by protein aggregates, inclusion bodies, plaques, lipofuscin, ceroid, and 'aggresomes' during oxidative stress, aging, and disease**. The International Journal of Biochemistry & Cell Biology *36*, 2519-2530, doi: https://doi.org/10.1016/j.biocel.2004.04.020.

Han, D., Lerner, A. G., Vande Walle, L., Upton, J.-P., Xu, W., Hagen, A., Backes, B. J., Oakes, S. A. and Papa, F. R. (2009). **IRE1α Kinase Activation Modes Control Alternate Endoribonuclease Outputs to Determine Divergent Cell Fates**. Cell *138*, 562-575, doi: 10.1016/j.cell.2009.07.017.

Han, J., Back, S. H., Hur, J., Lin, Y.-H., Gildersleeve, R., Shan, J., Yuan, C. L., Krokowski, D., Wang, S., Hatzoglou, M., Kilberg, M. S., Sartor, M. A. and Kaufman, R. J. (2013). **ER-stress-induced transcriptional regulation increases protein synthesis leading to cell death**. Nature Cell Biology *15*, 481-490, doi: 10.1038/ncb2738.

Harrison, D. E., Strong, R., Sharp, Z. D., Nelson, J. F., Astle, C. M., Flurkey, K., Nadon, N. L., Wilkinson, J. E., Frenkel, K., Carter, C. S., Pahor, M., Javors, M. A., Fernandez, E. and Miller, R. A. (2009). **Rapamycin fed late in life extends lifespan in genetically heterogeneous mice**. Nature *460*, 392-395, doi: 10.1038/nature08221.

Havranek, E. P., Froshaug, D. B., Emserman, C. D. B., Hanratty, R., Krantz, M. J., Masoudi, F. A., Dickinson, L. M. and Steiner, J. F. (2008). **Left ventricular hypertrophy and cardiovascular mortality by race and ethnicity**. The American journal of medicine *121*, 870-875, doi: 10.1016/j.amjmed.2008.05.034.

Hay, B. A., Abrams, B., Zumbrunn, A. Y., Valentine, J. J., Warren, L. C., Petras, S. F., Shelly, L. D., Xia, A., Varghese, A. H., Hawkins, J. L., Van Camp, J. A., Robbins, M. D., Landschulz, K. and Harwood, H. J. (2007). **Aminopyrrolidineamide inhibitors of site-1 protease**. Bioorganic & Medicinal Chemistry Letters *17*, 4411-4414, doi: https://doi.org/10.1016/j.bmcl.2007.06.031.

Haze, K., Yoshida, H., Yanagi, H., Yura, T. and Mori, K. (1999). **Mammalian Transcription Factor ATF6 Is Synthesized as a Transmembrane Protein and Activated by Proteolysis in Response to Endoplasmic Reticulum Stress**. Molecular Biology of the Cell *10*, 3787-3799, doi: 10.1091/mbc.10.11.3787.

Heineke, J. and Molkentin, J. D. (2006). **Regulation of cardiac hypertrophy by intracellular signalling pathways**. Nat Rev Mol Cell Biol *7*, 589-600, doi: 10.1038/nrm1983.

Heinzel, F. R., Hohendanner, F., Jin, G., Sedej, S. and Edelmann, F. (2015). **Myocardial hypertrophy and its role in heart failure with preserved ejection fraction**. Journal of applied physiology (Bethesda, Md. : 1985) *119*, 1233-1242, doi: 10.1152/japplphysiol.00374.2015.

Henis-Korenblit, S., Zhang, P., Hansen, M., McCormick, M., Lee, S.-J., Cary, M. and Kenyon, C. (2010). **Insulin/IGF-1 signaling mutants reprogram ER stress response regulators to promote longevity**. Proceedings of the National Academy of Sciences *107*, 9730, doi: 10.1073/pnas.1002575107.

Hetz, C. and Papa, F. R. (2018). **The Unfolded Protein Response and Cell Fate Control**. Molecular Cell *69*, 169-181, doi: https://doi.org/10.1016/j.molcel.2017.06.017.

Hidalgo San Jose, L., Sunshine, M. J., Dillingham, C. H., Chua, B. A., Kruta, M., Hong, Y., Hatters, D. M. and Signer, R. A. J. (2020). **Modest Declines in Proteome Quality Impair Hematopoietic Stem Cell Self-Renewal**. Cell Reports *30*, 69-80.e66, doi: 10.1016/j.celrep.2019.12.003.

Higa, A., Taouji, S., Lhomond, S., Jensen, D., Fernandez-Zapico, M. E., Simpson, J. C., Pasquet, J.-M., Schekman, R. and Chevet, E. (2014). **Endoplasmic Reticulum Stress-Activated Transcription Factor ATF6α Requires the Disulfide Isomerase PDIA5 To Modulate Chemoresistance**. Molecular and Cellular Biology *34*, 1839, doi: 10.1128/MCB.01484-13.

Hill, J. A. and Olson, E. N. (2008). **Cardiac Plasticity**. New England Journal of Medicine *358*, 1370-1380, doi: 10.1056/NEJMra072139.

Hipp, M. S., Kasturi, P. and Hartl, F. U. (2019). **The proteostasis network and its decline in ageing**. Nature Reviews Molecular Cell Biology *20*, 421-435, doi: 10.1038/s41580-019-0101-y.

Ho, S. Y. and Nihoyannopoulos, P. (2006). **Anatomy, echocardiography, and normal right ventricular dimensions**. Heart (British Cardiac Society) *92 Suppl 1*, i2-i13, doi: 10.1136/hrt.2005.077875.

Hofmann, C., Blackwood, E. A., Jakobi, T., Sandmann, C., Groß, J., Herzog, N., Kaufman, R. J., Katus, H. A., Völkers, M., Glembotski, C. C. and Doroudgar, S. (2021). **Age-related decline of the unfolded protein response in the heart promotes protein misfolding and cardiac pathology**. bioRxiv, 2021.2006.2016.448596, doi: 10.1101/2021.06.16.448596.

Hofmann, C., Katus Hugo, A. and Doroudgar, S. (2019). **Protein Misfolding in Cardiac Disease**. Circulation *139*, 2085-2088, doi: 10.1161/CIRCULATIONAHA.118.037417.

Hollien, J. and Weissman, J. S. (2006). **Decay of Endoplasmic Reticulum-Localized mRNAs During the Unfolded Protein Response**. Science *313*, 104, doi: 10.1126/science.1129631.

Hood, W. P., Rackley, C. E. and Rolett, E. L. (1968). **Wall stress in the normal and hypertrophied human left ventricle**. The American Journal of Cardiology *22*, 550-558, doi: https://doi.org/10.1016/0002-9149(68)90161-6.

Hsu, J. J., Ziaeian, B. and Fonarow, G. C. (2017). **Heart Failure With Mid-Range (Borderline) Ejection Fraction**. JACC: Heart Failure *5*, 763, doi: 10.1016/j.jchf.2017.06.013.

Huang, D. W., Sherman, B. T. and Lempicki, R. A. (2009). **Systematic and integrative analysis of large gene lists using DAVID bioinformatics resources**. Nature Protocols *4*, 44-57, doi: 10.1038/nprot.2008.211.

Huang, J., Wan, L., Lu, H. and Li, X. (2018). **High expression of active ATF6 aggravates endoplasmic reticulum stress-induced vascular endothelial cell apoptosis through the mitochondrial apoptotic pathway**. Molecular medicine reports *17*, 6483-6489, doi: 10.3892/mmr.2018.8658.

Hunt, S. A., Abraham, W. T., Chin, M. H., Feldman, A. M., Francis, G. S., Ganiats, T. G., Jessup, M., Konstam, M. A., Mancini, D. M., Michl, K., Oates, J. A., Rahko, P. S., Silver, M. A., Stevenson, L. W. and Yancy, C. W. (2009). **2009 Focused Update Incorporated Into the ACC/AHA 2005 Guidelines for the Diagnosis and Management of Heart Failure in Adults**. Journal of the American College of Cardiology *53*, e1, doi: 10.1016/j.jacc.2008.11.013.

Husom, A. D., Peters, E. A., Kolling, E. A., Fugere, N. A., Thompson, L. V. and Ferrington, D. A. (2004). **Altered proteasome function and subunit composition in aged muscle**. Archives of Biochemistry and Biophysics *421*, 67-76, doi: https://doi.org/10.1016/j.abb.2003.10.010.

Hussain, S. G. and Ramaiah, K. V. A. (2007). **Reduced eIF2α phosphorylation and increased proapoptotic proteins in aging**. Biochemical and Biophysical Research Communications *355*, 365-370, doi: https://doi.org/10.1016/j.bbrc.2007.01.156.

Iurlaro, R. and Muñoz-Pinedo, C. (2016). **Cell death induced by endoplasmic reticulum stress**. The FEBS Journal *283*, 2640-2652, doi: 10.1111/febs.13598.

Jackson, R. J., Hellen, C. U. T. and Pestova, T. V. (2010). **The mechanism of eukaryotic translation initiation and principles of its regulation**. Nat Rev Mol Cell Biol *11*, 113-127, doi: http://www.nature.com/nrm/journal/v11/n2/suppinfo/nrm2838_S1.html.

Jan, C. H., Williams, C. C. and Weissman, J. S. (2014). **Principles of ER cotranslational translocation revealed by proximity-specific ribosome profiling**. Science *346*, doi: 10.1126/science.1257521.

Jan, C. H., Williams, C. C. and Weissman, J. S. (2015). **Response to Comment on "Principles of ER cotranslational translocation revealed by proximity-specific ribosome profiling"**. Science *348*, 1217-1217, doi: 10.1126/science.aaa8299.

Jin, J. K., Blackwood, E. A., Azizi, K. M., Thuerauf, D. J., Fahem, A. G., Hofmann, C., Kaufman, R. J., Doroudgar, S. and Glembotski, C. C. (2016). **ATF6 Decreases Myocardial Ischemia/Reperfusion Damage and Links ER Stress and Oxidative Stress Signaling Pathways in the Heart**. Circ Res, doi: 10.1161/CIRCRESAHA.116.310266.

Johnson, N., Powis, K. and High, S. (2013). **Post-translational translocation into the endoplasmic reticulum**. Biochimica et Biophysica Acta (BBA) - Molecular Cell Research *1833*, 2403-2409, doi: https://doi.org/10.1016/j.bbamcr.2012.12.008.

Jurkin, J., Henkel, T., Nielsen, A. F., Minnich, M., Popow, J., Kaufmann, T., Heindl, K., Hoffmann, T., Busslinger, M. and Martinez, J. (2014). **The mammalian tRNA ligase complex mediates splicing of XBP1 mRNA and controls antibody secretion in plasma cells**. The EMBO Journal *33*, 2922-2936, doi: 10.15252/embj.201490332.

Kanda, S., Yanagitani, K., Yokota, Y., Esaki, Y. and Kohno, K. (2016). **Autonomous translational pausing is required for XBP1u mRNA recruitment to the ER via the SRP pathway**. Proceedings of the National Academy of Sciences of the United States of America *113*, E5886-E5895, doi: 10.1073/pnas.1604435113.

Kannel, W. B., Gordon, T., Castelli, W. P. and Margolis, J. R. (1970). **Electrocardiographic Left Ventricular Hypertrophy and Risk of Coronary Heart Disease: The Framingham Study**. Annals of Internal Medicine *72*, 813-822, doi: 10.7326/0003-4819-72-6-813.

Karali, E., Bellou, S., Stellas, D., Klinakis, A., Murphy, C. and Fotsis, T. (2014). **VEGF Signals through ATF6 and PERK to Promote Endothelial Cell Survival and Angiogenesis in the Absence of ER Stress**. Molecular Cell *54*, 559-572, doi: http://dx.doi.org/10.1016/j.molcel.2014.03.022.

Katholi, R. E. and Couri, D. M. (2011). **Left ventricular hypertrophy: major risk factor in patients with hypertension: update and practical clinical applications**. International journal of hypertension *2011*, 495349-495349, doi: 10.4061/2011/495349.

Kaushik, S. and Cuervo, A. M. (2015). **Proteostasis and aging**. Nature Medicine *21*, 1406-1415, doi: 10.1038/nm.4001.

Kawel, N., Turkbey Evrim, B., Carr, J. J., Eng, J., Gomes Antoinette, S., Hundley, W. G., Johnson, C., Masri Sofia, C., Prince Martin, R., van der Geest Rob, J., Lima João, A. C. and Bluemke David, A. (2012). **Normal Left Ventricular Myocardial Thickness for Middle-Aged and Older Subjects With Steady-State Free Precession Cardiac Magnetic Resonance**. Circulation: Cardiovascular Imaging *5*, 500-508, doi: 10.1161/CIRCIMAGING.112.973560.

Kikis, E. A., Gidalevitz, T. and Morimoto, R. I. (2010). **Protein homeostasis in models of aging and age-related conformational disease**. Advances in experimental medicine and biology *694*, 138-159, doi: 10.1007/978-1-4419-7002-2_11.

Kim, G. H., Uriel, N. and Burkhoff, D. (2018). **Reverse remodelling and myocardial recovery in heart failure**. Nature Reviews Cardiology *15*, 83-96, doi: 10.1038/nrcardio.2017.139.

Kohl, S., Zobor, D., Chiang, W.-C., Weisschuh, N., Staller, J., Menendez, I. G., Chang, S., Beck, S. C., Garrido, M. G., Sothilingam, V., Seeliger, M. W., Stanzial, F., Benedicenti, F., Inzana, F., Héon, E., Vincent, A., Beis, J., Strom, T. M., Rudolph, G., Roosing, S., Hollander, A. I. d., Cremers, F. P. M., Lopez, I., Ren, H., Moore, A. T., Webster, A. R., Michaelides, M., Koenekoop, R. K., Zrenner, E., Kaufman, R. J., Tsang, S. H., Wissinger, B. and Lin, J. H. (2015). **Mutations in the unfolded protein response regulator ATF6 cause the cone dysfunction disorder achromatopsia**. Nature Genetics *47*, 757-765, doi: 10.1038/ng.3319.

Kokame, K., Kato, H. and Miyata, T. (2001). **Identification of ERSE-II, a New cis-Acting Element Responsible for the ATF6-dependent Mammalian Unfolded Protein Response ***. Journal of Biological Chemistry *276*, 9199-9205, doi: 10.1074/jbc.M010486200.

Konstam Marvin, A., Kiernan Michael, S., Bernstein, D., Bozkurt, B., Jacob, M., Kapur Navin, K., Kociol Robb, D., Lewis Eldrin, F., Mehra Mandeep, R., Pagani Francis, D., Raval Amish, N. and Ward, C. (2018). **Evaluation and Management of Right-Sided Heart Failure: A Scientific Statement From the American Heart Association**. Circulation *137*, e578-e622, doi: 10.1161/CIR.0000000000000560.

Koren, M. J., Devereux, R. B., Casale, P. N., Savage, D. D. and Laragh, J. H. (1991). **Relation of Left Ventricular Mass and Geometry to Morbidity and Mortality in Uncomplicated Essential Hypertension**. Annals of Internal Medicine *114*, 345-352, doi: 10.7326/0003-4819-114-5-345.

Kosmaczewski, S. G., Edwards, T. J., Han, S. M., Eckwahl, M. J., Meyer, B. I., Peach, S., Hesselberth, J. R., Wolin, S. L. and Hammarlund, M. (2014). **The RtcB RNA ligase is an essential component of the metazoan unfolded protein response**. EMBO reports *15*, 1278-1285, doi: 10.15252/embr.201439531.

Kraut-Cohen, J., Afanasieva, E., Haim-Vilmovsky, L., Slobodin, B., Yosef, I., Bibi, E. and Gerst, J. E. (2013). **Translation- and SRP-independent mRNA targeting to the endoplasmic reticulum in the yeast Saccharomyces cerevisiae**. Molecular Biology of the Cell *24*, 3069-3084, doi: 10.1091/mbc.E13-01-0038.

Labbadia, J. and Morimoto, R. I. (2014). **Proteostasis and longevity: when does aging really begin?** F1000prime reports *6*, 7-7, doi: 10.12703/P6-7.

Labbadia, J. and Morimoto, R. I. (2015a). **The Biology of Proteostasis in Aging and Disease**. Annual Review of Biochemistry *84*, 435-464, doi: 10.1146/annurev-biochem-060614-033955.

Labbadia, J. and Morimoto, Richard I. (2015b). **Repression of the Heat Shock Response Is a Programmed Event at the Onset of Reproduction**. Molecular Cell *59*, 639-650, doi: https://doi.org/10.1016/j.molcel.2015.06.027.

Labunskyy, V. M., Gerashchenko, M. V., Delaney, J. R., Kaya, A., Kennedy, B. K., Kaeberlein, M. and Gladyshev, V. N. (2014). **Lifespan Extension Conferred by Endoplasmic Reticulum Secretory Pathway Deficiency Requires Induction of the Unfolded Protein Response**. PLOS Genetics *10*, e1004019, doi: 10.1371/journal.pgen.1004019.

Lang, R. M., Badano, L. P., Mor-Avi, V., Afilalo, J., Armstrong, A., Ernande, L., Flachskampf, F. A., Foster, E., Goldstein, S. A., Kuznetsova, T., Lancellotti, P., Muraru, D., Picard, M. H., Rietzschel, E. R., Rudski, L., Spencer, K. T., Tsang, W. and Voigt, J.-U. (2015). **Recommendations for Cardiac Chamber Quantification by Echocardiography in Adults: An Update from the American Society of Echocardiography and the European Association of Cardiovascular Imaging**. Journal of the American Society of Echocardiography *28*, 1-39.e14, doi: 10.1016/j.echo.2014.10.003.

Langmead, B. and Salzberg, S. L. (2012). **Fast gapped-read alignment with Bowtie 2**. Nature Methods *9*, 357-359, doi: 10.1038/nmeth.1923.

Lebeau, P., Byun, J. H., Yousof, T. and Austin, R. C. (2018). **Pharmacologic inhibition of S1P attenuates ATF6 expression, causes ER stress and contributes to apoptotic cell death**. Toxicology and Applied Pharmacology *349*, 1-7, doi: https://doi.org/10.1016/j.taap.2018.04.020.

Lee, C.-K., Klopp, R. G., Weindruch, R. and Prolla, T. A. (1999). **Gene Expression Profile of Aging and Its Retardation by Caloric Restriction**. Science *285*, 1390, doi: 10.1126/science.285.5432.1390.

Lee, E.-J., Chiang, W.-C. J., Kroeger, H., Bi, C. X., Chao, D. L., Skowronska-Krawczyk, D., Mastey, R. R., Tsang, S. H., Chea, L., Kim, K., Lambert, S. R., Grandjean, J. M. D., Baumann, B., Audo, I., Kohl, S., Moore, A. T., Wiseman, R. L., Carroll, J. and Lin, J. H. (2020). **Multiexon deletion alleles of ATF6 linked to achromatopsia**. JCI Insight *5*, doi: 10.1172/jci.insight.136041.

Lee, J. H., Budanov, A. V., Park, E. J., Birse, R., Kim, T. E., Perkins, G. A., Ocorr, K., Ellisman, M. H., Bodmer, R., Bier, E. and Karin, M. (2010). **Sestrin as a feedback inhibitor of TOR that prevents age-related pathologies**. Science (New York, N.Y.) *327*, 1223-1228, doi: 10.1126/science.1182228.

Lerner, A. G., Upton, J.-P., Praveen, P. V. K., Ghosh, R., Nakagawa, Y., Igbaria, A., Shen, S., Nguyen, V., Backes, B. J., Heiman, M., Heintz, N., Greengard, P., Hui, S., Tang, Q., Trusina, A., Oakes, S. A. and Papa, F. R. (2012). **IRE1α induces thioredoxin-interacting protein to activate the NLRP3 inflammasome and promote programmed cell death under irremediable ER stress**. Cell metabolism *16*, 250-264, doi: 10.1016/j.cmet.2012.07.007.

Levy, D., Garrison, R. J., Savage, D. D., Kannel, W. B. and Castelli, W. P. (1990). **Prognostic Implications of Echocardiographically Determined Left Ventricular Mass in the Framingham Heart Study**. New England Journal of Medicine *322*, 1561-1566, doi: 10.1056/NEJM199005313222203.

Levy, D., Kenchaiah, S., Larson, M. G., Benjamin, E. J., Kupka, M. J., Ho, K. K. L., Murabito, J. M. and Vasan, R. S. (2002). **Long-Term Trends in the Incidence of and Survival with Heart Failure**. New England Journal of Medicine *347*, 1397-1402, doi: 10.1056/NEJMoa020265.

Levy, D., Savage, D. D., Garrison, R. J., Anderson, K. M., Kannel, W. B. and Castelli, W. P. (1987). **Echocardiographic criteria for left ventricular hypertrophy: The Framingham heart study**. American Journal of Cardiology *59*, 956-960, doi: 10.1016/0002-9149(87)91133-7.

Li, F., Wang, X., Capasso, J. M. and Gerdes, A. M. (1996). **Rapid transition of cardiac myocytes from hyperplasia to hypertrophy during postnatal development**. J Mol Cell Cardiol *28*, 1737-1746, doi: 10.1006/jmcc.1996.0163.

Liao, Y., Smyth, G. K. and Shi, W. (2019). **The R package Rsubread is easier, faster, cheaper and better for alignment and quantification of RNA sequencing reads**. Nucleic acids research *47*, e47-e47, doi: 10.1093/nar/gkz114.

Lin, J. H., Li, H., Yasumura, D., Cohen, H. R., Zhang, C., Panning, B., Shokat, K. M., LaVail, M. M. and Walter, P. (2007). **IRE1 Signaling Affects Cell Fate During the Unfolded Protein Response**. Science *318*, 944, doi: 10.1126/science.1146361.

Litviňuková, M., Talavera-López, C., Maatz, H., Reichart, D., Worth, C. L., Lindberg, E. L., Kanda, M., Polanski, K., Heinig, M., Lee, M., Nadelmann, E. R., Roberts, K., Tuck, L., Fasouli, E. S., DeLaughter, D. M., McDonough, B., Wakimoto, H., Gorham, J. M., Samari, S., Mahbubani, K. T., Saeb-Parsy, K., Patone, G., Boyle, J. J., Zhang, H., Zhang, H., Viveiros, A., Oudit, G. Y., Bayraktar, O. A., Seidman, J. G., Seidman, C. E., Noseda, M., Hubner, N. and Teichmann, S. A. (2020). **Cells of the adult human heart**. Nature *588*, 466-472, doi: 10.1038/s41586-020-2797-4.

Liu, X., Kwak, D., Lu, Z., Xu, X., Fassett, J., Wang, H., Wei, Y., Cavener, D. R., Hu, X., Hall, J., Bache, R. J. and Chen, Y. (2014). **Endoplasmic reticulum stress sensor protein kinase R-like endoplasmic reticulum kinase (PERK) protects against pressure overload-induced heart failure and lung remodeling**. Hypertension (Dallas, Tex. : 1979) *64*, 738-744, doi: 10.1161/HYPERTENSIONAHA.114.03811.

Locke, M. and Tanguay, R. M. (1996). **Diminished heat shock response in the aged myocardium**. Cell stress & chaperones *1*, 251-260, doi: 10.1379/1466-1268(1996)001<0251:dhsrit>2.3.co;2.

Lu, P. D., Jousse, C., Marciniak, S. J., Zhang, Y., Novoa, I., Scheuner, D., Kaufman, R. J., Ron, D. and Harding, H. P. (2004). **Cytoprotection by pre-emptive conditional phosphorylation of translation initiation factor 2**. The EMBO journal *23*, 169-179, doi: 10.1038/sj.emboj.7600030.

Lu, Y., Liang, F.-X. and Wang, X. (2014). **A Synthetic Biology Approach Identifies the Mammalian UPR RNA Ligase RtcB**. Molecular Cell *55*, 758-770, doi: 10.1016/j.molcel.2014.06.032.

Lynch, J. M., Maillet, M., Vanhoutte, D., Schloemer, A., Sargent, M. A., Blair, N. S., Lynch, K. A., Okada, T., Aronow, B. J., Osinska, H., Prywes, R., Lorenz, J. N., Mori, K., Lawler, J., Robbins, J. and Molkentin, J. D. (2012). **A thrombospondin-dependent pathway for a protective ER stress response**. Cell *149*, 1257-1268, doi: 10.1016/j.cell.2012.03.050.

Lyon, R. C., Lange, S. and Sheikh, F. (2013). **Breaking down protein degradation mechanisms in cardiac muscle**. Trends in molecular medicine *19*, 239-249, doi: 10.1016/j.molmed.2013.01.005.

Maillet, M., van Berlo, J. H. and Molkentin, J. D. (2013). **Molecular basis of physiological heart growth: fundamental concepts and new players**. Nat Rev Mol Cell Biol *14*, 38-48, doi: 10.1038/nrm3495.

Martindale, J. J., Fernandez, R., Thuerauf, D., Whittaker, R., Gude, N., Sussman, M. A. and Glembotski, C. C. (2006). **Endoplasmic Reticulum Stress Gene Induction and Protection From Ischemia/Reperfusion Injury in the Hearts of Transgenic Mice With a Tamoxifen-Regulated Form of ATF6**. Circulation Research *98*, 1186-1193, doi: 10.1161/01.RES.0000220643.65941.8d.

Masiero, E., Agatea, L., Mammucari, C., Blaauw, B., Loro, E., Komatsu, M., Metzger, D., Reggiani, C., Schiaffino, S. and Sandri, M. (2009). **Autophagy Is Required to Maintain Muscle Mass**. Cell Metabolism *10*, 507-515, doi: 10.1016/j.cmet.2009.10.008.

Matai, L., Sarkar, G. C., Chamoli, M., Malik, Y., Kumar, S. S., Rautela, U., Jana, N. R., Chakraborty, K. and Mukhopadhyay, A. (2019). **Dietary restriction improves proteostasis and increases life span through endoplasmic reticulum hormesis**. Proceedings of the National Academy of Sciences *116*, 17383, doi: 10.1073/pnas.1900055116.

Matecic, M., Smith, D. L., Jr., Pan, X., Maqani, N., Bekiranov, S., Boeke, J. D. and Smith, J. S. (2010). **A Microarray-Based Genetic Screen for Yeast Chronological Aging Factors**. PLOS Genetics *6*, e1000921, doi: 10.1371/journal.pgen.1000921.

Maurel, M., Chevet, E., Tavernier, J. and Gerlo, S. (2014). **Getting RIDD of RNA: IRE1 in cell fate regulation**. Trends in Biochemical Sciences *39*, 245-254, doi: 10.1016/j.tibs.2014.02.008.

McFarland, T. P., Milstein, M. L. and Cala, S. E. (2010). **Rough endoplasmic reticulum to junctional sarcoplasmic reticulum trafficking of calsequestrin in adult cardiomyocytes**. Journal of Molecular and Cellular Cardiology *49*, 556-564, doi: 10.1016/j.yjmcc.2010.05.012.

McKee, P. A., Castelli, W. P., McNamara, P. M. and Kannel, W. B. (1971). **The Natural History of Congestive Heart Failure: The Framingham Study**. New England Journal of Medicine *285*, 1441-1446, doi: 10.1056/NEJM197112232852601.

McLendon, P. M. and Robbins, J. (2015). **Proteotoxicity and cardiac dysfunction**. Circulation research *116*, 1863-1882, doi: 10.1161/CIRCRESAHA.116.305372.

Meerson, F. Z. (1961). **On the mechanism of compensatory hyperfunction and insufficiency of the heart**. Cor Vasa *3*, 161-177.

Mohammadi, M., Abouissa, A., Azizah, I., Xie, Y., Cordero, J., Shirvani, A., Gigina, A., Engelhardt, M., Trogisch, F. A., Geffers, R., Dobreva, G., Bauersachs, J. and Heineke, J. (2019). **Induction of cardiomyocyte proliferation and angiogenesis protects neonatal mice from pressure overload-associated maladaptation**. JCI insight *5*, e128336, doi: 10.1172/jci.insight.128336.

Mohammed, S. F., Mirzoyev, S. A., Edwards, W. D., Dogan, A., Grogan, D. R., Dunlay, S. M., Roger, V. L., Gertz, M. A., Dispenzieri, A., Zeldenrust, S. R. and Redfield, M. M. (2014). **Left Ventricular Amyloid Deposition in Patients With Heart Failure and Preserved Ejection Fraction**. JACC: Heart Failure *2*, 113-122, doi: https://doi.org/10.1016/j.jchf.2013.11.004.

Moore, K. and Hollien, J. (2015). **Ire1-mediated decay in mammalian cells relies on mRNA sequence, structure, and translational status**. Molecular Biology of the Cell *26*, 2873-2884, doi: 10.1091/mbc.E15-02-0074.

Morishima, N., Nakanishi, K. and Nakano, A. (2011). **Activating Transcription Factor-6 (ATF6) Mediates Apoptosis with Reduction of Myeloid Cell Leukemia Sequence 1 (Mcl-1) Protein via Induction of WW Domain Binding Protein 1**. Journal of Biological Chemistry *286*, 35227-35235, doi: 10.1074/jbc.M111.233502.

Naidoo, N., Ferber, M., Master, M., Zhu, Y. and Pack, A. I. (2008). **Aging Impairs the Unfolded Protein Response to Sleep Deprivation and Leads to Proapoptotic Signaling**. The Journal of Neuroscience *28*, 6539, doi: 10.1523/JNEUROSCI.5685-07.2008.

Nakamura, M. and Sadoshima, J. (2018). **Mechanisms of physiological and pathological cardiac hypertrophy**. Nature Reviews Cardiology *15*, 387-407, doi: 10.1038/s41569-018-0007-y.

Nakanishi, K., Sudo, T. and Morishima, N. (2005). **Endoplasmic reticulum stress signaling transmitted by ATF6 mediates apoptosis during muscle development**. J Cell Biol *169*, 555-560, doi: 10.1083/jcb.200412024.

Nathans, D. (1964). **Puromycin Inhibition of Protein Synthesis: Incorporation of Puromycin into Peptide Chains**. Proceedings of the National Academy of Sciences of the United States of America *51*, 585-592, doi: 10.1073/pnas.51.4.585.

Nguyen, D. T., Kebache, S., Fazel, A., Wong, H. N., Jenna, S., Emadali, A., Lee, E. H., Bergeron, J. J., Kaufman, R. J., Larose, L. and Chevet, E. (2004). **Nck-dependent activation of extracellular signal-regulated kinase-1 and regulation of cell survival during endoplasmic reticulum stress**. Mol Biol Cell *15*, 4248-4260, doi: 10.1091/mbc.E03-11-0851.

Novoa, I., Zeng, H., Harding, H. P. and Ron, D. (2001). **Feedback inhibition of the unfolded protein response by GADD34-mediated dephosphorylation of eIF2alpha**. The Journal of cell biology *153*, 1011-1022, doi: 10.1083/jcb.153.5.1011.

Nyathi, Y., Wilkinson, B. M. and Pool, M. R. (2013). **Co-translational targeting and translocation of proteins to the endoplasmic reticulum**. Biochimica et Biophysica Acta (BBA) - Molecular Cell Research *1833*, 2392-2402, doi: https://doi.org/10.1016/j.bbamcr.2013.02.021.

Ohlmeier, C., Mikolajczyk, R., Frick, J., Prütz, F., Haverkamp, W. and Garbe, E. (2015). **Incidence, prevalence and 1-year all-cause mortality of heart failure in Germany: a study based on electronic healthcare data of more than six million persons**. Clinical Research in Cardiology *104*, 688-696, doi: 10.1007/s00392-015-0841-4.

Oka, O. B. V., van Lith, M., Rudolf, J., Tungkum, W., Pringle, M. A. and Bulleid, N. J. (2019). **ERp18 regulates activation of ATF6α during unfolded protein response**. The EMBO Journal *38*, e100990, doi: 10.15252/embj.2018100990.

Okada, K.-i., Minamino, T., Tsukamoto, Y., Liao, Y., Tsukamoto, O., Takashima, S., Hirata, A., Fujita, M., Nagamachi, Y., Nakatani, T., Yutani, C., Ozawa, K., Ogawa, S., Tomoike, H., Hori, M. and Kitakaze, M. (2004). **Prolonged Endoplasmic Reticulum Stress in Hypertrophic and Failing Heart After Aortic Constriction**. Possible Contribution of Endoplasmic Reticulum Stress to Cardiac Myocyte Apoptosis *110*, 705-712, doi: 10.1161/01.cir.0000137836.95625.d4.

Ozcan, U., Ozcan, L., Yilmaz, E., Düvel, K., Sahin, M., Manning, B. D. and Hotamisligil, G. S. (2008). **Loss of the Tuberous Sclerosis Complex Tumor Suppressors Triggers the Unfolded Protein Response to Regulate Insulin Signaling and Apoptosis**. Molecular Cell *29*, 541-551, doi: http://dx.doi.org/10.1016/j.molcel.2007.12.023.

Pagliarini, V., Giglio, P., Bernardoni, P., De Zio, D., Fimia, G. M., Piacentini, M. and Corazzari, M. (2015). **Downregulation of E2F1 during ER stress is required to induce apoptosis**. Journal of Cell Science *128*, 1166, doi: 10.1242/jcs.164103.

Palade, G. (1975). **Intracellular aspects of the process of protein synthesis**. Science *189*, 347-358, doi: 10.1126/science.1096303.

Pattison, J. S., Sanbe, A., Maloyan, A., Osinska, H., Klevitsky, R. and Robbins, J. (2008). **Cardiomyocyte expression of a polyglutamine preamyloid oligomer causes heart failure**. Circulation *117*, 2743-2751, doi: 10.1161/CIRCULATIONAHA.107.750232.

Paz Gavilán, M., Vela, J., Castaño, A., Ramos, B., del Río, J. C., Vitorica, J. and Ruano, D. (2006). **Cellular environment facilitates protein accumulation in aged rat hippocampus**. Neurobiology of Aging *27*, 973-982, doi: https://doi.org/10.1016/j.neurobiolaging.2005.05.010.

Pelliccia, A., Maron Barry, J., De Luca, R., Di Paolo Fernando, M., Spataro, A. and Culasso, F. (2002). **Remodeling of Left Ventricular Hypertrophy in Elite Athletes After Long-Term Deconditioning**. Circulation *105*, 944-949, doi: 10.1161/hc0802.104534.

Perrino, C., Prasad, S. V. N., Mao, L., Noma, T., Yan, Z., Kim, H.-S., Smithies, O. and Rockman, H. A. (2006). **Intermittent pressure overload triggers hypertrophy-independent cardiac dysfunction and vascular rarefaction**. The Journal of Clinical Investigation *116*, 1547-1560, doi: 10.1172/JCI25397.

Pinto, A. R., Ilinykh, A., Ivey, M. J., Kuwabara, J. T., D'Antoni, M. L., Debuque, R., Chandran, A., Wang, L., Arora, K., Rosenthal, N. A. and Tallquist, M. D. (2016). **Revisiting Cardiac Cellular Composition**. Circulation research *118*, 400-409, doi: 10.1161/CIRCRESAHA.115.307778.

Plate, L., Rius, B., Nguyen, B., Genereux, J. C., Kelly, J. W. and Wiseman, R. L. (2019). **Quantitative Interactome Proteomics Reveals a Molecular Basis for ATF6-Dependent Regulation of a Destabilized Amyloidogenic Protein**. Cell Chemical Biology *26*, 913-925.e914, doi: 10.1016/j.chembiol.2019.04.001.

Plumb, R., Zhang, Z.-R., Appathurai, S. and Mariappan, M. (2015). **A functional link between the co-translational protein translocation pathway and the UPR**. eLife *4*, e07426, doi: 10.7554/eLife.07426.

Ponikowski, P., Anker, S. D., AlHabib, K. F., Cowie, M. R., Force, T. L., Hu, S., Jaarsma, T., Krum, H., Rastogi, V., Rohde, L. E., Samal, U. C., Shimokawa, H., Budi Siswanto, B., Sliwa, K. and Filippatos, G. (2014). **Heart failure: preventing disease and death worldwide**. ESC Heart Failure *1*, 4-25, doi: 10.1002/ehf2.12005.

Ponikowski, P., Voors, A. A., Anker, S. D., Bueno, H., Cleland, J. G. F., Coats, A. J. S., Falk, V., González-Juanatey, J. R., Harjola, V.-P., Jankowska, E. A., Jessup, M., Linde, C., Nihoyannopoulos, P., Parissis, J. T., Pieske, B., Riley, J. P., Rosano, G. M. C., Ruilope, L.

M., Ruschitzka, F., Rutten, F. H., van der Meer, P. and Group, E. S. C. S. D. (2016). **2016 ESC Guidelines for the diagnosis and treatment of acute and chronic heart failure: The Task Force for the diagnosis and treatment of acute and chronic heart failure of the European Society of Cardiology (ESC)Developed with the special contribution of the Heart Failure Association (HFA) of the ESC**. European Heart Journal *37*, 2129-2200, doi: 10.1093/eurheartj/ehw128.

Rainer, P., Dong, P., Sorge, M., Fert-Bober, J., Holewinski Ronald, J., Wang, Y., Foss Catherine, A., An Steven, S., Baracca, A., Solaini, G., Glabe Charles, G., Pomper Martin, G., Van Eyk Jennifer, E., Tomaselli Gordon, F., Paolocci, N. and Agnetti, G. (2018). **Desmin Phosphorylation Triggers Preamyloid Oligomers Formation and Myocyte Dysfunction in Acquired Heart Failure**. Circulation Research *122*, e75-e83, doi: 10.1161/CIRCRESAHA.117.312082.

Rao, J., Yue, S., Fu, Y., Zhu, J., Wang, X., Busuttil, R. W., Kupiec-Weglinski, J. W., Lu, L. and Zhai, Y. (2014). **ATF6 mediates a pro-inflammatory synergy between ER stress and TLR activation in the pathogenesis of liver ischemia-reperfusion injury**. American journal of transplantation : official journal of the American Society of Transplantation and the American Society of Transplant Surgeons *14*, 1552-1561, doi: 10.1111/ajt.12711.

Ravi, V., Jain, A., Ahamed, F., Fathma, N., Desingu, P. A. and Sundaresan, N. R. (2018). **Systematic evaluation of the adaptability of the non-radioactive SUnSET assay to measure cardiac protein synthesis**. Scientific Reports *8*, 4587, doi: 10.1038/s41598-018-22903-8.

Reid, David W., Chen, Q., Tay, Angeline S. L., Shenolikar, S. and Nicchitta, Christopher V. (2014). **The Unfolded Protein Response Triggers Selective mRNA Release from the Endoplasmic Reticulum**. Cell *158*, 1362-1374, doi: http://dx.doi.org/10.1016/j.cell.2014.08.012.

Reid, D. W. and Nicchitta, C. V. (2012). **Primary role for endoplasmic reticulum-bound ribosomes in cellular translation identified by ribosome profiling**. J Biol Chem *287*, 5518-5527, doi: 10.1074/jbc.M111.312280.

Reid, D. W. and Nicchitta, C. V. (2015). **Comment on "Principles of ER cotranslational translocation revealed by proximity-specific ribosome profiling"**. Science *348*, 1217-1217, doi: 10.1126/science.aaa7257.

Robinson, M. D., McCarthy, D. J. and Smyth, G. K. (2010). **edgeR: a Bioconductor package for differential expression analysis of digital gene expression data**. Bioinformatics (Oxford, England) *26*, 139-140, doi: 10.1093/bioinformatics/btp616.

Rockman, H. A., Ross, R. S., Harris, A. N., Knowlton, K. U., Steinhelper, M. E., Field, L. J., Ross, J. and Chien, K. R. (1991). **Segregation of atrial-specific and inducible expression of an atrial natriuretic factor transgene in an in vivo murine model of cardiac hypertrophy**. Proceedings of the National Academy of Sciences *88*, 8277, doi: 10.1073/pnas.88.18.8277.

Roehr, J. T., Dieterich, C. and Reinert, K. (2017). **Flexbar 3.0 – SIMD and multicore parallelization**. Bioinformatics *33*, 2941-2942, doi: 10.1093/bioinformatics/btx330.

Ron, D. and Walter, P. (2007). **Signal integration in the endoplasmic reticulum unfolded protein response**. Nature Reviews Molecular Cell Biology *8*, 519-529, doi: 10.1038/nrm2199.

Roth, G. A., Forouzanfar, M. H., Moran, A. E., Barber, R., Nguyen, G., Feigin, V. L., Naghavi, M., Mensah, G. A. and Murray, C. J. L. (2015). **Demographic and Epidemiologic Drivers of Global Cardiovascular Mortality**. New England Journal of Medicine *372*, 1333-1341, doi: 10.1056/NEJMoa1406656.

Rubin, J. and Maurer, M. S. (2020). **Cardiac Amyloidosis: Overlooked, Underappreciated, and Treatable**. Annual Review of Medicine *71*, 203-219, doi: 10.1146/annurev-med-052918-020140.

Rubinsztein, David C., Mariño, G. and Kroemer, G. (2011). **Autophagy and Aging**. Cell *146*, 682-695, doi: 10.1016/j.cell.2011.07.030.

Rueden, C. T., Schindelin, J., Hiner, M. C., DeZonia, B. E., Walter, A. E., Arena, E. T. and Eliceiri, K. W. (2017). **ImageJ2: ImageJ for the next generation of scientific image data**. BMC Bioinformatics *18*, 529, doi: 10.1186/s12859-017-1934-z.

Ruggiano, A., Foresti, O. and Carvalho, P. (2014). **ER-associated degradation: Protein quality control and beyond**. Journal of Cell Biology *204*, 869-879, doi: 10.1083/jcb.201312042.

Saez, I. and Vilchez, D. (2014). **The Mechanistic Links Between Proteasome Activity, Aging and Age-related Diseases**. Current genomics *15*, 38-51, doi: 10.2174/1389202915011403061133 44.

Sala, A. J., Bott, L. C. and Morimoto, R. I. (2017). **Shaping proteostasis at the cellular, tissue, and organismal level**. Journal of Cell Biology *216*, 1231-1241, doi: 10.1083/jcb.201612111.

Sanbe, A., Osinska, H., Saffitz, J. E., Glabe, C. G., Kayed, R., Maloyan, A. and Robbins, J. (2004). **Desmin-related cardiomyopathy in transgenic mice: a cardiac amyloidosis**. Proceedings of the National Academy of Sciences of the United States of America *101*, 10132-10136, doi: 10.1073/pnas.0401900101.

Savarese, G. and Lund, L. H. (2017). **Global Public Health Burden of Heart Failure**. Cardiac failure review *3*, 7-11, doi: 10.15420/cfr.2016:25:2.

Schiattarella, G. G., Altamirano, F., Tong, D., French, K. M., Villalobos, E., Kim, S. Y., Luo, X., Jiang, N., May, H. I., Wang, Z. V., Hill, T. M., Mammen, P. P. A., Huang, J., Lee, D. I., Hahn, V. S., Sharma, K., Kass, D. A., Lavandero, S., Gillette, T. G. and Hill, J. A. (2019).

Nitrosative stress drives heart failure with preserved ejection fraction. Nature *568*, 351-356, doi: 10.1038/s41586-019-1100-z.

Schiattarella, G. G. and Hill, J. A. (2015). **Inhibition of Hypertrophy Is a Good Therapeutic Strategy in Ventricular Pressure Overload**. Circulation *131*, 1435-1447, doi: 10.1161/CIRCULATIONAHA.115.013894.

Schiattarella, G. G., Hill, T. M. and Hill, J. A. (2017). **Is Load-Induced Ventricular Hypertrophy Ever Compensatory?** Circulation *136*, 1273-1275, doi: 10.1161/CIRCULATIONAHA.117.030730.

Schindelin, J., Arganda-Carreras, I., Frise, E., Kaynig, V., Longair, M., Pietzsch, T., Preibisch, S., Rueden, C., Saalfeld, S., Schmid, B., Tinevez, J.-Y., White, D. J., Hartenstein, V., Eliceiri, K., Tomancak, P. and Cardona, A. (2012). **Fiji: an open-source platform for biological-image analysis**. Nature methods *9*, 676-682, doi: 10.1038/nmeth.2019.

Schirmer, H., Lunde, P. and Rasmussen, K. (1999). **Prevalence of left ventricular hypertrophy in a general population; The Tromsø Study**. European Heart Journal *20*, 429-438, doi: 10.1053/euhj.1998.1314.

Schlossarek, S., Frey, N. and Carrier, L. (2014). **Ubiquitin-proteasome system and hereditary cardiomyopathies**. Journal of Molecular and Cellular Cardiology *71*, 25-31, doi: https://doi.org/10.1016/j.yjmcc.2013.12.016.

Schmidt, E. K., Clavarino, G., Ceppi, M. and Pierre, P. (2009). **SUnSET, a nonradioactive method to monitor protein synthesis**. Nature Methods *6*, 275-277, doi: 10.1038/nmeth.1314.

Schubert, U., Antón, L. C., Gibbs, J., Norbury, C. C., Yewdell, J. W. and Bennink, J. R. (2000). **Rapid degradation of a large fraction of newly synthesized proteins by proteasomes**. Nature *404*, 770-774, doi: 10.1038/35008096.

Sekiya, M., Maruko-Otake, A., Hearn, S., Sakakibara, Y., Fujisaki, N., Suzuki, E., Ando, K. and Iijima, K. M. (2017). **EDEM Function in ERAD Protects against Chronic ER Proteinopathy and Age-Related Physiological Decline in Drosophila**. Developmental cell *41*, 652-664.e655, doi: 10.1016/j.devcel.2017.05.019.

Shamu, C. E. and Walter, P. (1996). **Oligomerization and phosphorylation of the Ire1p kinase during intracellular signaling from the endoplasmic reticulum to the nucleus**. The EMBO Journal *15*, 3028-3039, doi: 10.1002/j.1460-2075.1996.tb00666.x.

Shen, J., Chen, X., Hendershot, L. and Prywes, R. (2002). **ER Stress Regulation of ATF6 Localization by Dissociation of BiP/GRP78 Binding and Unmasking of Golgi Localization Signals**. Developmental Cell *3*, 99-111, doi: 10.1016/S1534-5807(02)00203-4.

Shen, J., Snapp, E. L., Lippincott-Schwartz, J. and Prywes, R. (2005). **Stable Binding of ATF6 to BiP in the Endoplasmic Reticulum Stress Response**. Molecular and Cellular Biology *25*, 921, doi: 10.1128/MCB.25.3.921-932.2005.

Shore, D. E., Carr, C. E. and Ruvkun, G. (2012). **Induction of Cytoprotective Pathways Is Central to the Extension of Lifespan Conferred by Multiple Longevity Pathways**. PLOS Genetics *8*, e1002792, doi: 10.1371/journal.pgen.1002792.

Shoulders, Matthew D., Ryno, Lisa M., Genereux, Joseph C., Moresco, James J., Tu, Patricia G., Wu, C., Yates, John R., Su, Andrew I., Kelly, Jeffery W. and Wiseman, R. L. (2013). **Stress-Independent Activation of XBP1s and/or ATF6 Reveals Three Functionally Diverse ER Proteostasis Environments**. Cell Reports *3*, 1279-1292, doi: https://doi.org/10.1016/j.celrep.2013.03.024.

Singh, S. R. and Robbins, J. (2018). **Desmin and Cardiac Disease: An Unfolding Story**. Circulation research *122*, 1324-1326, doi: 10.1161/CIRCRESAHA.118.312965.

Slade, A. M. and Severs, N. J. (1985). **Rough endoplasmic reticulum in the adult mammalian cardiac muscle cell**. J Submicrosc Cytol *17*, 531-536.

Sleiman, N. H., McFarland, T. P., Jones, L. R. and Cala, S. E. (2015). **Transitions of protein traffic from cardiac ER to junctional SR**. Journal of molecular and cellular cardiology *81*, 34-45, doi: 10.1016/j.yjmcc.2014.12.025.

Stauffer, T. W., Arrieta, A., Blackwood, A. E. and Glembotski, C. C. (2020a). **Sledgehammer to Scalpel: Broad Challenges to the Heart and Other Tissues Yield Specific Cellular Responses via Transcriptional Regulation of the ER-Stress Master Regulator ATF6α**. International Journal of Molecular Sciences *21*, doi: 10.3390/ijms21031134.

Stauffer, W. T., Blackwood, E. A., Azizi, K., Kaufman, R. J. and Glembotski, C. C. (2020b). **The ER Unfolded Protein Response Effector, ATF6, Reduces Cardiac Fibrosis and Decreases Activation of Cardiac Fibroblasts**. International Journal of Molecular Sciences *21*, doi: 10.3390/ijms21041373.

Steenman, M. and Lande, G. (2017). **Cardiac aging and heart disease in humans**. Biophysical reviews *9*, 131-137, doi: 10.1007/s12551-017-0255-9.

Steiner, I. (1987). **The prevalence of isolated atrial amyloid**. The Journal of Pathology *153*, 395-398, doi: 10.1002/path.1711530413.

Tadimalla, A., Belmont, P. J., Thuerauf, D. J., Glassy, M. S., Martindale, J. J., Gude, N., Sussman, M. A. and Glembotski, C. C. (2008). **Mesencephalic Astrocyte-Derived Neurotrophic Factor Is an Ischemia-Inducible Secreted Endoplasmic Reticulum Stress Response Protein in the Heart**. Circulation Research *103*, 1249-1258, doi: 10.1161/circresaha.108.180679.

Tannous, P., Zhu, H., Nemchenko, A., Berry, J. M., Johnstone, J. L., Shelton, J. M., Miller, F. J., Jr., Rothermel, B. A. and Hill, J. A. (2008). **Intracellular protein aggregation is a**

proximal trigger of cardiomyocyte autophagy. Circulation *117*, 3070-3078, doi: 10.1161/CIRCULATIONAHA.107.763870.

Tanskanen, M., Peuralinna, T., Polvikoski, T., Notkola, I. L., Sulkava, R., Hardy, J., Singleton, A., Kiuru-Enari, S., Paetau, A., Tienari, P. J. and Myllykangas, L. (2008). **Senile systemic amyloidosis affects 25% of the very aged and associates with genetic variation in alpha2-macroglobulin and tau: A population-based autopsy study**. Annals of Medicine *40*, 232-239, doi: 10.1080/07853890701842988.

Taylor, R. C. (2016). **Aging and the UPR(ER)**. Brain Research *1648*, 588-593, doi: https://doi.org/10.1016/j.brainres.2016.04.017.

Taylor, R. C. and Dillin, A. (2013). **XBP-1 is a cell-nonautonomous regulator of stress resistance and longevity**. Cell *153*, 1435-1447, doi: 10.1016/j.cell.2013.05.042.

The Criteria Committee of the New York Heart Association. Boston, M. L. B. (1994). **Nomenclature and criteria for diagnosis of diseases of the heart and great vessels (9th ED.)**

Thuerauf, D. J., Hoover, H., Meller, J., Hernandez, J., Su, L., Andrews, C., Dillmann, W. H., McDonough, P. M. and Glembotski, C. C. (2001). **Sarco/endoplasmic Reticulum Calcium ATPase-2 Expression Is Regulated by ATF6 during the Endoplasmic Reticulum Stress Response: INTRACELLULAR SIGNALING OF CALCIUM STRESS IN A CARDIAC MYOCYTE MODEL SYSTEM**. Journal of Biological Chemistry *276*, 48309-48317, doi: 10.1074/jbc.M107146200.

Thuerauf, D. J., Marcinko, M., Belmont, P. J. and Glembotski, C. C. (2007). **Effects of the Isoform-specific Characteristics of ATF6α and ATF6β on Endoplasmic Reticulum Stress Response Gene Expression and Cell Viability**. Journal of Biological Chemistry *282*, 22865-22878, doi: 10.1074/jbc.M701213200.

Thuerauf, D. J., Morrison, L. and Glembotski, C. C. (2004). **Opposing Roles for ATF6α and ATF6β in Endoplasmic Reticulum Stress Response Gene Induction**. Journal of Biological Chemistry *279*, 21078-21084, doi: 10.1074/jbc.M400713200.

Toko, H., Takahashi, H., Kayama, Y., Okada, S., Minamino, T., Terasaki, F., Kitaura, Y. and Komuro, I. (2010). **ATF6 is important under both pathological and physiological states in the heart**. Journal of Molecular and Cellular Cardiology *49*, 113-120, doi: https://doi.org/10.1016/j.yjmcc.2010.03.020.

Tomaru, U., Takahashi, S., Ishizu, A., Miyatake, Y., Gohda, A., Suzuki, S., Ono, A., Ohara, J., Baba, T., Murata, S., Tanaka, K. and Kasahara, M. (2012). **Decreased Proteasomal Activity Causes Age-Related Phenotypes and Promotes the Development of Metabolic Abnormalities**. The American Journal of Pathology *180*, 963-972, doi: 10.1016/j.ajpath.2011.11.012.

Tóth, M. L., Sigmond, T., Borsos, É., Barna, J., Erdélyi, P., Takács-Vellai, K., Orosz, L., Kovács, A. L., Csikós, G., Sass, M. and Vellai, T. (2008). **Longevity pathways converge on**

autophagy genes to regulate life span in Caenorhabditis elegans. Autophagy *4*, 330-338, doi: 10.4161/auto.5618.

Tsujimoto, Y., Nakagawa, T. and Shimizu, S. (2006). **Mitochondrial membrane permeability transition and cell death**. Biochimica et Biophysica Acta (BBA) - Bioenergetics *1757*, 1297-1300, doi: https://doi.org/10.1016/j.bbabio.2006.03.017.

Tsujita, Y., Kato, T. and Sussman, M. A. (2005). **Evaluation of Left Ventricular Function in Cardiomyopathic Mice by Tissue Doppler and Color M-Mode Doppler Echocardiography**. Echocardiography *22*, 245-253, doi: 10.1111/j.0742-2822.2005.04014.x.

Upton, J.-P., Wang, L., Han, D., Wang, E. S., Huskey, N. E., Lim, L., Truitt, M., McManus, M. T., Ruggero, D., Goga, A., Papa, F. R. and Oakes, S. A. (2012). **IRE1α Cleaves Select microRNAs During ER Stress to Derepress Translation of Proapoptotic Caspase-2**. Science *338*, 818, doi: 10.1126/science.1226191.

Urra, H., Dufey, E., Lisbona, F., Rojas-Rivera, D. and Hetz, C. (2013). **When ER stress reaches a dead end**. Biochimica et Biophysica Acta (BBA) - Molecular Cell Research *1833*, 3507-3517, doi: https://doi.org/10.1016/j.bbamcr.2013.07.024.

Vattem, K. M. and Wek, R. C. (2004). **Reinitiation involving upstream ORFs regulates ATF4 mRNA translation in mammalian cells**. Proceedings of the National Academy of Sciences of the United States of America *101*, 11269-11274, doi: 10.1073/pnas.0400541101.

Vekich, J. A., Belmont, P. J., Thuerauf, D. J. and Glembotski, C. C. (2012). **Protein Disulfide Isomerase-associated 6 is an ATF6-inducible ER Stress Response Protein that Protects Cardiac Myocytes from Ischemia/Reperfusion-mediated Cell Death**. Journal of molecular and cellular cardiology *53*, 259-267, doi: 10.1016/j.yjmcc.2012.05.005.

Velagaleti, R. S., Gona, P., Pencina, M. J., Aragam, J., Wang, T. J., Levy, D., D'Agostino, R. B., Lee, D. S., Kannel, W. B., Benjamin, E. J. and Vasan, R. S. (2014). **Left ventricular hypertrophy patterns and incidence of heart failure with preserved versus reduced ejection fraction**. The American journal of cardiology *113*, 117-122, doi: 10.1016/j.amjcard.2013.09.028.

Vernace, V. A., Arnaud, L., Schmidt-Glenewinkel, T. and Figueiredo-Pereira, M. E. (2007). **Aging perturbs 26S proteasome assembly in Drosophila melanogaster**. FASEB journal : official publication of the Federation of American Societies for Experimental Biology *21*, 2672-2682, doi: 10.1096/fj.06-6751com.

Völkers, M., Weidenhammer, C., Herzog, N., Qiu, G., Spaich, K., Wegner, F. V., Peppel, K., Müller, O. J., Schinkel, S., Rabinowitz, J. E., Hippe, H.-J., Brinks, H., Katus, H. A., Koch, W. J., Eckhart, A. D., Friedrich, O. and Most, P. (2011). **The inotropic peptide βARKct improves βAR responsiveness in normal and failing cardiomyocytes through G(βγ)-**

mediated L-type calcium current disinhibition. Circulation research *108*, 27-39, doi: 10.1161/CIRCRESAHA.110.225201.

Walter, P. and Ron, D. (2011). **The Unfolded Protein Response: From Stress Pathway to Homeostatic Regulation**. Science *334*, 1081, doi: 10.1126/science.1209038.

Walther, Dirk M., Kasturi, P., Zheng, M., Pinkert, S., Vecchi, G., Ciryam, P., Morimoto, Richard I., Dobson, Christopher M., Vendruscolo, M., Mann, M. and Hartl, F. U. (2015). **Widespread Proteome Remodeling and Aggregation in Aging C. elegans**. Cell *161*, 919-932, doi: 10.1016/j.cell.2015.03.032.

Wang, P., Li, J., Tao, J. and Sha, B. (2018). **The luminal domain of the ER stress sensor protein PERK binds misfolded proteins and thereby triggers PERK oligomerization**. The Journal of biological chemistry *293*, 4110-4121, doi: 10.1074/jbc.RA117.001294.

Wang, X., Osinska, H., Klevitsky, R., Gerdes, A. M., Nieman, M., Lorenz, J., Hewett, T. and Robbins, J. (2001). **Expression of R120G–αB-Crystallin Causes Aberrant Desmin and αB-Crystallin Aggregation and Cardiomyopathy in Mice**. Circulation Research *89*, 84-91, doi: 10.1161/hh1301.092688.

Wang, X. and Robbins, J. (2006). **Heart Failure and Protein Quality Control**. Circulation Research *99*, 1315-1328, doi: 10.1161/01.RES.0000252342.61447.a2.

Wang, Y., Shen, J., Arenzana, N., Tirasophon, W., Kaufman, R. J. and Prywes, R. (2000). **Activation of ATF6 and an ATF6 DNA Binding Site by the Endoplasmic Reticulum Stress Response**. Journal of Biological Chemistry *275*, 27013-27020, doi: 10.1016/S0021-9258(19)61473-0.

Wang, Y., Zhang, Y., Ding, G., May, H. I., Xu, J., Gillette, T. G., Wang, H. and Wang, Z. V. (2017). **Temporal dynamics of cardiac hypertrophic growth in response to pressure overload**. American journal of physiology. Heart and circulatory physiology *313*, H1119-H1129, doi: 10.1152/ajpheart.00284.2017.

Wehner, G. J., Jing, L., Haggerty, C. M., Suever, J. D., Leader, J. B., Hartzel, D. N., Kirchner, H. L., Manus, J. N. A., James, N., Ayar, Z., Gladding, P., Good, C. W., Cleland, J. G. F. and Fornwalt, B. K. (2019). **Routinely reported ejection fraction and mortality in clinical practice: where does the nadir of risk lie?** European Heart Journal *41*, 1249-1257, doi: 10.1093/eurheartj/ehz550.

Willis, M. S. and Patterson, C. (2013). **Proteotoxicity and cardiac dysfunction--Alzheimer's disease of the heart?** N Engl J Med *368*, 455-464, doi: 10.1056/NEJMra1106180.

Wu, J., Rutkowski, D. T., Dubois, M., Swathirajan, J., Saunders, T., Wang, J., Song, B., Yau, G. D. Y. and Kaufman, R. J. (2007). **ATF6α Optimizes Long-Term Endoplasmic Reticulum Function to Protect Cells from Chronic Stress**. Developmental Cell *13*, 351-364, doi: https://doi.org/10.1016/j.devcel.2007.07.005.

Yamamoto, K., Sato, T., Matsui, T., Sato, M., Okada, T., Yoshida, H., Harada, A. and Mori, K. (2007). **Transcriptional Induction of Mammalian ER Quality Control Proteins Is Mediated by Single or Combined Action of ATF6α and XBP1**. Developmental Cell *13*, 365-376, doi: 10.1016/j.devcel.2007.07.018.

Yamamoto, K., Yoshida, H., Kokame, K., Kaufman, R. J. and Mori, K. (2004). **Differential Contributions of ATF6 and XBP1 to the Activation of Endoplasmic Reticulum Stress-Responsive cis-Acting Elements ERSE, UPRE and ERSE-II**. The Journal of Biochemistry *136*, 343-350, doi: 10.1093/jb/mvh122.

Yanagitani, K., Kimata, Y., Kadokura, H. and Kohno, K. (2011). **Translational Pausing Ensures Membrane Targeting and Cytoplasmic Splicing of XBP1u mRNA**. Science *331*, 586, doi: 10.1126/science.1197142.

Yancy, C. W., Jessup, M., Bozkurt, B., Butler, J., Casey, D. E., Drazner, M. H., Fonarow, G. C., Geraci, S. A., Horwich, T., Januzzi, J. L., Johnson, M. R., Kasper, E. K., Levy, W. C., Masoudi, F. A., McBride, P. E., McMurray, J. J. V., Mitchell, J. E., Peterson, P. N., Riegel, B., Sam, F., Stevenson, L. W., Tang, W. H. W., Tsai, E. J. and Wilkoff, B. L. (2013). **2013 ACCF/AHA Guideline for the Management of Heart Failure**. Journal of the American College of Cardiology *62*, e147, doi: 10.1016/j.jacc.2013.05.019.

Yancy, W., Jessup, M., Bozkurt, B., Butler, J., Casey Donald, E., Colvin Monica, M., Drazner Mark, H., Filippatos Gerasimos, S., Fonarow Gregg, C., Givertz Michael, M., Hollenberg Steven, M., Lindenfeld, J., Masoudi Frederick, A., McBride Patrick, E., Peterson Pamela, N., Stevenson Lynne, W. and Westlake, C. (2017). **2017 ACC/AHA/HFSA Focused Update of the 2013 ACCF/AHA Guideline for the Management of Heart Failure: A Report of the American College of Cardiology/American Heart Association Task Force on Clinical Practice Guidelines and the Heart Failure Society of America**. Circulation *136*, e137-e161, doi: 10.1161/CIR.0000000000000509.

Yao, Y., Lu, Q., Hu, Z., Yu, Y., Chen, Q. and Wang, Q. K. (2017). **A non-canonical pathway regulates ER stress signaling and blocks ER stress-induced apoptosis and heart failure**. Nature communications *8*, 133-133, doi: 10.1038/s41467-017-00171-w.

Yoshida, H., Matsui, T., Yamamoto, A., Okada, T. and Mori, K. (2001). **XBP1 mRNA Is Induced by ATF6 and Spliced by IRE1 in Response to ER Stress to Produce a Highly Active Transcription Factor**. Cell *107*, 881-891, doi: https://doi.org/10.1016/S0092-8674(01)00611-0.

Yoshida, H., Okada, T., Haze, K., Yanagi, H., Yura, T., Negishi, M. and Mori, K. (2000). **ATF6 Activated by Proteolysis Binds in the Presence of NF-Y (CBF) Directly to the cis-Acting Element Responsible for the Mammalian Unfolded Protein Response**. Molecular and Cellular Biology *20*, 6755, doi: 10.1128/MCB.20.18.6755-6767.2000.

Yoshida, H., Oku, M., Suzuki, M. and Mori, K. (2006). **pXBP1(U) encoded in XBP1 pre-mRNA negatively regulates unfolded protein response activator pXBP1(S) in mammalian**

ER stress response. The Journal of cell biology *172*, 565-575, doi: 10.1083/jcb.200508145.

Zarrinkoub, R., Wettermark, B., Wändell, P., Mejhert, M., Szulkin, R., Ljunggren, G. and Kahan, T. (2013). **The epidemiology of heart failure, based on data for 2.1 million inhabitants in Sweden**. European Journal of Heart Failure *15*, 995-1002, doi: 10.1093/eurjhf/hft064.

Zhang, G., Wang, X., Bi, X., Li, C., Deng, Y., Al-Hashimi, A. A., Luo, X., Gillette, T. G., Austin, R. C., Wang, Y. and Wang, Z. V. (2019). **GRP78 (Glucose-Regulated Protein of 78 kDa) Promotes Cardiomyocyte Growth Through Activation of GATA4 (GATA-Binding Protein 4)**. Hypertension (Dallas, Tex. : 1979) *73*, 390-398, doi: 10.1161/HYPERTENSIONAHA.118.12084.

Zhao, D., Liu, J., Xie, W. and Qi, Y. (2015). **Cardiovascular risk assessment: a global perspective**. Nature Reviews Cardiology *12*, 301-311, doi: 10.1038/nrcardio.2015.28.

Zhou, C., Slaughter, Brian D., Unruh, Jay R., Guo, F., Yu, Z., Mickey, K., Narkar, A., Ross, Rhonda T., McClain, M. and Li, R. (2014). **Organelle-Based Aggregation and Retention of Damaged Proteins in Asymmetrically Dividing Cells**. Cell *159*, 530-542, doi: http://dx.doi.org/10.1016/j.cell.2014.09.026.

Zhou, J., Chong, S. Y., Lim, A., Singh, B. K., Sinha, R. A., Salmon, A. B. and Yen, P. M. (2017). **Changes in macroautophagy, chaperone-mediated autophagy, and mitochondrial metabolism in murine skeletal and cardiac muscle during aging**. Aging *9*, 583-599, doi: 10.18632/aging.101181.

Ziaeian, B. and Fonarow, G. C. (2016). **Epidemiology and aetiology of heart failure**. Nature Reviews Cardiology *13*, 368-378, doi: 10.1038/nrcardio.2016.25.

9 Contributions

This thesis was conducted in a collaboration between the research groups ‘Cardiac Proteostasis’ lead by Shirin Doroudgar, Ph.D., ‘Molecular Cardiology’ lead by Prof. Christopher C. Glembotski and ‘Molecular Biology of Cell Growth’ lead by Dr. Mirko Völkers. The study was conceptualized together with Shirin Doroudgar, Ph.D. and Prof. Christopher C. Glembotski and is based on a large number of methods and previous results that have already been established in the different laboratories. Dr. Mirko Völkers assisted in the conceptualization of the study. Isolation of primary cardiomyocytes was performed majorly by Nicole Herzog and Verena Kamuf-Schenk. ATF6 knockout mice were provided by Prof. Christopher C. Glembotski. Dr. Tobias Jakobi performed the differential gene expression analysis of the sequencing data obtained from ATF6 knockout mice. Transverse aortic constriction surgeries were performed by Eva Riechert. qPCRs of Figure 30B and Figure 30D were performed by Erik A. Blackwood. I performed the remaining experiments and created the figures under the supervision of Shirin Doroudgar, Ph.D.

10 Acknowledgments

First and foremost, I would like to express my sincere gratitude to my supervisor Shirin Doroudgar, Ph.D. for her consistent guidance and encouragement throughout the years.

I also want to thank Dr. Mirko Völkers for being an outstanding mentor and his incredible support.

Working with Prof. Christopher C. Glembotski was an extraordinary experience and I want to thank him for giving me a chance to be part of his laboratory.

I am very thankful to all the members of the Doroudgar lab, the Völkers lab and the Glembotski lab for being good friends and their continuous assistance.

I also would like to acknowledge and thank Xunlei Zhou, Ph.D. and Gonzalo Alvarez-Bolado, M.D., Ph.D., for introducing me to the world of science and truly being an inspiration for me.

Most importantly, none of this could have happened without my family. I am forever grateful for your unconditional love and want to thank all of you for knowing that I can always count on you.

11 Eidesstattliche Versicherung

1. Bei der eingereichten Dissertation zu dem Thema

Hypertrophic Growth Control by Activating Transcription Factor 6 in the Neonatal and Adult Heart

handelt es sich um meine eigenständig erbrachte Leistung.

2. Ich habe nur die angegebenen Quellen und Hilfsmittel benutzt und mich keiner unzulässigen Hilfe Dritter bedient. Insbesondere habe ich wörtlich oder sinngemäß aus anderen Werken übernommene Inhalte als solche kenntlich gemacht.

3. Die Arbeit oder Teile davon habe ich bislang nicht an einer Hochschule des In- oder Auslands als Bestandteil einer Prüfung- oder Qualifikationsleistung vorgelegt.

4. Die Richtigkeit der vorstehenden Erklärungen bestätige ich.

5. Die Bedeutung der eidesstattlichen Versicherung und die strafrechtlichen Folgen einer unrichtigen oder unvollständigen eidesstattlichen Versicherung sind mir bekannt. Ich versichere an Eides statt, dass ich nach bestem Wissen die reine Wahrheit erklärt und nichts verschwiegen habe.

_____

Heidelberg, 21.06.2021 Christoph Hofmann